Numerical Studies of Rotating Bose-Einstein Condensates via Rotating Lagrangian Coordinates

CAO XIAOMENG

(B.Sc.(Hons.), NUS,

Diplôme de l'Ecole Polytechnique)

A THESIS SUBMITTED FOR THE DEGREE OF

MASTER OF SCIENCE

DEPARTMENT OF MATHEMATICS

NATIONAL UNIVERSITY OF SINGAPORE

2012

Acknowledgements

I would like to extend my heartfelt gratitude to my supervisor: Prof Bao Weizhu, for his guidance and advice throughout the research process. He has provided me great ideas and strong encouragement.

In addition, I'd like to express special thanks to Mr. Tang Qinglin for all his help and guidance.

Moreover, I'd like to thank the professors in National University of Singapore and Ecole Polytechnique in France, for their guidance through out my two years studies in Singapore and two years studies in France under the French-Grandes Ecoles Double Degree Program (FDDP). I'd like to thank Assoc. Prof. Wong Yan Loi for his coordination and help in FDDP during the years.

And finally, I wish to thank my parents for their understanding, unconditional support and sacrifice over the years. I would never arrive at this stage without them.

Contents

Summary

Since the realization of Bose-Einstein Condensation (BEC) in dilute bosonic atomic gases [54, 5, 16], significant experimental and theoretical advances have been developed in the field of research [56, 64, 4, 3, 13, 35, 33] which permits an intriguing glimpse into the macroscopic quantum world. Quantized vortices in rotating BEC have been observed by several groups experimentally, e.g. the JILA group [56], the ENS group [54], and the MIT group [64]. There are various methods to generate quantized vortices, including imposing a rotating laser beam with angular velocity on the magnetic trap [21] and adding a narrow, moving Gaussian potential to the stationary magnetic trap [45]. These observations have spurred great excitement in studying superfluidity.

In this thesis, the dynamics of rotating BEC is studied analytically and numerically based on introducing a rotating Lagrangian coordinate. Based on the mean field theory, the rotating one-component BEC is described by a single Gross-Pitaevskii equation (GPE) in a rotating frame. By introducing a rotating Lagrangian coordinate transform, the angular momentum term has been removed from the original GPE and is replaced by a time-dependent potential. We find the formulation for energy and proved its conservation. And we study the conservation and dynamical laws of angular momentum expectation and condensate width. We investigate the center of mass with initial ground state with a shift. A numerical method, which is explicit, stable, spectral accurate is presented. Extensive numerical results are presented to demonstrate the dynamical results.

Finally, these numerical results are extended to two-component rotating BEC.

The first chapter of this thesis will focus on the background of BEC and existing numerical methods. The work in this thesis will be introduced as well.

Chapter 2 will focus on the single-component BEC. We apply the coordinate transformation methodology. The dynamical laws of the rotating BEC under the new coordinate system will be discussed and presented in details. We approximate the rotating BEC using time splitting method for temporal direction and spectral discretization method for spatial direction. Numerical results will also be presented.

Our investigation is extended to two-component rotating BEC in Chapter 3. We apply a similar approach to the coupled GPE where the dynamics is studied both analytically and numerically.

List of Tables

List of Figures

Chapter 1

Introduction

1.1 Bose-Einstein condensates

A Bose-Einstein condensate (BEC) is a state of matter of a dilute gas of weakly interacting bosons which is cooled to temperatures near absolute zero and confined in an external potential. Under these conditions, quantum effects become apparent on a macroscopic scale, as a large fraction of bosons will spontaneously occupy the lowest quantum state of the external potential [41].

The idea of BEC was first predicted by Albert Einstein in 1924. He has predicted the existence of a singular quantum state produced by the slowing of atoms using cooling apparatus [31]. He reviewed and generalized the work of Satyendra Nath Bose [14] on the statistical mechanics of photons. The result of the combined efforts of Bose and Einstein forms the concept of a Bose gas, governed by Bose-Einstein statistics, which describes the statistical distribution of identical particles with integer spin, known as bosons. In 1938, Fritz London proposed BEC as a mechanism for superfluidity in liquid helium and superconductivity [15, 53]. Superfluid helium has many exceptional properties, including zero viscosity and the existence of quantized vortices. It was later discovered that these properties also appear in the gaseous BEC, after the first experimental realization of BEC, by Eric Cornell, Carl Wieman and co-workers at JILA on June 5, 1995 in vapours of ^{87}Rb (cf. Fig. 1.1) [5]. About four months later, an independent effort led by Wolfgang Ketterle at MIT created a condensate

made of ^{23}Na [29]. The condensate had about a hundred more atoms, allowing him to obtain several important experimental results, such as the observation of quantum mechanical interference between two different condensates. Cornell, Wieman and Ketterle won the 2011 Nobel Prize in Physics for their achievements. One month after the JILA work, a group led by Randall Hulet at Rice University announced the create of a condensate of ^{7}Li atoms [16]. Later, it was achieved in many other alkali gases, including ^{85}Rb [27],^{41}K [57], ^{133}Cs [73], spin-polarized hydrogen [36] and metastable triplet ^{4}He [65, 67]. These systems have become a subject of explosion of research.

The most striking feature of BEC is that due to the condensation of a large

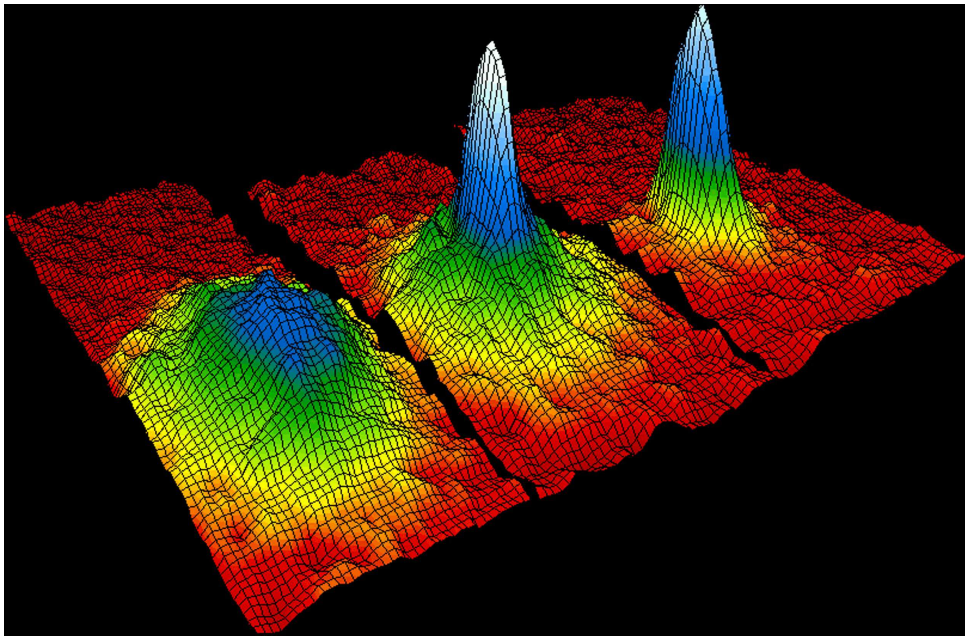

Figure 1.1: Velocity-distribution data of a gas of Rubidium (Rb) atoms, confirming the discovery of a new phase of matter, the Bose-Einstein condensate. Left: just before the appearance of a Bose-Einstein condensate. Center: just after the appearance of the condensate. Right: after further evaporation, leaving a sample of nearly pure condensate.

fraction of identical atoms into the same quantum state, the wave-like behaviour is exhibited on a macroscopic scale, which is distinguishable to the behaviours of particles following classical Newton's second law. Another intriguing property is the unrestricted flow of particles in the sample, such as the flow of currents without observable viscosity and the flow of electric currents without observable

resistance [75]. These properties can be explained by the macroscopic occupation of a quantized mode which provides a stabilized mechanism. Many experiments have been carried out to study the superfluid properties of BEC, which has a particularly interesting signature of supporting quantized vortex states [35, 48, 72]. In 1999, a vortex was first created experimentally at JILA using ^{87}Rb containing two different hyperfine components [56]. Soon after, the ENS group has created vortex in elongated rotating cigar-shaped one component condensate, with small vortex arrays of up to 11 vortices being observed [24, 26, 54, 55]. Recently, MIT group has created larger rotating condensates with up to 130 vortices being observed [1]. More recently Leanhardt et al have created a coreless vortex in a spinor $F = 1$ BEC using "topological phase imprinting" [51]. It is hence of great importance to study the quantized vortex state to better understand the above observations as well as superfluidity [35, 48, 68, 17]. Quantized vortex states can be detected in the experiments of rotating single-component BEC, rotating two-component and spin $F = 1$ BEC. Mean-field theory is widely applied to approximate the BEC. The main idea of the theory is to replace interactions of all particles in the system to any one body with an average or effective interaction, sometimes called a molecular field [23]. The multi-body problem can be reduced into a one-body problem. In this case, the interactions between particles in a dilute atomic gas are very weak and the system can be regarded as being dominated by the wave-like condensate. One can hence apply the main-field theory and sum the interaction of all of the particles to get an effective one-body problem, which can be approximated using Gross-Pitaevskii equation (GPE) [28, 30].

1.2 The Gross-Pitaevskii equation

The Gross-Pitaevskii equation was first derived in the early 1960s and named after Eugene P. Gross [42] and Lev Petrovich Pitaevskii [62]. According to theory, the rotating one-component condensate can be described by a single GPE in a rotating frame [4, 12, 21, 35, 39, 37]. At temperature T which is much smaller

than the critical temperature T_c, a BEC could be described by the macroscopic wave function $\psi := \psi(\tilde{\mathbf{x}}, t)$, whose evolution is governed by a self-consistent, mean field nonlinear Schrödinger equation (NLSE) in a rotational frame, also known as the GPE with the angular momentum rotation term [21, 8, 34]:

$$\begin{cases} i\partial_t \psi = -\frac{1}{2}\nabla^2\psi + V_{hos}(\tilde{\mathbf{x}})\psi - \Omega L_{\tilde{z}}\psi + \beta|\psi|^2\psi, \\ \\ \psi(\tilde{\mathbf{x}}, 0) = \psi^0(\tilde{\mathbf{x}}), \quad \tilde{\mathbf{x}} \in R^d, \ d = 2, 3. \end{cases} \tag{1.1}$$

Here, $\tilde{\mathbf{x}} = (\tilde{x}, \tilde{y})^T$ 2D and $\tilde{\mathbf{x}} = (\tilde{x}, \tilde{y}, \tilde{z})^T$ in 3D, is the Cartesian coordinate vector, and t is time, $\psi = \psi(\tilde{\mathbf{x}}, t)$ is the dimensionless wave function, $V_{hos}(\tilde{\mathbf{x}})$ is the dimensionless homogeneous external trapping potential, which is often harmonic and thus can be written as $\frac{1}{2}(\gamma_x^2\tilde{x}^2 + \gamma_y^2\tilde{y}^2)$ in 2D, and resp., $V_{hos}(\tilde{\mathbf{x}}) = \frac{1}{2}(\gamma_x^2\tilde{x}^2 + \gamma_y^2\tilde{y}^2 + \gamma_z^2\tilde{z}^2)$ in 3D, with $\gamma_x > 0, \gamma_y > 0$ and $\gamma_z > 0$. $L_{\tilde{z}} = -i(\tilde{x}\partial_y - \tilde{y}\partial_x) = iJ_{\tilde{z}}$ is the $z-$component of the angular momentum. Ω is the dimensionless angular momentum rotating speed. β is a constant characterizing the particle interactions. When $\Omega = 0$, (1.1) is the expression for single-component non-rotating BEC. The rotating two-component condensates are governed by the coupled GPEs [38, 40, 48, 58, 69]. The coupled GPEs for two-component BEC will be discussed in Chapter 3.

1.3 Existing numerical methods

To study the dynamics of BEC, it is essential to have an efficient and accurate numerical method to analyse the time-dependent GPE. In literature, many numerical methods have been proposed to study the dynamics of non-rotating single component BEC, which can be grouped into two types. One is finite difference method, such as explicit finite difference method [22], Crank-Nicolson finite difference method [66] and alternating direction method [71]. Generally, the accuracy can be second or fourth order in space. The other method is pseudo-spectral method, for example, Bao [13] has proposed a fourth-order time-splitting Fourier pseudo-spectral method (TSSP) and a fourth-order time-

splitting Laguerre-Hermite pseudo-spectral method (TSLH) [11], Adhikari et al. have proposed Runge-Kutta pseudospectral method [2, 59]. Researches have demonstrated that pseudospectral method is more accurate and stable than finite difference method. However, for a rotating BEC, due to the appearance of the angular rotating term, the above methods can no longer be applied directly. Limited numerical methods have been proposed to study the dynamics of rotating BEC, but they are usually low-order finite difference methods [4, 20, 19, 75, 18]. Some better performed methods were designed, for example, Bao et al. [8] has proposed a numerical method by decoupling the nonlinearity in the GPE and adopting the polar coordinates or cylindrical coordinates to make the angular rotating term constant. It is of spectral accuracy in transverse direction but of second or fourth-order accuracy in radial direction. Another leap-frog spectral method is proposed, which is of spectral accuracy in space and second-order accuracy in time [76]. However, it has a stability time constraint for time step [76].

For coupled-GPEs, there have also been quite a few existing numerical methods, such as finite difference method and pseudospectral method [6, 38, 25]. But for rotating coupled-GPEs, due to the rotational term, difficulties have been introduced as the case for single-component BEC.

1.4 Purpose of the study and structure of the thesis

Hence, it is of a strong interest to develop an accurate, stable and efficient numerical method. In this paper, we have proposed such a numerical method and studied the dynamics of the rotating BEC by using it. The key feature of the method is: By taking an orthogonal time-dependent Lagrangian transformation, the rotational term in GPE can be eliminated under the new rotating Lagrangian coordinate. We can therefore apply previous numerical methods proposed for non-rotating BEC on the transformed GPE. In this paper, we have studied the rotating single component BEC and rotating two-component BEC. We have applied a second-order time splitting method and spectral method in space, which

is very efficient and accurate. New forms of energy, angular momentum as well as center of mass for the transformed rotating BEC are defined and presented both analytically and numerically.

The paper is organized as follows: In Chapter 2, we analyse the rotating single component BEC. And in Chapter 3, we extend the numerical methods to two-component BEC. The two chapters follow the same structure. We first begin by presenting the dynamical laws of the BEC. We proceed to apply the orthogonal time dependent matrix transformation method and study the dynamics of the rotating BEC under the new Lagrangian coordinates, we redefined and studied the conservation of density and energy, as well as angular momentum conservation under certain conditions. Dynamical laws for condensate width and analytical solutions for center of mass are presented as well. We follow by presenting an efficient and accurate numerical method for the simulation of transformed rotating BEC. Numerical results after applying the numerical method are discussed in section 4, which include accuracy test, dynamical results and quantized vortex interaction. Finally, some conclusion and further study directions are drawn.

Chapter 2

Methods and analysis for rotating BEC

In this chapter, we study the dynamics of rotating single-component Bose-Einstein condensation (BEC) based on the Gross-Pitaevskii equation (GPE) with an angular momentum rotational term. We first begin by reviewing the dynamical laws of the BEC according to previous researches. We follow by taking a rotating Lagrangian coordinate which as a result, removes the angular rotational term in the GPE. We proceed to redefine and study the dynamical laws of the BEC under the new coordinate system, such as density, energy, angular momentum expectation, condensate width and center of mass. Finally, an accurate and efficient numerical method is demonstrated and various numerical results have been presented.

2.1 Dynamical laws in the Cartesian coordinate

There have been many researches done to study the dynamics of rotating BEC [76, 8], we present a brief review of the dynamical laws of rotating BEC in the Cartesian coordinate.

I). Energy and density.

There are two important invariants: density and energy and they are defined as

follows:

$$N(\psi) = \int_{\mathbb{R}^d} |\psi(\tilde{\mathbf{x}}, t)|^2 \, \mathrm{d}\tilde{\mathbf{x}}, \quad t \geq 0, \tag{2.1}$$

$$E(\psi) = \int_{\mathbb{R}^d} \left[\frac{1}{2} |\nabla \psi|^2 + V_{hos}(\tilde{\mathbf{x}}, t) |\psi|^2 + \frac{\beta}{2} |\psi|^4 - \Omega \psi^* L_{\tilde{z}} \psi \right] \mathrm{d}\tilde{\mathbf{x}}, \tag{2.2}$$

where ψ^* denotes the complex conjugate of ψ.

II). Angular momentum expectation.

Angular momentum expectation is defined as:

$$\langle L_{\tilde{z}} \rangle (t) := \int_{\mathbb{R}^d} \psi^* L_{\tilde{z}} \psi \, \mathrm{d}\tilde{\mathbf{x}}, \quad t \geq 0, \quad d = 2, 3. \tag{2.3}$$

Theorem 2.1.1.

$$\frac{d \langle L_{\tilde{z}} \rangle (t)}{dt} = \frac{\gamma_x^2 - \gamma_y^2}{2} \tilde{\eta}(t), \tag{2.4}$$

with

$$\tilde{\eta}(t) := \int_{R^2} \tilde{x} \tilde{y} |\psi(\tilde{\boldsymbol{x}}, t)|^2 \, \mathrm{d}\tilde{\boldsymbol{x}}. \tag{2.5}$$

Thus, we have the conservation of angular momentum expectation and energy for the non-rotating part, at least in the following cases:

(i): For any given initial data, if we have $\gamma_x = \gamma_y$, i.e. the trapping potential is radially symmetric.

(ii): For any given γ_x, γ_y, if we have $\Omega = 0$ and the initial data ψ^0 is even in either x or y.

III). Condensate width

We define the condensate width as follows along the α-axis ($\alpha = x, y, z$ for 3D), to quantify the dynamics of the problem (2.13):

$$\langle \delta_\alpha \rangle (t) = \sqrt{\delta_\alpha(t)}, \text{ with } \delta_\alpha = \langle \alpha^2 \rangle (t) = \int_{\mathbb{R}^d} \alpha^2 |\psi|^2 \, \mathrm{d}\tilde{\mathbf{x}}, \ \alpha = \tilde{x}, \tilde{y}, \tilde{z}. \tag{2.6}$$

We have the following dynamical law for the condensate width:

Theorem 2.1.2. *i) Generally, for d=2,3, with any potential and initial data,*

the condensate width satisfies:

$$\frac{d^2\delta_\alpha(t)}{d^2t} = \int_{\mathbb{R}^d}\Big[(\partial_{\tilde{y}}\alpha-\partial_{\tilde{x}}\alpha)(4i\Omega\psi^*(\tilde{x}\partial_{\tilde{y}}+\tilde{y}\partial_{\tilde{x}})\psi+2\Omega^2(\tilde{x}^2-\tilde{y}^2)|\psi|^2) +2|\partial_\alpha\psi|^2+\beta|\psi|^4-2\alpha|\psi|^2\partial_\alpha V_{hos}\Big]\,\mathrm{d}\tilde{\boldsymbol{x}},$$

with

$$\delta_\alpha(0)=:\delta_\alpha^{(0)}=\int_{\mathbb{R}^d}\alpha^2|\psi^0|^2\,\mathrm{d}\tilde{\boldsymbol{x}},$$

$$\dot{\delta}_\alpha(0)=:\delta_\alpha^{(1)}=2\int_{\mathbb{R}^d}\alpha\,\big[\ Im((\psi^0)^*\partial_\alpha\psi^0)-\Omega|\psi^0|^2(\tilde{x}\partial_{\tilde{y}}-\tilde{y}\partial_{\tilde{x}})\alpha\big]\,\mathrm{d}\tilde{\boldsymbol{x}}.$$

ii) In 2D with a radially symmetric trap, i.e. $d=2,\gamma_x=\gamma_y:=\gamma_r$, *we have*

$$\begin{cases}\delta_r(t)=\frac{E(\psi_0)+\Omega\langle L_{\tilde{z}}\rangle(0)}{\gamma_r^2}\left[1-\cos(2\gamma_r t)\right]+\delta_r^{(0)}\cos(2\gamma_r t)+\frac{\delta_r^{(1)}}{2\gamma_r}\sin(2\gamma_r t),\\ \delta_r(0)=:\delta_r^{(0)}=\delta_{\tilde{x}}(0)+\delta_{\tilde{y}}(0)=\int_{\mathbb{R}^d}(\tilde{x}^2+\tilde{y}^2)|\psi^0|^2\,\mathrm{d}\tilde{\boldsymbol{x}},\\ \dot{\delta}_r(0)=:\delta_r^{(1)}=\dot{\delta}_{\tilde{x}}(0)+\dot{\delta}_{\tilde{y}}(0).\end{cases}\tag{2.7}$$

Moreover, if $\psi_0(\tilde{\boldsymbol{x}})=f(r)e^{im\theta}$, *with* $m\in\boldsymbol{Z}$ *and* $f(0)=0$ *when* $m\neq 0$, *we have, for any* $t\geq 0$,

$$\delta_{\tilde{x}}(t)=\delta_{\tilde{y}}(t)=\frac{1}{2}\delta_r(t)=\frac{E(\psi_0)+m\Omega}{2\gamma_x^2}\left[1-\cos(2\gamma_x t)\right]+\delta_{\tilde{x}}^{(0)}\cos(2\gamma_x t)+\frac{\delta_{\tilde{x}}^{(1)}}{2\gamma_x}\sin(2\gamma_x t).\tag{2.8}$$

iii) For all other cases, we have , for $t\geq 0$,

$$\delta_\alpha(t)=\frac{E(\psi_0)+\Omega\left\langle L_z\right\rangle(0)}{\gamma_\alpha^2}\left[1-\cos(2\gamma_\alpha t)\right]+\delta_\alpha^{(0)}\cos(2\gamma_\alpha t)+\frac{\delta_\alpha^{(1)}}{2\gamma_\alpha}\sin(2\gamma_\alpha t)+f_\alpha(t),\tag{2.9}$$

where $\tilde{f}_\alpha(t)$ *is the solution of the following equations:*

$$\frac{d^2\tilde{f}_\alpha(t)}{d^2t}+4\gamma_\alpha^2\tilde{f}_\alpha(t)=\tilde{F}_\alpha(t),\quad \tilde{f}_\alpha(0)=\frac{d\tilde{f}_\alpha(0)}{dt}=0,$$

with

$$\begin{aligned}\tilde{F}_\alpha(t) \;:=\; \int_{\mathbb{R}^d}\Big[&2(|\partial_\alpha\psi|^2-|\nabla\psi|^2)-\beta|\psi|^4+(2\gamma_\alpha^2\alpha^2-4V_{hos})|\psi|^2+4\Omega\,\langle L_{\tilde{z}}\rangle\,(t)\\&+(\partial_y\alpha-\partial_x\alpha)\left(4i\Omega\psi^*(\tilde{x}\partial_y+\tilde{y}\partial_x)\psi+2\Omega^2(\tilde{x}^2-\tilde{y}^2)|\psi|^2\right)\Big]\,\mathrm{d}\tilde{\boldsymbol{x}}.\end{aligned}$$

IV). Center of mass.

The center of mass is defined as follows:

$$\langle\tilde{\mathbf{x}}\rangle\,(t)=\int_{\mathbb{R}^d}\tilde{\mathbf{x}}|\psi|^2\,\mathrm{d}\tilde{\mathbf{x}}=:(\tilde{x}_c(t),\tilde{y}_c(t),\tilde{z}_c(t))^T. \tag{2.10}$$

By [8], the center of mass satisfies a 2nd order ODE and can be solved analytically.

2.2 GPE under a rotating Lagrangian coordinate

Since the rotational term L_z is the key 'bottle-neck' when one derives a numerical method, we now take an orthogonal rotational transformation for (1.1) in spatial space to deduce this rotational term and waive the difficulty. Denote the orthogonal rotational matrix as follows:

$$A(t):=\begin{bmatrix}\cos(\Omega t) & -\sin(\Omega t)\\ \sin(\Omega t) & \cos(\Omega t)\end{bmatrix}, \tag{2.11}$$

if $d=2$, and

$$A(t):=\begin{bmatrix}\cos(\Omega t) & -\sin(\Omega t) & 0\\ \sin(\Omega t) & \cos(\Omega t) & 0\\ 0 & 0 & 1\end{bmatrix}, \tag{2.12}$$

if $d=3$.

Take transformation $\mathbf{x}=A(t)\tilde{\mathbf{x}}$, $\phi(\mathbf{x},t)=\psi(A(t)\tilde{\mathbf{x}},t)$, and we substitute them into (1.1). We notice that

$$L_{\tilde{z}}\psi=L_z\phi,\;\; i\partial_t\psi=i\partial_t\phi+\Omega L_z\phi,$$

we can therefore cancel the rotational term in (1.1) and instead solve the following problem:

$$\begin{cases} i\partial_t\phi = -\frac{1}{2}\nabla^2\phi + V(\mathbf{x},t)\phi + \beta|\phi|^2\phi, \\ \phi(\mathbf{x},0) = \phi^0(\mathbf{x}), \quad \mathbf{x}\in R^d,\ d=2,3, \end{cases} \tag{2.13}$$

where

$$V(\mathbf{x},t) := V_{rot}(\mathbf{x}.t) + V_{hos}(\mathbf{x}), \tag{2.14}$$

with

$$\begin{aligned} V_{rot}(\mathbf{x}.t) &:= \frac{(\gamma_x^2-\gamma_y^2)\left[\sin^2(\Omega t)(y^2-x^2)+\sin(2\Omega t)xy\right]}{2}, \\ V_{hos}(\mathbf{x}) &:= \begin{cases} \frac{\gamma_x^2x^2+\gamma_y^2y^2}{2} & d=2, \\ \frac{\gamma_x^2x^2+\gamma_y^2y^2+\gamma_z^2z^2}{2} & d=3. \end{cases} \end{aligned}$$

2.3 Dynamical laws in the Lagrangian coordinate

In this section, we provide some analytical results on the definition and the dynamical laws of the following quantities for the inhomogeneous GPE (2.13): energy, density, angular momentum expectation, condensate width and the center of mass.

I). Energy and density.

We introduce two important invariants of (2.13), which are the normalization of the wave function:

$$N(\phi) = \int_{\mathbb{R}^d} |\phi(\mathbf{x},t)|^2\,\mathrm{d}\mathbf{x}, \quad t\geq 0, \tag{2.15}$$

and the energy

$$E(\phi) := E_1(\phi) + E_{rot}(\phi), \quad t\geq 0, \tag{2.16}$$

where

$$\begin{aligned} E_1(\phi) &:= \int_{\mathbb{R}^d}\left[\frac{1}{2}|\nabla\phi(\mathbf{x},t)|^2 + V(\mathbf{x},t)|\phi(\mathbf{x},t)|^2 + \frac{\beta}{2}|\phi(\mathbf{x},t)|^4\right]\mathrm{d}\mathbf{x}, \quad (2.17) \\ E_{rot}(\phi) &:= -\int_{\mathbb{R}^d}\int_0^t \partial_s V(\mathbf{x},s)|\phi(\mathbf{x},s)|^2 ds\,\mathrm{d}\mathbf{x}. \quad (2.18) \end{aligned}$$

We have the following theorem for the conservation of energy and density:

Theorem 2.3.1. *Conservation law for the energy and density:*

$$\frac{dN(\phi)}{dt} = \frac{dE(\phi)}{dt} = 0.$$

Proof. Following the properties of the GPE under a rotating Lagrangian coordinate, we have:

$$N(\phi) = \int |\phi(\mathbf{x})|^2 \, \mathrm{d}\mathbf{x} = \int |\psi(\tilde{\mathbf{x}})|^2 det(A) \, \mathrm{d}\tilde{\mathbf{x}} = N(\psi). \tag{2.19}$$

Conservation of $N(\phi)$ follows directly from the conservation of $N(\psi)$. We begin with the equation (2.13) to show the energy conservation. Starting from

$$i\partial_t \phi = -\frac{1}{2}\nabla^2 \phi + V(\mathbf{x}, t)\phi + \beta|\phi|^2\phi, \tag{2.20}$$

we have:

$$\begin{cases} i\partial_t\phi\partial_t\phi^* = \left(-\frac{1}{2}\nabla^2\phi + V(\mathbf{x},t)\phi + \beta|\phi|^2\phi\right)\partial_t\phi^*, \\ -i\partial_t\phi^*\partial_t\phi = \left(-\frac{1}{2}\nabla^2\phi^* + V(\mathbf{x},t)\phi^* + \beta|\phi|^2\phi^*\right)\partial_t\phi. \end{cases} \tag{2.21}$$

Sum the two equations in (2.21) together, we obtain

$$\begin{aligned} 0 &= -\frac{1}{2}\int_{\mathbb{R}^d} (\nabla^2\phi\partial_t\phi^* + \nabla^2\phi^*\partial_t\phi)\, \mathrm{d}\mathbf{x} + \int_{\mathbb{R}^d} V(\mathbf{x},t)\partial_t|\phi|^2 \, \mathrm{d}\mathbf{x} + \frac{1}{2}\partial_t \int_{\mathbb{R}^d} \beta|\phi|^4 \, \mathrm{d}\mathbf{x} \\ &= \partial_t\left[\frac{1}{2}\int_{\mathbb{R}^d} |\nabla\phi|^2 \, \mathrm{d}\mathbf{x} + \frac{\beta}{2}\int_{\mathbb{R}^d} |\phi|^4 \, \mathrm{d}\mathbf{x}\right] + \partial_t \int_{\mathbb{R}^d} V(\mathbf{x},t)|\phi|^2 \, \mathrm{d}\mathbf{x} - \int_{\mathbb{R}^d} \partial_t V(\mathbf{x},t)|\phi|^2 \, \mathrm{d}\mathbf{x} \\ &= \partial_t \int_{\mathbb{R}^d} \left[\frac{1}{2}|\nabla\phi(x,t)|^2 + V(x,t)|\phi(x,t)|^2 + \frac{\beta}{2}|\phi(x,t)|^4 - \int_0^t \partial_s V(x,s)|\phi(x,s)|^2 ds\right] \mathrm{d}\mathbf{x} \\ &= \frac{dE(\phi)}{dt}. \end{aligned}$$

Hence we have the energy conservation law as stated above. □

II). Angular momentum expectation.

Angular momentum is another important quantity to study the dynamics of

rotating BEC. It is a measure of the vortex flux and is defined as follows:

$$\langle L_z \rangle (t) = \int_{\mathbb{R}^d} \phi^* L_z \phi \, \mathrm{d}\mathbf{x}, \quad t \geq 0, \quad d = 2, 3. \tag{2.22}$$

For this quantity, we have the following dynamical law:

Theorem 2.3.2.

$$\frac{d \langle L_z \rangle (t)}{dt} = \int_{\mathbb{R}^d} |\phi|^2 J_z V \, \mathrm{d}\boldsymbol{x} = \int_{\mathbb{R}^d} |\phi|^2 \partial_t V \, \mathrm{d}\boldsymbol{x} = \frac{\gamma_x^2 - \gamma_y^2}{2} \, \eta(t), \tag{2.23}$$

where J_z and $\eta(t)$ are respectively defined as:

$$J_z = y\partial_x - x\partial_y = -iL_z, \tag{2.24}$$

$$\eta(t) = \int_{R^2} \left[2\cos(2\Omega t)xy + (y^2 - x^2)\sin(2\Omega t) \right] |\phi(\boldsymbol{x}, t)|^2 \, \mathrm{d}\boldsymbol{x}, \tag{2.25}$$

for $t \geq 0$. Hence, the energy can be rewritten in another equivalent form:

$$E(\phi) = \int_{\mathbb{R}^d} \left[\frac{1}{2} |\nabla \phi|^2 + V(\boldsymbol{x}, t)|\phi|^2 + \frac{\beta}{2} |\phi|^4 \right] \mathrm{d}\boldsymbol{x} - \Omega \langle L_z \rangle (t). \tag{2.26}$$

Thus, we have the conservation of angular momentum expectation, at least in the following cases:

(i): For any given initial data, if we have $\gamma_x = \gamma_y$, i.e. the trapping potential is radially symmetric;

(ii): For any given γ_x, γ_y, if we have $\Omega = 0$ and the initial data ϕ^0 is even in either x or y.

We have the following conservation laws

$$\langle L_z \rangle (t) = \langle L_z \rangle (0), \qquad E_1(\phi(\boldsymbol{x}, t)) = E_1(\phi^0),$$

where, E_1 is defined in (2.17).

Proof. Differentiating (2.22) with respect to t, noticing (2.13), integrating by

parts, and taking into account that ϕ decreases to 0 when $|\mathbf{x}| \to \infty$, we have

$$\begin{aligned}
\frac{d\langle L_z\rangle(t)}{dt} &= \int_{\mathbb{R}^d} (\phi_t^* L_z\phi + \phi^* L_z\phi_t)\,\mathrm{d}\mathbf{x} \\
&= \int_{\mathbb{R}^d} [-(i\phi_t)^* J_z\phi + \phi^* J_z(i\phi_t)]\,\mathrm{d}\mathbf{x} \\
&= -\int_{\mathbb{R}^d} \left[\left(-\frac{1}{2}\nabla^2\phi + V(\mathbf{x},t)\phi + \beta|\phi|^2\phi\right) J_z\phi^* \right. \\
&\quad \left. + \left(-\frac{1}{2}\nabla^2\phi^* + V(\mathbf{x},t)\phi^* + \beta|\phi|^2\phi^*\right) J_z\phi \right] \mathrm{d}\mathbf{x} \\
&= \frac{1}{2}\int_{\mathbb{R}^d} \left[\nabla^2\phi J_z\phi^* + \nabla^2\phi^* J_z\phi\right]\,\mathrm{d}\mathbf{x} - \int_{\mathbb{R}^d} V(\mathbf{x},t)(\phi J_z\phi^* + \phi^* J_z\phi)\,\mathrm{d}\mathbf{x} \\
&\quad + \frac{\beta}{2}\int_{\mathbb{R}^d} J_z|\phi|^4\,\mathrm{d}\mathbf{x} \\
&= -\frac{1}{2}\int_{\mathbb{R}^d} [\nabla\phi\nabla(J_z\phi^*)]\,\mathrm{d}\mathbf{x} - \frac{1}{2}\int_{\mathbb{R}^d} [\nabla\phi^*\nabla(J_z\phi)]\,\mathrm{d}\mathbf{x} \\
&\quad - \int_{\mathbb{R}^d} V(\mathbf{x},t)\phi J_z\phi^*\,\mathrm{d}\mathbf{x} + \int_{\mathbb{R}^d} \phi\,[V(\mathbf{x},t)J_z\phi^* + \phi^* J_z V(\mathbf{x},t)]\,\mathrm{d}\mathbf{x} \\
&= \frac{\gamma_x^2 - \gamma_y^2}{2}\,\eta(t),
\end{aligned}$$

with $\eta(t)$ defined in (2.25).

For case (i), when $\gamma_x = \gamma_y$, we could easily arrive at the conclusion that the angular momentum expectation $\langle L_z\rangle$ is conserved from the ODE:

$$\frac{d\langle L_z\rangle(t)}{dt} = 0, \quad t \geq 0.$$

For case (ii), we know that the solution $\phi(\mathbf{x},t)$ is even in first variable x or second variable y due to the assumption of the initial data and symmetry of $V(\mathbf{x})$. Then when $\Omega = 0$, with $|\phi(\mathbf{x},t)|$ even in either x or y, we easily have the conservation of angular momentum.

Referring to (2.26), we have

$$\frac{dE_1(t)}{dt} = \frac{dE(t)}{dt} + \Omega\frac{d}{dt}\langle L_z\rangle(t) = 0. \tag{2.27}$$

□

III). Condensate width

We define the condensate width as follows along the α-axis ($\alpha = x, y, z$ for 3D), to quantify the dynamics of the problem (2.13):

$$\langle \delta_\alpha \rangle (t) = \sqrt{\delta_\alpha(t)}, \text{ with } \delta_\alpha = \langle \alpha^2 \rangle (t) = \int_{\mathbb{R}^d} \alpha^2 |\phi|^2 \, \mathrm{d}\mathbf{x}, \ \alpha = x, y, z, \tag{2.28}$$

we have the following dynamical law for the condensate width:

Theorem 2.3.3. *i) Generally, for d=2,3, and any potential and initial data, the condensate width satisfies:*

$$\begin{cases} \frac{d^2\delta_\alpha(t)}{d^2t} + 2\gamma_\alpha^2 \delta_\alpha(t) = \int_{\mathbb{R}^d} \left[2|\partial_\alpha \phi|^2 + \beta|\phi|^4 - 2\alpha|\phi|^2 \partial_\alpha V_{rot} \right] \mathrm{d}\boldsymbol{x}, \\ \delta_\alpha(0) =: \delta_\alpha^{(0)} = \int_{\mathbb{R}^d} \alpha^2 |\phi^0|^2 \, \mathrm{d}\boldsymbol{x}, \\ \dot{\delta}_\alpha(0) =: \delta_\alpha^{(1)} = 2 \int_{\mathbb{R}^d} \alpha \ Im((\phi^0)^* \partial_\alpha \phi^0) \, \mathrm{d}\boldsymbol{x}. \end{cases} \tag{2.29}$$

ii) In 2D with a radially symmetric trap, i.e. $d = 2, \gamma_x = \gamma_y := \gamma_r$, we have

$$\begin{cases} \delta_r(t) = \frac{E(\phi_0) + \Omega \langle L_z \rangle (0)}{\gamma_r^2} \left[1 - \cos(2\gamma_r t) \right] + \delta_r^{(0)} \cos(2\gamma_r t) + \frac{\delta_r^{(1)}}{2\gamma_r} \sin(2\gamma_r t), \\ \delta_r(0) =: \delta_r^{(0)} = \delta_x(0) + \delta_y(0) = \int_{\mathbb{R}^d} (x^2 + y^2) |\phi^0|^2 \, \mathrm{d}\boldsymbol{x}, \\ \dot{\delta}_r(0) =: \delta_r^{(1)} = \dot{\delta}_x(0) + \dot{\delta}_y(0). \end{cases} \tag{2.30}$$

Moreover, if the $\phi_0(\boldsymbol{x}) = f(r) e^{im\theta}$, with $m \in \boldsymbol{Z}$ and $f(0) = 0$ when $m \neq 0$, we have, for any $t \geq 0$,

$$\delta_x(t) = \delta_y(t) = \frac{1}{2}\delta_r(t) = \frac{E(\phi_0) + m\Omega}{2\gamma_x^2} \left[1 - \cos(2\gamma_x t) \right] + \delta_x^{(0)} \cos(2\gamma_x t) + \frac{\delta_x^{(1)}}{2\gamma_x} \sin(2\gamma_x t). \tag{2.31}$$

iii) For all other cases, we have , for $t \geq 0$,

$$\delta_\alpha(t) = \frac{E(\phi_0) + \Omega \langle L_z \rangle (0)}{\gamma_\alpha^2} \left[1 - \cos(2\gamma_\alpha t) \right] + \delta_\alpha^{(0)} \cos(2\gamma_\alpha t) + \frac{\delta_\alpha^{(1)}}{2\gamma_\alpha} \sin(2\gamma_\alpha t) + f_\alpha(t), \tag{2.32}$$

where $f_\alpha(t)$ is the solution of the following equations:

$$\frac{d^2 f_\alpha(t)}{d^2 t} + 4\gamma_\alpha^2 f_\alpha(t) = F_\alpha(t), \quad f_\alpha(0) = \frac{df_\alpha(0)}{dt} = 0,$$

with

$$F_\alpha(t) = \int_{\mathbb{R}^d} \left[2(|\partial_\alpha \phi|^2 - |\nabla \phi|^2) - (2\alpha \partial_\alpha V_{rot}(\boldsymbol{x}, t) - 4V(x,t))|\phi|^2 + 4\Omega \langle L_z \rangle (t)\right] \mathrm{d}\boldsymbol{x}.$$

Proof. i). Differentiate (2.28) directly with respect to t, noticing (2.13), integrate by parts, we have:

$$\begin{aligned}
\frac{d\delta_\alpha(t)}{dt} &= \frac{d}{dt}\int_{\mathbb{R}^d} \alpha^2 |\phi|^2 \,\mathrm{d}\mathbf{x} = \int_{\mathbb{R}^d} \alpha^2(\phi \partial_t \phi^* + \phi^* \partial_t \phi)\,\mathrm{d}\mathbf{x} \\
&= i\int_{\mathbb{R}^d} \alpha^2 \left[\phi(i\partial_t \phi)^* - \phi^*(i\partial_t \phi)\right] \mathrm{d}\mathbf{x} \\
&= \frac{i}{2}\int_{\mathbb{R}^d} \alpha^2 \left[\phi(i\partial_t \phi)^* - \phi^*(i\partial_t \phi)\right] \mathrm{d}\mathbf{x} \\
&= \frac{i}{2}\int_{\mathbb{R}^d} \left[\nabla\phi^*(\alpha^2 \nabla\phi + \phi\nabla\alpha^2) - \nabla\phi(\alpha^2\nabla\phi^* + \phi^*\nabla\alpha^2)\right] \mathrm{d}\mathbf{x} \\
&= i\int_{\mathbb{R}^d} \alpha(\phi\phi_\alpha^* - \phi^*\phi_\alpha)\,\mathrm{d}\mathbf{x}. \qquad (2.33)
\end{aligned}$$

And we differentiate (2.33) with respect to t:

$$\begin{aligned}
\frac{d^2\delta_\alpha(t)}{dt^2} &= i\int_{\mathbb{R}^d} \alpha(\phi_t\phi_\alpha^* + \phi\phi_{t\alpha}^* - \phi_t^*\phi_\alpha - \phi^*\phi_{t\alpha})\,\mathrm{d}\mathbf{x} \\
&= i\int_{\mathbb{R}^d} \alpha(\phi_t\phi_\alpha^* - \phi_t^*\phi_\alpha)\,\mathrm{d}\mathbf{x} - i\int_{\mathbb{R}^d} [\phi_t^*(\alpha\phi_\alpha + \phi) - \phi_t(\alpha\phi_\alpha^* + \phi^*)]\,\mathrm{d}\mathbf{x} \\
&= \int_{\mathbb{R}^d} \left[2|\partial_\alpha\phi|^2 + \beta|\phi|^4 - 2\alpha|\phi|^2\partial_\alpha V\right] \mathrm{d}\mathbf{x} \\
&= -2\gamma_\alpha^2\delta_\alpha(t) + \int_{\mathbb{R}^d} \left[2|\partial_\alpha\phi|^2 + \beta|\phi|^4 - 2\alpha|\phi|^2\partial_\alpha V_{rot}\right] \mathrm{d}\mathbf{x}.
\end{aligned}$$

(ii). If $d = 2$, we have:

$$\begin{cases} \frac{d^2\delta_x(t)}{d^2t} + 2\gamma_x^2\delta_x(t) = \int_{\mathbb{R}^d} \left[2|\partial_x\phi|^2 + \beta|\phi|^4 - 2x|\phi|^2\partial_x V_{rot}\right] \mathrm{d}\mathbf{x}, \\ \frac{d^2\delta_y(t)}{d^2t} + 2\gamma_y^2\delta_y(t) = \int_{\mathbb{R}^d} \left[2|\partial_y\phi|^2 + \beta|\phi|^4 - 2y|\phi|^2\partial_y V_{rot}\right] \mathrm{d}\mathbf{x}. \end{cases} \qquad (2.34)$$

Add (2.34) and with $\gamma_x = \gamma_y = \gamma_r$, we have the ODE for $\delta_r(t)$:

$$\begin{aligned}
\frac{d^2\delta_r(t)}{d^2t} &= -2\gamma_r^2\delta_r(t) + 4\int_{\mathbb{R}^d} \left[\frac{1}{2}|\nabla\phi|^2 + V(x,t)|\phi|^2 + \frac{\beta}{2}|\phi|^4 - \Omega\mathbf{Re}\langle L_z\rangle(t)\right] \mathrm{d}\mathbf{x} \\
&\quad -4\int_{\mathbb{R}^d} V(x,t)|\phi|^2\,\mathrm{d}\mathbf{x} + 4\Omega\langle L_z\rangle(t) - 2\int_{\mathbb{R}^d} (x\partial_x V_{rot} + y\partial_y V_{rot})|\phi|^2\,\mathrm{d}\mathbf{x}.
\end{aligned}$$

Noticing that when $\gamma_x = \gamma_y = \gamma_r$, we have:

$$\frac{d}{dt}E(\phi) = \frac{d}{dt}\langle L_z\rangle(t) = V_{rot} \equiv 0. \tag{2.35}$$

We substitute (2.35) and (2.27) into (2.35), and using the energy conservation law, we get:

$$\frac{d^2\delta_r(t)}{d^2t} = -4\gamma_r^2\delta_r(t) + 4E(\phi_0) + 4\Omega\langle L_z\rangle(0). \tag{2.36}$$

The initial condition now is:

$$\begin{cases} \delta_r(0) =: \delta_r^{(0)} = \delta_x(0) + \delta_y(0) = \int_{\mathbb{R}^d}(x^2+y^2)|\phi_0|^2\,\mathrm{d}\mathbf{x}, \\ \dot{\delta}_r(0) =: \delta_r^{(1)} = \dot{\delta}_x(0) + \dot{\delta}_y(0). \end{cases} \tag{2.37}$$

We solve the ODE (2.36) with the initial data given in (2.37), we could find the following unique solution:

$$\delta_r(t) = \frac{E(\phi_0) + \Omega\langle L_z\rangle(0)}{\gamma_r^2}[1-\cos(2\gamma_r t)] + \delta_r^{(0)}\cos(2\gamma_r t) + \frac{\delta_r^{(1)}}{2\gamma_r}\sin(2\gamma_r t). \tag{2.38}$$

In addition, if the initial data has radial symmetric structure:

$$\phi_0(\mathbf{x}, 0) = f(r)e^{im\theta},$$

with $m \in \mathbf{Z}$ and $f(0) = 0$ when $m \neq 0$, then, since $V(x,t) = V_{hos}$, which ensures the radial symmetric property of the solution $\phi(x,t)$ if the initial condition is assumed to be radially symmetric, we have, for any $t \geq 0$,

$$\begin{aligned} \delta_x(t) &= \int_{\mathbb{R}^d} x^2|\phi|^2\,\mathrm{d}\mathbf{x} = \int_0^\infty\int_0^{2\pi} r^2\cos^2\theta|f(r,t)|^2 r\,d\theta\,dr \\ &= \pi\int_0^\infty r^2|f(r,t)|^2 r\,dr = \int_0^\infty\int_0^{2\pi} r^2\sin^2\theta|f(r,t)|^2 r\,d\theta\,dr \\ &= \int_{\mathbb{R}^d} y^2|\phi|^2\,\mathrm{d}\mathbf{x} = \delta_y(t) = \frac{1}{2}\delta_r(t). \end{aligned}$$

Thus we could show the result above in (2.31).

(iii). In general, we take a similar approach as what we have done in (2.35) and

(2.36), by combining energy expression as in (2.27), we have:

$$\frac{d^2\delta_\alpha(t)}{d^2t} = -4\gamma_\alpha^2\delta_\alpha(t) + 4E(\phi_0) + f_\alpha(t), \tag{2.39}$$

where $f_\alpha(t)$ satisfying the 2nd-order ODE:

$$\frac{d^2 f_\alpha(t)}{d^2t} + 4\gamma_\alpha^2 f_\alpha(t) = F_\alpha(t), \quad f_\alpha = \frac{df_\alpha}{dt} = 0,$$

with

$$F_\alpha(t) = \int_{\mathbb{R}^d} \left[2(|\partial_\alpha\phi|^2 - |\nabla\phi|^2) - (2\alpha\partial_\alpha V_{rot}(\mathbf{x},t) - 4V(x,t))|\phi|^2 + 4\Omega\mathbf{Re}\left\langle L_z\right\rangle(t)\right] \mathrm{d}\mathbf{x}.$$

We solve the second-order ODE and could get a unique solution as defined in (2.32). □

IV). Center of mass.

In this section, we would like to study the analytical solutions for the center of mass. Denote ϕ as the solution of GPE, the center of mass is defined as:

$$\langle \mathbf{x}\rangle(t) = \int_{\mathbb{R}^d} \mathbf{x}|\phi|^2 \,\mathrm{d}\mathbf{x} =: (x_c(t), y_c(t), z_c(t))^T. \tag{2.40}$$

Then, for any given initial data, we have:

Lemma 2.3.4.

$$\begin{cases} \frac{d^2\langle \boldsymbol{x}\rangle(t)}{dt^2} + B(t)\langle \boldsymbol{x}\rangle(t) = 0, \\ \langle \boldsymbol{x}\rangle(0) = \boldsymbol{x}_0, \\ \dot{\langle \boldsymbol{x}\rangle}(0) = 0, \end{cases} \tag{2.41}$$

with $B(t) = A^T(t)\Lambda A(t)$, *where* $\Lambda = diag(\gamma_x, \gamma_y)$ *in 2-d and* $diag(\gamma_x, \gamma_y, \gamma_z)$ *in 3-d, i.e.*

$$B(t) = \frac{1}{2}\begin{bmatrix} \gamma_x^2+\gamma_y^2 & 0 \\ 0 & \gamma_x^2+\gamma_y^2 \end{bmatrix} + \frac{\gamma_x^2-\gamma_y^2}{2}\begin{bmatrix} \cos(2\Omega t) & \sin(2\Omega t) \\ \sin(2\Omega t) & -\cos(2\Omega t) \end{bmatrix}, \tag{2.42}$$

if $d = 2$, *and*

$$B(t) = \frac{1}{2}\begin{bmatrix} \gamma_x^2+\gamma_y^2 & 0 & 0 \\ 0 & \gamma_x^2+\gamma_y^2 & 0 \\ 0 & 0 & 2\gamma_z^2 \end{bmatrix} + \frac{\gamma_x^2-\gamma_y^2}{2}\begin{bmatrix} \cos(2\Omega t) & \sin(2\Omega t) & 0 \\ \sin(2\Omega t) & -\cos(2\Omega t) & 0 \\ 0 & 0 & 0 \end{bmatrix}, \tag{2.43}$$

for $d = 3$.

Proof. By differentiating (2.40) with respect to t, we have

$$\begin{aligned} \frac{d\langle \mathbf{x}\rangle(t)}{dt} &= \int_{\mathbb{R}^d} \mathbf{x}(\phi_t^*\phi + \phi^*\phi_t)\,\mathrm{d}\mathbf{x} = i\int_{\mathbb{R}^d} \mathbf{x}\left[(-i\phi_t^*)\phi - \phi^*(i\phi_t)\right]\,\mathrm{d}\mathbf{x} \\ &= i\int_{\mathbb{R}^d} \mathbf{x}\left[-\frac{1}{2}\nabla^2\phi^*\phi + \frac{1}{2}\nabla^2\phi\phi^*\right]\,\mathrm{d}\mathbf{x} = \frac{i}{2}\int_{\mathbb{R}^d}(\nabla\phi^*\phi - \nabla\phi\phi^*)\,\mathrm{d}\mathbf{x} \\ &= -i\int_{\mathbb{R}^d}\phi^*\nabla\phi\,\mathrm{d}\mathbf{x}. \end{aligned} \tag{2.44}$$

Furthermore, differentiate (2.44) with respect to t again, we get

$$\begin{aligned} \frac{d^2\langle \mathbf{x}\rangle(t)}{dt^2} &= -i\int_{\mathbb{R}^d}(\phi_t^*\nabla\phi + \phi^*\nabla\phi_t)\,\mathrm{d}\mathbf{x} = i\int_{\mathbb{R}^d}(\phi_t\nabla\phi^* - \phi_t^*\nabla\phi)\,\mathrm{d}\mathbf{x} \\ &= \int_{\mathbb{R}^d} V(\mathbf{x},t)\nabla|\phi|^2\,\mathrm{d}\mathbf{x} = -\int_{\mathbb{R}^d}\nabla V(\mathbf{x},t)|\phi|^2\,\mathrm{d}\mathbf{x}. \end{aligned}$$

Substitute the expression for $V(\mathbf{x},t)$ as in (2.14) and we define $B(t)$ as

$$B(t) := \nabla V(\mathbf{x},t).$$

which is stated explicitly in (2.42) for 2D and (2.43) for 3D. Hence we have

$$\frac{d^2\langle \mathbf{x}\rangle(t)}{d^2t} + B(t)\langle \mathbf{x}\rangle(t) = 0. \tag{2.45}$$

□

We proceed to solve the second-order ODE (2.41) and the analytical solutions are as follows:

Case I: $\gamma_x = \gamma_y = \gamma_r$ or $\Omega = 0$, we have $B(t) = \mathrm{diag}(\gamma_x^2, \gamma_y^2, \gamma_z^2)$, and the solution

should be of the form:

$$\alpha_c(t) = a_\alpha \cos(\gamma_\alpha t) + b_\alpha \sin(\gamma_\alpha t), \quad \alpha = x, y, z. \tag{2.46}$$

With the initial condition defined in (2.41), we have the explicit solution as:

$$\alpha_c(t) = \alpha_0 \cos(\gamma_\alpha t), \quad \alpha = x, y, z. \tag{2.47}$$

Case II: $\gamma_x \neq \gamma_y$ and $\Omega \neq 0$. Actually, if we take the inverse transformation

$$\mathbf{x} = A(t)\tilde{\mathbf{x}},$$

where we use $\mathbf{x}$ to represent the transformed variable and $\tilde{\mathbf{x}}$ the original one, which implies that

$$\langle \mathbf{x} \rangle (t) = A(t) \langle \tilde{\mathbf{x}} \rangle (t),$$

and plug into equation (2.41), we have

$$\frac{d^2}{d^2t} A(t) \langle \tilde{\mathbf{x}} \rangle (t) + 2\frac{d}{dt} A(t) \frac{d}{dt} \langle \tilde{\mathbf{x}} \rangle (t) + A(t) \frac{d^2}{d^2t} \langle \tilde{\mathbf{x}} \rangle (t) + A\Lambda \langle \tilde{\mathbf{x}} \rangle (t) = 0, \tag{2.48}$$

by noticing that $\frac{d^2}{d^2t} A(t) = -\Omega^2 \tilde{I}^2 A(t)$ with

$$\tilde{I} = I_2, \qquad \text{if} \quad \text{d=2}, \quad \text{and} \quad \tilde{I} = \begin{bmatrix} 1 & 0 & 0 \\ 0 & 1 & 0 \\ 0 & 0 & 0 \end{bmatrix}, \quad \text{if} \quad \text{d=3},$$

and

$$A(t)^T \frac{d}{dt} A(t) = \Omega \begin{bmatrix} 0 & -1 \\ 1 & 0 \end{bmatrix} =: C, \quad if \ d = 2,$$

$$A(t)^T \frac{d}{dt} A(t) = \Omega \begin{bmatrix} 0 & -1 & 0 \\ 1 & 0 & 0 \\ 0 & 0 & 0 \end{bmatrix} =: C, \quad if \ d = 3.$$

By multipling (2.48) to the orthogonal matrix $A(t)$, we have:

$$\frac{d^2}{d^2t}\left\langle \tilde{\mathbf{x}} \right\rangle (t) + 2\Omega C \frac{d}{dt}\left\langle \tilde{\mathbf{x}} \right\rangle (t) + (\Lambda - \Omega^2 \tilde{I})\left\langle \tilde{\mathbf{x}} \right\rangle (t) = 0,$$

which is now the orignial form of the dynamical law of the center mass of the original non-transformed equation. Now, we can solve equation (2.41) by the old method proposed in previous research [76] and take transformation back again. Different cases and their respected results will be presented in section 2.5.

2.4 Numerical methods

In this section, we present an accurate and efficient numerical method which solves the transformed rotating GPE under a rotating Lagrangian coordinate as shown in (2.13). Without loss of generality, we take $d = 2$.

Different from other studies to solve the rotating BEC, by introducing an orthogonal transformation, we have reduced the rotational term in the GPE. We finally have a standard GPE with inhomogeneous potential, which could be solved by standard numerical methods in a more stable way, compared to previous researches done in this area.

We begin by applying the time splitting method, and then proceed with Fourier spectral method in x and y direction.

2.4.1 Time splitting method

We take $\Delta t > 0$ as a time step. For $n = 0, 1, 2, \ldots, N$ from time $t = t_n = n\Delta t$ to $t = t_{n+1} = t_n + \Delta t$, we could solve the transformed GPE (2.13) in the following two steps:

Step I:

$$\begin{cases} i\partial_t \phi = -\frac{1}{2}\nabla^2 \phi, \\ \phi(\mathbf{x}, 0) = \phi^0(\mathbf{x}), \quad \mathbf{x} \in R^d, \ d = 2, 3. \end{cases} \tag{2.49}$$

Step II:

$$\begin{cases} i\partial_t\phi = V(\mathbf{x},t)\phi + \beta|\phi|^2\phi, \\ \phi(\mathbf{x},0) = \phi^0(\mathbf{x}), \quad \mathbf{x}\in R^d,\ d=2,3. \end{cases} \tag{2.50}$$

These two steps are solved for the same time step of length Δt. A point need to be noted that compared to the non-rotating BEC, the time step has not been much affected with a small Ω. For a very big Ω, a smaller time step is required to well capture the rotation. For step I (2.49), we will discuss in details in the following two subsections. Step II (2.50) can be solved analytically. We first demonstrate that the ODE is linear by showing:

$$\begin{aligned} \frac{d|\phi(\mathbf{x},t)|^2}{dt} &= (\phi_t^*\phi + \phi^*\phi_t) = -i\left[-(i\phi_t)^*\phi + \phi^*(i\phi_t)\right] \\ &= -i\Bigg[\left(-\frac{1}{2}\nabla^2\phi + V(\mathbf{x},t)\phi + \beta|\phi|^2\phi\right)\phi^* \\ &\quad -\phi\left(-\frac{1}{2}\nabla^2\phi^* + V(\mathbf{x},t)\phi^* + \beta|\phi|^2\phi^*\right)\Bigg] = 0. \end{aligned}$$

which gives us

$$|\phi(\mathbf{x},t)|^2 = |\phi(\mathbf{x},t_n)|^2, \quad t\in[t_n,t_{n+1}]. \tag{2.51}$$

Then solve the ODE in (2.50) directly which gives us:

$$\phi(\mathbf{x},t) = \exp\left[-i\left(\int_{t_n}^{t} V(\mathbf{x},s)ds + \beta|\phi(\mathbf{x},t_n)|^2\right)(t-t_n)\right]. \tag{2.52}$$

Take $d=2$ and substitute (2.14) in (2.52) and integrate, we have the exact analytical solution given by:

For $\gamma_x=\gamma_y=\gamma_r$,

$$\int_{t_n}^{t} V(\mathbf{x},s)ds = \frac{1}{2}\gamma_r^2(x^2+y^2)(t-t_n). \tag{2.53}$$

For $\gamma_x \neq \gamma_y$,

$$\int_{t_n}^{t} V(\mathbf{x},s)ds = \frac{1}{2}(\gamma_x^2 x^2 + \gamma_y^2 y^2)(t-t_n) + \frac{\gamma_x^2-\gamma_y^2}{4}\left[(y^2-x^2)\left(t-t_n - \frac{1}{2\Omega}(\sin 2\Omega t - \sin 2\Omega t_n)\right) + \frac{xy}{\Omega}(\cos 2\Omega t - \cos 2\Omega t_n)\right] \quad (2.54)$$

We can also apply numerical quadrature method, e.g. Simposon rule to approximate $\int_{t_n}^{t_{n+1}} V(\mathbf{x},s)ds$.

2.4.2 Discretization in 2D

We apply the Fourier spectral method to discretize (2.49). We suppose that $\phi(x,y,t)$ is defined in domain $[a,b]\times[c,d]$.

Let

$$\phi(x,y,t) = \sum_{l=-\frac{N_x}{2}}^{\frac{N_x}{2}-1}\sum_{k=-\frac{N_y}{2}}^{\frac{N_y}{2}-1} \hat{\phi}_{lk}(t) e^{i\mu_l^x(x-a)} e^{i\mu_k^y(y-c)}, \quad (2.55)$$

with

$$\mu_l^x = \frac{2\pi l}{b-a}, \quad \mu_k^y = \frac{2\pi k}{d-c},$$

$$l = -\frac{N_x}{2}, -\frac{N_x}{2}+1, \ldots, \frac{N_x}{2}-1, \quad k = -\frac{N_y}{2}, -\frac{N_y}{2}+1, \ldots, \frac{N_y}{2}-1.$$

$\hat{\phi}_{lk}(t)$ is the Fourier coefficient for the lth mode in x and kth mode in y.

Differentiate (2.55) with respect to t, and noticing the orthogonality of the Fourier functions, we obtain:

$$\partial_t \hat{\phi}_{lk}(t) = -\frac{i}{2}\left[(\mu_l^x)^2 + (\mu_k^y)^2\right]\hat{\phi}_{lk}(t),$$

which can be solved analytically to have

$$\hat{\phi}_{lk}(t) = e^{-\frac{i}{2}\left[(\mu_l^x)^2+(\mu_k^y)^2\right](t-t_n)}\hat{\phi}_{lk}(t_n),$$

for $t \in [t_n, t_{n+1}]$. Starting from t_n, $\phi(t_n)$ is known. We take a Fast Fourier Transform to obtain $\hat{\phi}_{lk}(t_n)$. And then by applying the above equation, we get $\hat{\phi}_{lk}(t_{n+1})$. We take an Inverse Fourier Transform to get $\hat{\phi}_{lk}(t_{n+1})$.

In practice, we often apply the second order Strang splitting [70, 76].

2.4.3 Discretization in 3D

When $d = 3$, for a defined domain $[a, b] \times [c, d] \times [e, f]$, we use a similar approach as what we have discussed above in (2.55). We take:

$$\phi(x, y, t) = \sum_{l=-\frac{N_x}{2}}^{\frac{N_x}{2}-1} \sum_{k=-\frac{N_y}{2}}^{\frac{N_y}{2}-1} \sum_{m=-\frac{N_z}{2}}^{\frac{N_z}{2}-1} \hat{\phi}_{lkm}(t) e^{i\mu_l^x (x-a)} e^{i\mu_k^y (y-c)} e^{i\mu_m^z (y-e)}, \tag{2.56}$$

with

$$\mu_l^x = \frac{2\pi l}{b-a}, \quad \mu_k^y = \frac{2\pi k}{d-c}, \quad \mu_m^z = \frac{2\pi m}{f-e},$$

$$l = -\frac{N_x}{2}, -\frac{N_x}{2}+1, \ldots, \frac{N_x}{2}-1, \quad k = -\frac{N_y}{2}, -\frac{N_y}{2}+1, \ldots, \frac{N_y}{2}-1,$$

$$m = -\frac{N_z}{2}, -\frac{N_z}{2}+1, \ldots, \frac{N_z}{2}-1,$$

here, $\hat{\phi}_{lkm}(t)$ is the Fourier coefficient for the lth mode in x, kth mode in y and mth mode in z.

2.5 Numerical results

Without loss of generality, we have taken $d = 2$ for numerical computations. The 3D case is quite similar. In this section, we first test the numerical accuracy of the method proposed in section 2. Then we proceed to study the dynamics of the quantities discussed above, by choosing a gaussian initial data $\phi_0(\mathbf{x})$ which is a stationary state with its center shifted. We will look at the conservation of energy and density, as well as the dynamical laws of angular momentum expectation, condensate width. For center of mass, we will compare the numerical solutions with the exact analytical solutions that we obtained by solving related ODE. We will also discuss the interaction between a few central vortices by looking at their trajectories.

2.5.1 Accuracy test

In this subsection, we will present the numerical results obtained to show a spectral accuracy in space and second order accuracy in time. To this end, we take the initial data as:

$$\phi_0(x,y) = \frac{(\gamma_x\gamma_y)^{1/4}}{(\pi)^{1/2}} e^{-\frac{\gamma_x(x-x_0)^2+\gamma_y(y-y_0)^2}{2}}. \tag{2.57}$$

We take $\gamma_x = 1, \gamma_y = 2, \Omega = 1$, and solve on the interval $[-16,16]\times[-16,16]$ with homogeneous Dirichlet boundary condition. Our numerical solution is computed using TSSP2 with a very fine mesh, e.g $h := dx = dy = \frac{1}{32}$, and a small time step $k := dt = 0.0001$. As we treat it as the 'exact' solution, denoted by $\phi_e(t)$. And we use $\phi^{h,k}(t)$ to represent the numerical solution obtained with mesh size h and time step k.

First, we test the spectral accuracy of TSSP2 in space. We have three different β, and for each one, we solve the numerical solution with a very small time step $k = 0.0001$ and different mesh sizes h, as shown in Table 2.1. Since the time step is chosen as small as our 'exact' solution, we could neglige the truncation error resulted from time discretization compared to space discretization.

Then we use a similar approach to test the time accuracy, as in Table 2.2. In

Table 2.1: Spatial error analysis: Error $||\phi_e(t) - \phi^{h,k}(t)||_{l^2}$ at $t = 2.0$ with $k = 1E-4$.

Mesh	h=1/2	h=1/4	h=1/8	h=1/16
$\beta = 10$	1.114E-2	9.932E-7	9.6613E-13	<E-13
$\beta = 20\sqrt{2}$	0.236	5.371E-4	6.903E-10	<E-13
$\beta = 80$	1.894	6.528E-2	2.556E-5	2.362E-12

a strong repulsive interaction regime or semi-classical regime, where $\beta \gg 1$, we are interested to find how to choose the "correct" mesh size h and time step $\triangle t$. After a rescaling of equation (2.13) under normalization, we get:

$$i\epsilon\partial_t\phi(\mathbf{x},t) = -\frac{\epsilon^2}{2}\nabla^2\phi + V_d(\mathbf{x},t)\phi + |\phi|^2\phi, \quad \mathbf{x}\in\mathbb{R}^d, \tag{2.58}$$

Table 2.2: Temporal error analysis: Error $||\phi_e(t) - \phi^{h,k}(t)||_{l^2}$ at $t = 2.0$ with $h = 1/32$.

Time step	k=1/20	k=1/40	k=1/80	k=1/160	k=1/320
$\beta = 10$	1.002E-3	2.582E-4	5.661E-5	1.153E-5	3.528E-6
$\beta = 20\sqrt{2}$	4.132E-3	1.341E-3	3.513E-4	9.382E-5	2.496E-5
$\beta = 80$	2.154E-2	5.381E-3	1.463E-3	3.652E-4	9.563E-5

with $\mathbf{x} \to \epsilon^{-1/2}\mathbf{x}$, $\phi \to \epsilon^{d/4}.\phi$, $\epsilon = \beta_d^{-2/(d+2)}$.

As also demonstrated in [8, 9, 10], the suitable meshing strategy which best approximates the "correct" solution should be:

$$h = O(\epsilon), \quad k = O(\epsilon).$$

Thus for a strong repulsive interaction, we take:

$$h = O(\epsilon) = O(1/\beta_d^{2/(d+2)}), \quad k = O(\epsilon) = O(1/\beta_d^{2/(d+2)}), \quad with\ d = 2, 3.$$

2.5.2 Dynamical results in 2D

To verify the analytical solutions obtained in section II like the density and mass conservation, and to study the dynamical laws of a rotating BEC under a Lagrangian coordinate, we take a Gaussian initial condition as stated in (2.57).

(I). Dynamics of density and energy

As defined in (2.16), the energy is expressed as:

$$\begin{aligned} E(\phi) &= \int_{\mathbb{R}^d} \left[\frac{1}{2}|\nabla\phi(x,t)|^2 + V(x,t)|\phi(x,t)|^2 + \frac{\beta}{2}|\phi(x,t)|^4 \right. \qquad (2.59) \\ &\quad \left. - \int_0^t \partial_s V(x,s)|\phi(x,s)|^2 ds \right] \mathrm{d}\mathbf{x} \\ &:= E_k(\phi) + E_{int}(\phi) + E_p(\phi) + E_{rot}(\phi), \qquad (2.60) \end{aligned}$$

where $E_k(\phi)$ is the kinetic energy, $E_{int}(\phi)$ stands for interaction energy, $E_p(\phi)$ is the potential energy and $E_{rot}(\phi)$ is the rotating energy.

We have energy and density conservation for any given initial state as discussed

above. We take $\beta = 10,\ T = 10,\ x_0 = y_0 = 1$. We have listed four cases as follows with different Ω and γ_x, γ_y: As we could see, in all the four cases, and also the other examples that we have not listed here, the energy and density are well conserved.

And when $\Omega = 0$ or $\gamma_x = \gamma_y$, as shown in Figure 2.1, Figure 2.2 and Figure 2.3, the rotating energy equals zero. This could be explained by our analytical results in (2.53), (2.54) and (2.16). By comparing Figure 2.1 and Figure 2.2 which are different by the value of γ_y, we could see that the period becomes smaller with an increasing γ_y. The same follows when we change γ_x.

(II). Dynamics of condensate width and angular momentum

We solve the problem on the domain $[-10, 10] \times [-10, 10]$ under a mesh size $h = 1/8$ and time step 0.001, with homogeneous Dirichlet boundary condition and initial condition defined in (2.57). We take $\beta = 100$ and $T = 10$, set different values for $\Omega, \gamma_x, \gamma_y$ and the starting point $x_0,\ y_0$ to show the dynamical laws of condensate width and angular momentum.

As discussed in Theorem 2.3.2, under the rotating Lagrangian coordinate, we have the angular momentum conservation law in two cases:

(i) $\gamma_x = \gamma_y$, for any initial data and Ω given. This is shown in Figure 2.5, where $\Omega = 1, \gamma_x = \gamma_y = 1, x_0 = 1, y_0 = 1$.

(ii) $\Omega = 0$ and the initial data $\phi_0(t)$ is symmetric in either x or y direction. We could find that in Figure 2.7, where $\Omega = 0, \gamma_x = 1, \gamma_y = 2, x_0 = 0, y_0 = 1$, initial data is symmetric in x direction, the angular momentum is conserved. To compare, Figure 2.8 has almost the same quantities except that $x_0 = 1, y_0 = 1$, where the initial data does not have any symmetric property, and the angular momentum is not conserved in this case. And in Figure 2.6, where $\Omega = 1, \gamma_x = 1, \gamma_y = 2, x_0 = 0, y_0 = 1$, we have a symmetric initial data but with a nonzero Ω, the angular momentum is not conserved.

For condensate width, as we have discussed in Theorem 2.3.3, when $\gamma_x = \gamma_y = \gamma_r$, δ_x and δ_y are periodic with period $T = \frac{2\pi}{\delta_r}$. This is shown in Figure 2.5. For other Figures, although the condensate width are not periodic, due to $\gamma_y = 2\gamma_x$, the oscillation frequency for δ_y is roughly double that of δ_x, and the amplitudes

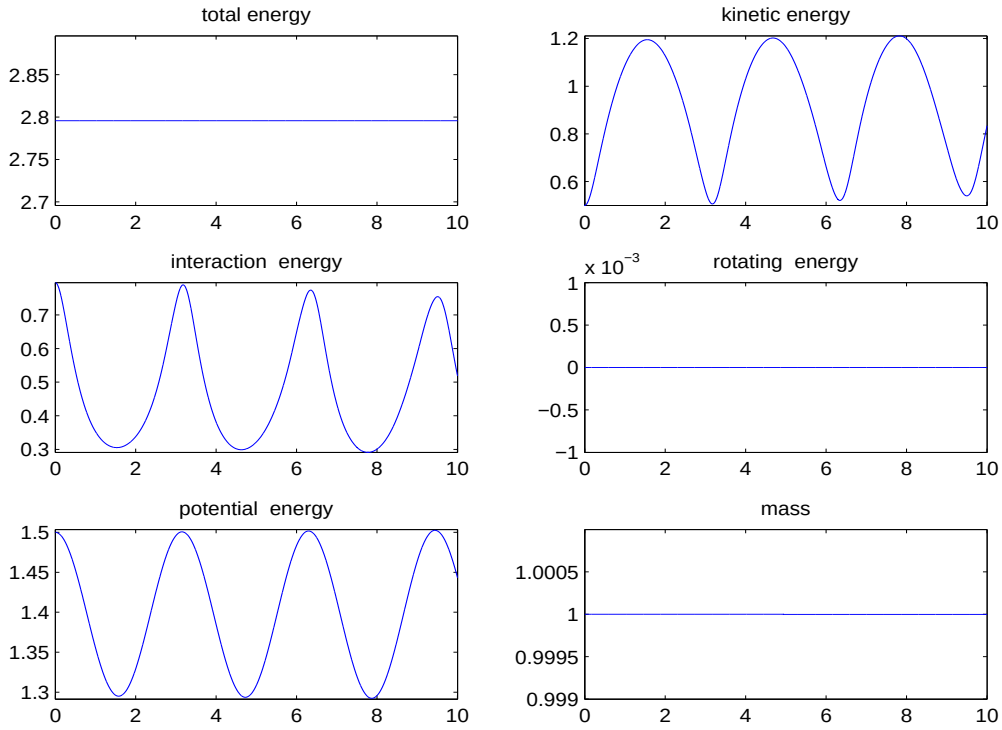

Figure 2.1: Dynamics of mass and energies under $\Omega = 0, \gamma_x = \gamma_y = 1$.

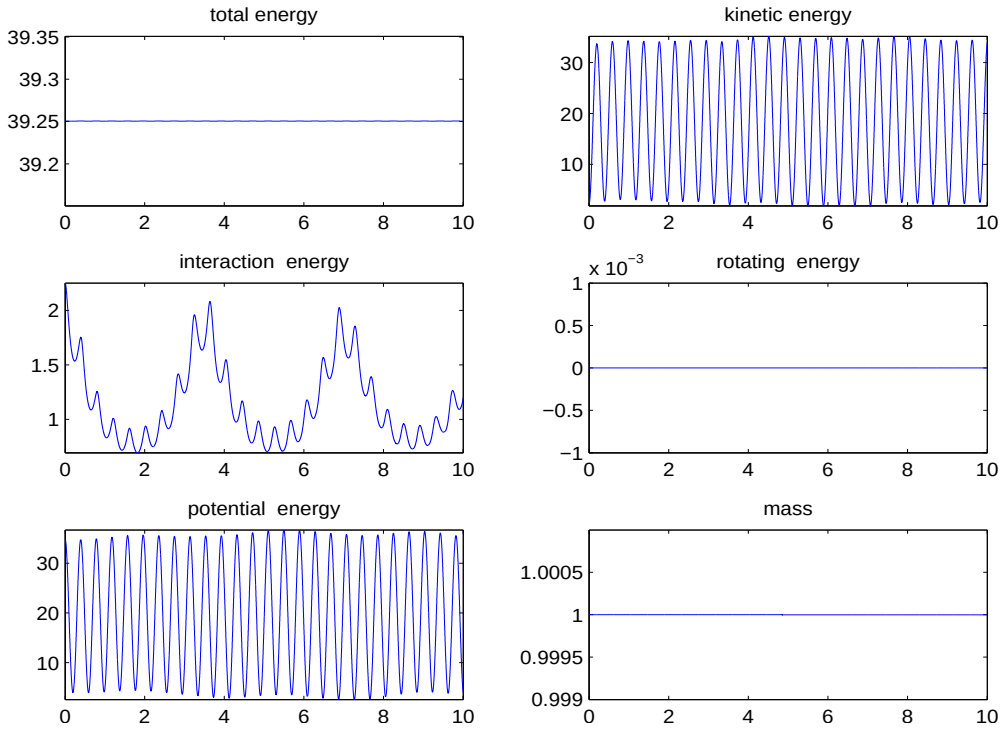

Figure 2.2: Dynamics of mass and energies under $\Omega = 0, \gamma_x = 1, \gamma_y = 8$.

of δ_x are in general larger than that of δ_y (cf. Fig. 2.7).

(III). Center of mass under new coordinate and original coordinate

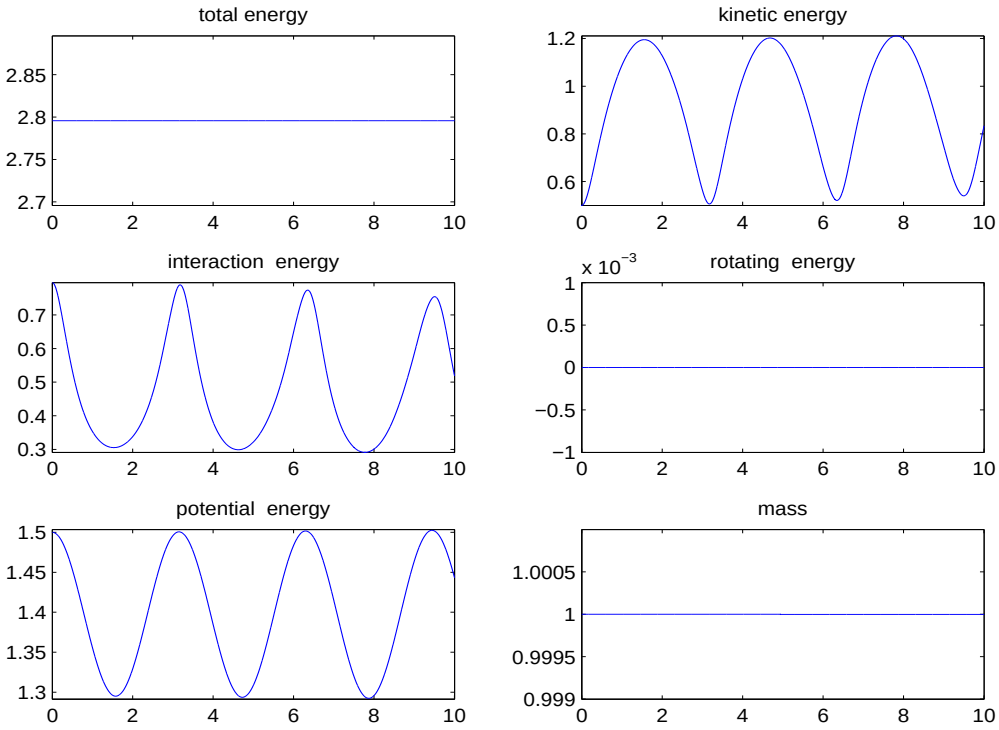

Figure 2.3: Dynamics of mass and energies under $\Omega = 1, \gamma_x = \gamma_y = 1$.

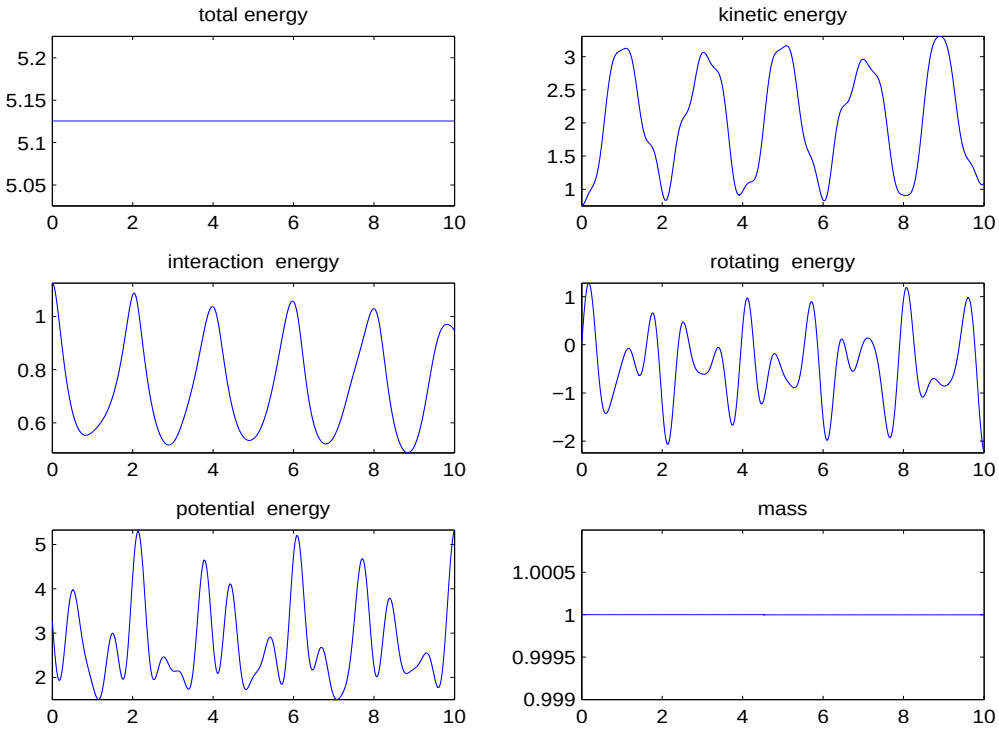

Figure 2.4: Dynamics of mass and energies under $\Omega = 4, \gamma_x = 1, \gamma_y = 2$.

As we have discussed in Theorem 2.3.4, the center of mass could be solved analytically. We are interested in comparing the numerical results obtained

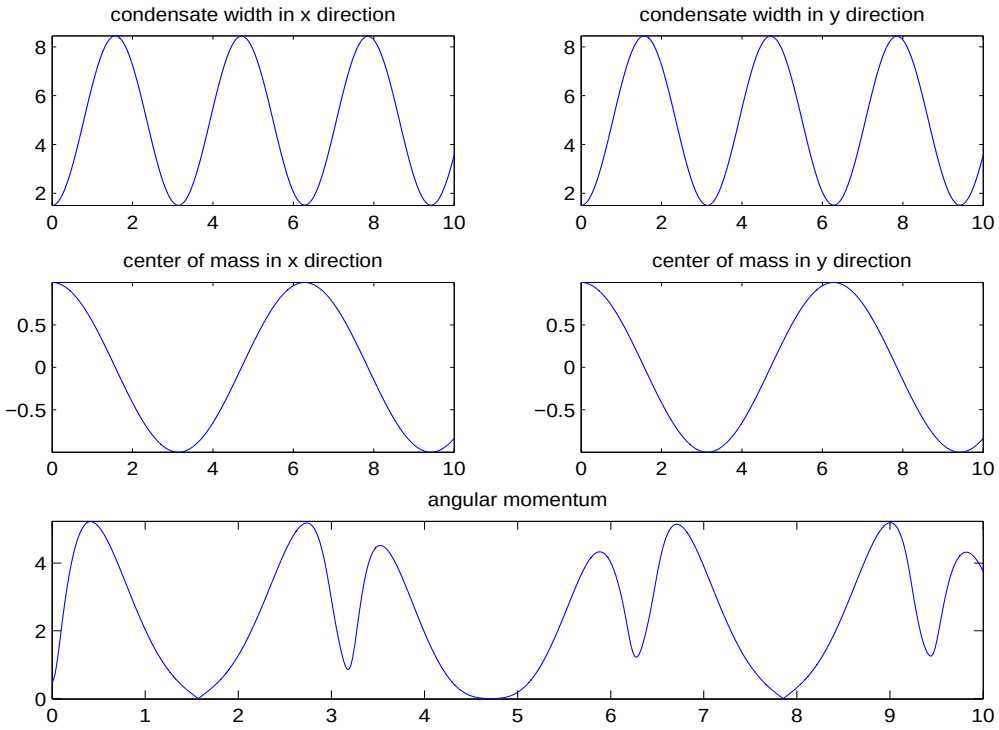

Figure 2.5: Dynamics of condensate width and angular momentum under $\Omega = 1, \gamma_x = \gamma_y = 1, x_0 = 1, y_0 = 1$.

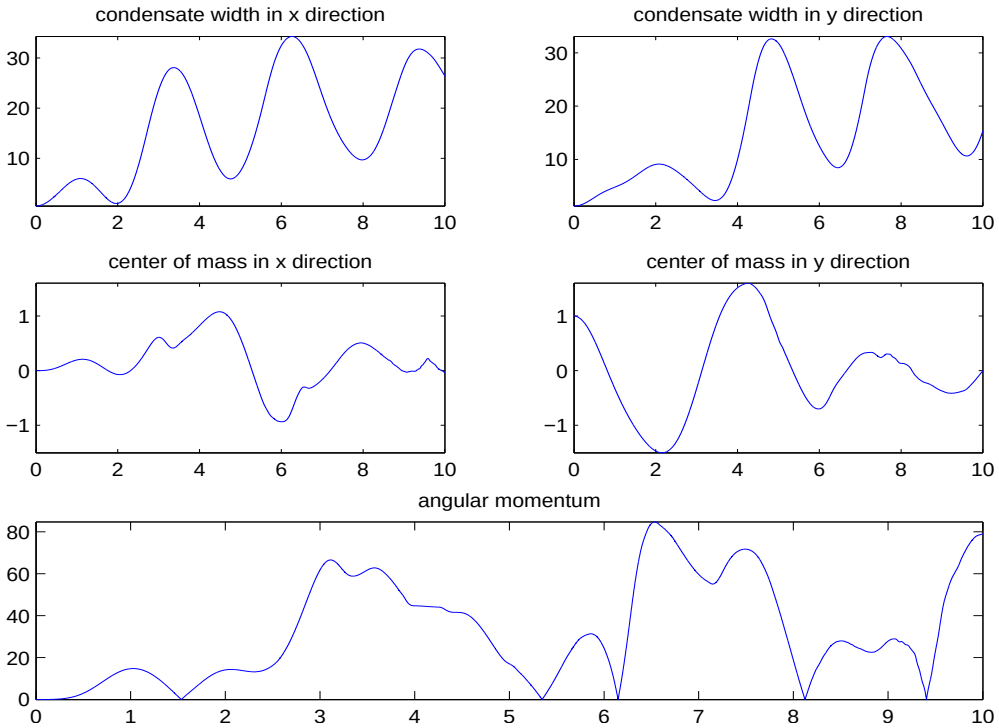

Figure 2.6: Dynamics of condensate width and angular momentum under $\Omega = 1, \gamma_x = 1, \gamma_y = 2, x_0 = 0, y_0 = 1$.

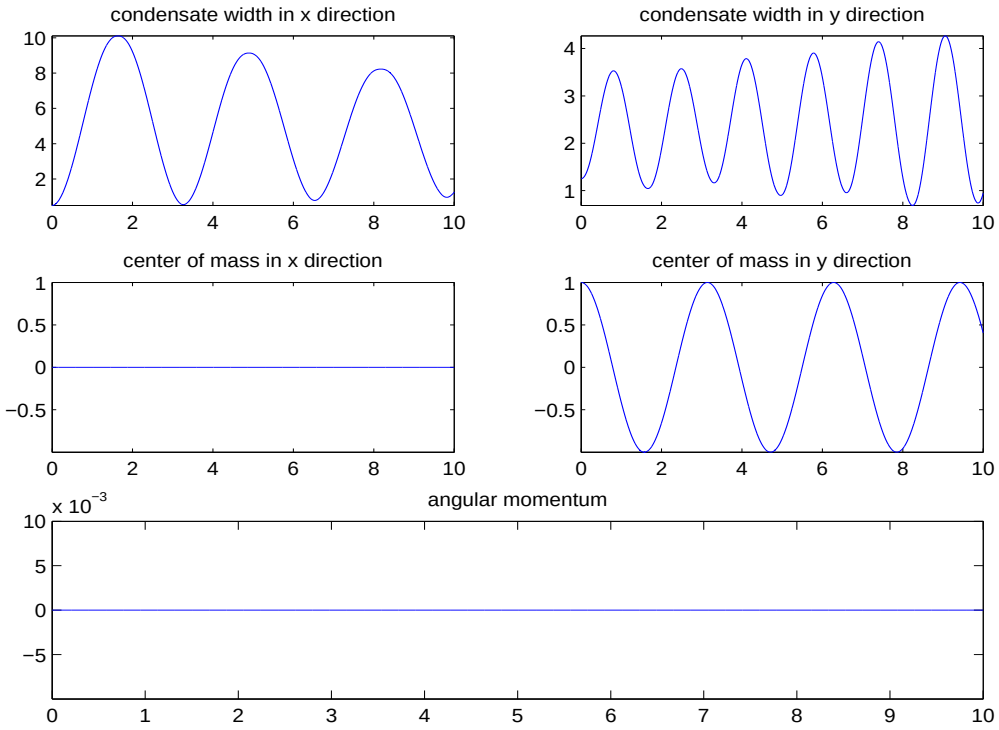

Figure 2.7: Dynamics of condensate width and angular momentum under $\Omega = 0, \gamma_x = 1, \gamma_y = 2, x_0 = 0, y_0 = 1$.

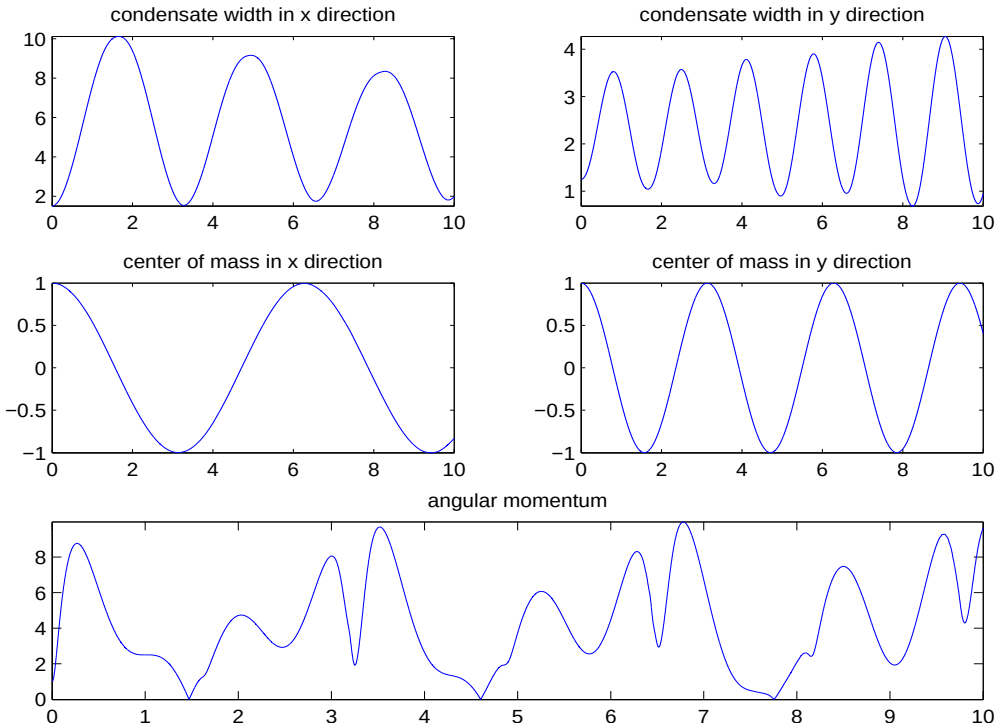

Figure 2.8: Dynamics of condensate width and angular momentum under $\Omega = 0, \gamma_x = 1, \gamma_y = 2, x_0 = 1, y_0 = 1$.

by the method proposed above with the analytical solution, and studying the motion of the center $\mathbf{x}(t)$ under the new coordinate as well as in the original ones. As far as we know, no previous studies are done for the motion of center of mass under a rotating Lagrangian coordinate. In the following figures, the red dash line represents the analytical solution and the blue solid line represents the numerical solution for the motion of center. As we could notice, the numerical solutions approximate quite well.

As we have discussed, we could categorize the motion of center of mass into five different cases, by different Ω, γ_x and γ_y.

Case(I): Non-rotating BEC.

For a non-rotating BEC, i.e. $\Omega = 0$, as we have discussed above in (2.47),

$$\alpha_c(t) = \alpha_0 \cos(\gamma_\alpha t) \quad \alpha = x, y.$$

We take $\mathbf{x}_0 = (1, 1)$. As shown in Figure 2.9, Figure 2.10 and Figure 2.11, the motion in each direction is a periodic function with period $T_\alpha = \frac{2\pi}{\gamma_\alpha}$. (i)If $\gamma_x = \gamma_y$, the trajectory is the straight line $y = x$ (cf. Fig. 2.9). (ii). If γ_x/γ_y is a rational number, then the center moves periodically (cf. Fig. 2.10). (iii). If γ_x/γ_y is irrational, then the center has a chaotic motion in the rectangle $[-|x_0|, |x_0|] \times [-|y_0|, |y_0|]$ (cf. Fig. 2.10).

Case(II): Rotating BEC with an isotropic potential.

For $\Omega \neq 0, \gamma_x = \gamma_y$, taking $\mathbf{x}_0 = (1, 1)$, the center of mass follows the same solution as Case (I), which is (2.47). And as a result, regardless of the value of Ω, the motion of transformed center of mass always follows the one in Figure 2.9. By taking a reverse transformation which is given by $\tilde{\mathbf{x}} = A(t)^T \mathbf{x}$, we could get the motion of center under the original coordinate system, which is dependent of Ω. As we could see from Figure 2.12 to Figure 2.17, Ω takes the value of $1/5, 4/5, 1, 3/2, 6, \pi$ respectively. When Ω is a rational number, i.e. $\Omega = m/n$ with m, n positive integers with no common factor, as shown from Figure 2.12 to Figure 2.16, the center moves periodically with a period $T = n\pi$ for m, n being odd and $T = 2n\pi$ if not [76]. And when Ω is irrational, then the center

has a chaotic motion in a circle with radius of $|\mathbf{x}_0|$ and centered at origin (cf. Fig. 2.17).

Case(III): Anisotropic potential: $0 < |\Omega| = \gamma_x$ *or* $|\Omega| = \gamma_y$.

These figures show that in the case $\Omega = 1, \gamma_x = 1, \gamma_y = 2$, the time evolution of the center for $\mathbf{x}_0 = (1, 1)$. As we can see in Figure 2.19, in the original frame, the trajectory of the center is a spiral coil going to infinity in x-direction.

Case(IV): Anisotropic potential: $\gamma_x < \gamma_y$, $0 < |\Omega| < \gamma_x$ *or* $|\Omega| > \gamma_y$ *or* $\gamma_x < |\Omega| < \gamma_y$.

The Figure 2.20 to Figure 2.26 show the motion of center $\mathbf{x}(t)$ with different Ω, γ_x and γ_y, where $\gamma_x < \gamma_y$ and $|\Omega| < \gamma_x$ or $|\Omega| > \gamma_y$. We could draw a conclusion that the center follows a chaotic motion in a bounded domain.

2.5.3 Quantized vortex interaction in 2D

In this subsection, we study the interaction between central vortices. In order to do so, we have defined the initial data in the following way:

$$\phi(\mathbf{x}, 0) = \frac{\prod_{j=1}^{M} \phi^{m_j}(\mathbf{x} - \mathbf{x}_j^0)}{\| \prod_{j=1}^{M} \phi^{m_j}(\mathbf{x} - \mathbf{x}_j^0) \|}, \tag{2.61}$$

where

$$\phi^{m_j}(x, y) = (x + i m_j y)\phi_e(x, y), \quad m_j \in \{1, -1\},$$

and $\phi_e(\mathbf{x})$ takes the form as in (2.57). M is the total number of interacting vortices.

We will take various cases to study the time evolution of the density. We set $\beta = 50, \Omega = 1, \gamma_x = \gamma_y = 1$ and $M = 2$.

We consider the following cases with different times:

$$
\begin{aligned}
(I) \quad & \mathbf{x}_1^0 = (0.5, 0), \mathbf{x}_2^0 = (-0.5, 0), (m_1, m_2) = (1, 1), \\
(II) \quad & \mathbf{x}_1^0 = (0.5, 0), \mathbf{x}_2^0 = (0, 0), (m_1, m_2) = (1, 1), \\
(III) \quad & \mathbf{x}_1^0 = (0.5, 0), \mathbf{x}_2^0 = (-0.5, 0), (m_1, m_2) = (1, -1), \\
(IV) \quad & \mathbf{x}_1^0 = (0.5, 0), \mathbf{x}_2^0 = (0, 0), (m_1, m_2) = (1, -1).
\end{aligned}
$$

Figures 2.28-2.31 shows the contour plot of the density at different time in different cases. As also discussed in [8], we can draw the following conclusions: if $m_1 = m_2$, the centers of the two vortices rotate symmetrically around the trap center if $\mathbf{x}_1^0$ and $\mathbf{x}_2^0$ are symmetric, as shown in Case I (c.f. Fig. 2.28) and nonsymmetrically if not as shown in Case II (c.f. Fig. 2.29). The two vortices do not collide at any time. For two central vortices with different indices, e.g. $m_1 = 1$ and $m_2 = -1$, the two vortices centers will always collide and merge, as shown in Case III (c.f. Fig. 2.30) and Case IV (c.f. Fig. 2.31).

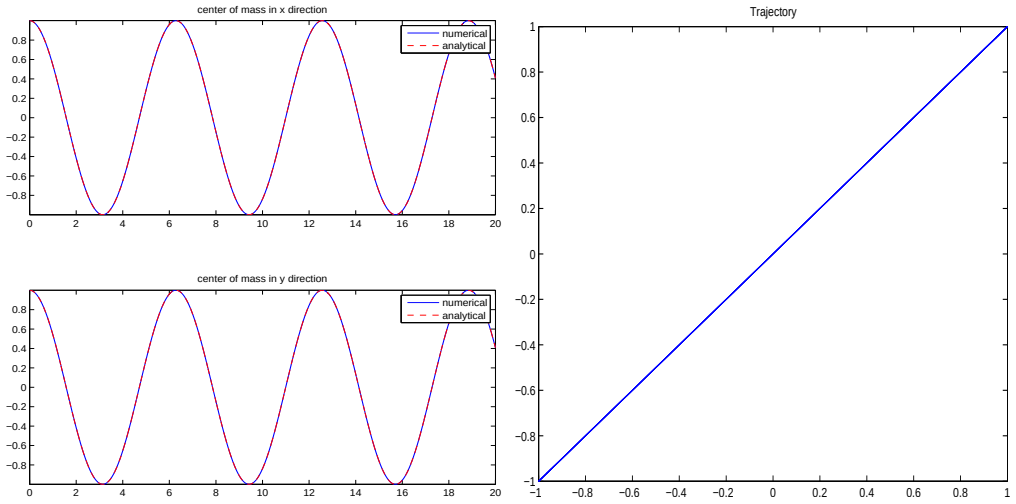

Figure 2.9: Trajectory of center of mass under original and transformed frame when $\gamma_x = \gamma_y$.

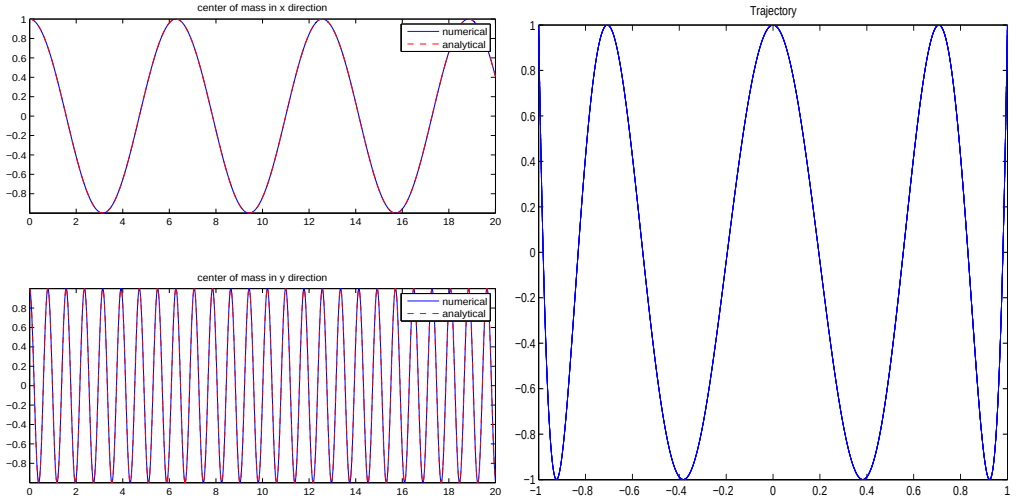

Figure 2.10: Trajectory of center of mass under original and transformed frame when $\Omega = 0, \gamma_x = 1, \gamma_y = 8$.

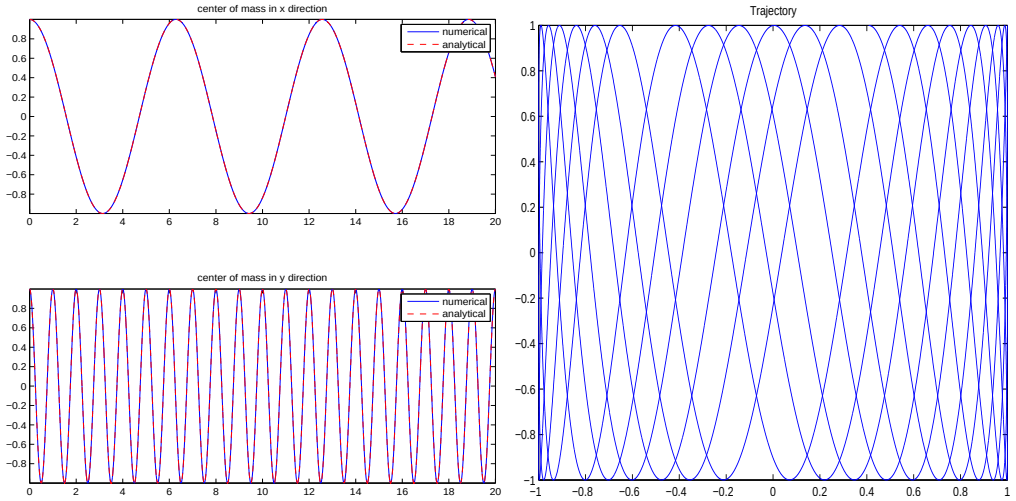

Figure 2.11: Trajectory of center of mass under original and transformed frame when $\Omega = 0, \gamma_x = 1, \gamma_y = 2\pi$.

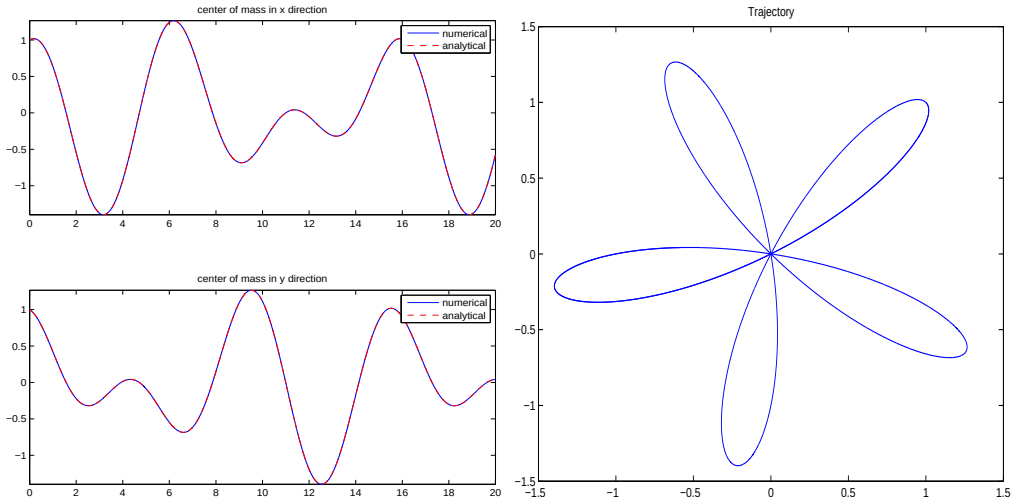

Figure 2.12: Trajectory of center of mass under original frame when $\Omega = 1/5, \gamma_x = \gamma_y = 1$.

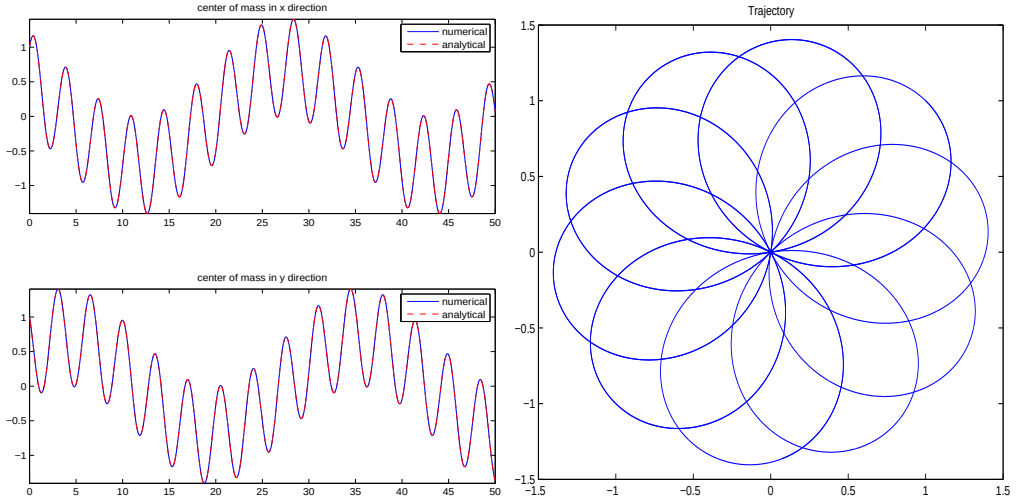

Figure 2.13: Trajectory of center of mass under original frame when $\Omega = 4/5, \gamma_x = \gamma_y = 1$.

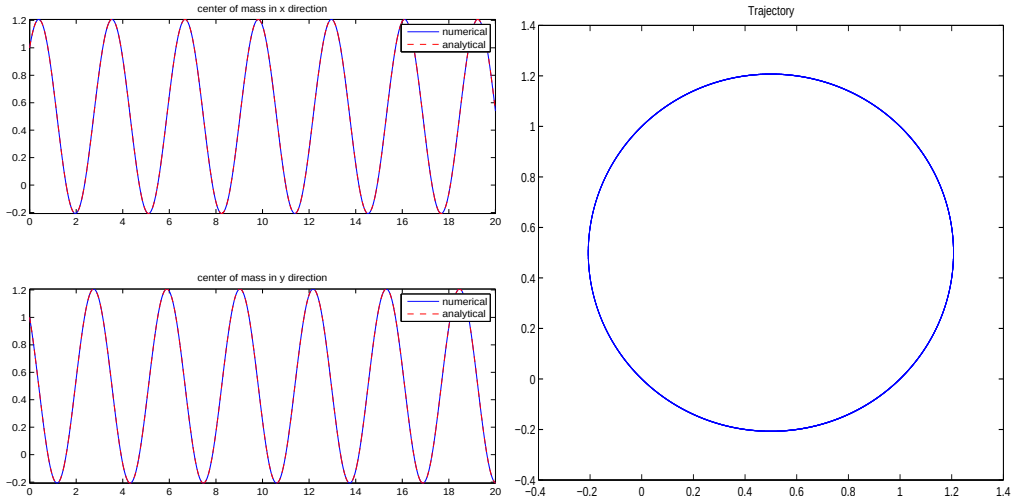

Figure 2.14: Trajectory of center of mass under original frame when $\Omega = 1, \gamma_x = \gamma_y = 1$.

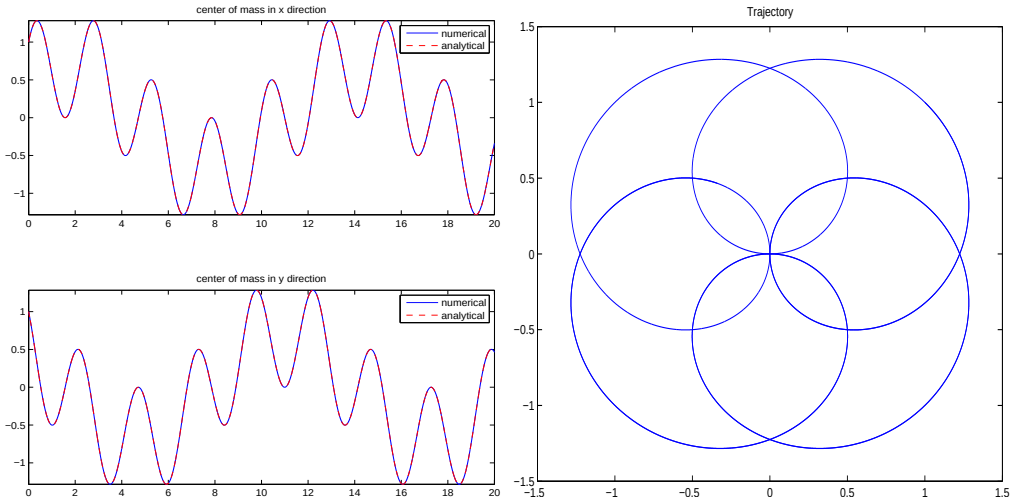

Figure 2.15: Trajectory of center of mass under original frame when $\Omega = 3/2, \gamma_x = \gamma_y = 1$.

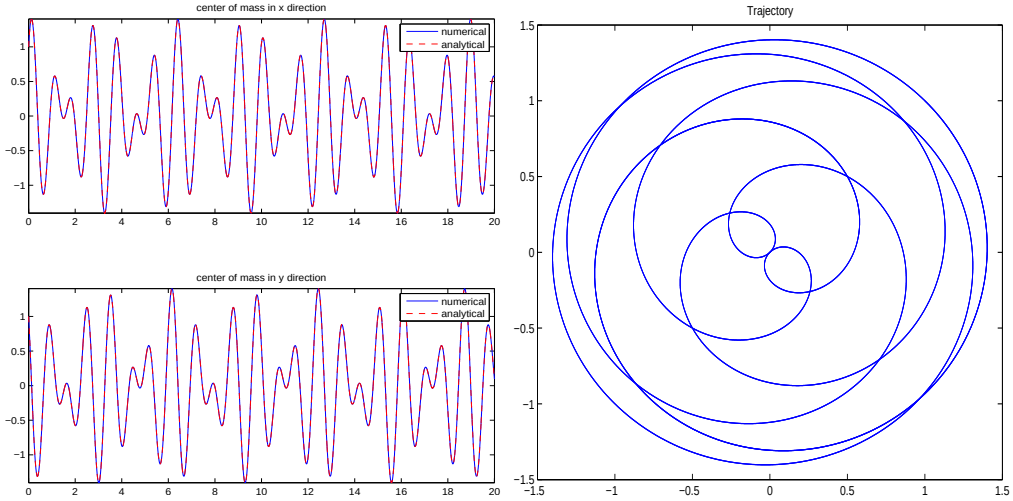

Figure 2.16: Trajectory of center of mass under original frame when $\Omega = 6, \gamma_x = \gamma_y = 1$.

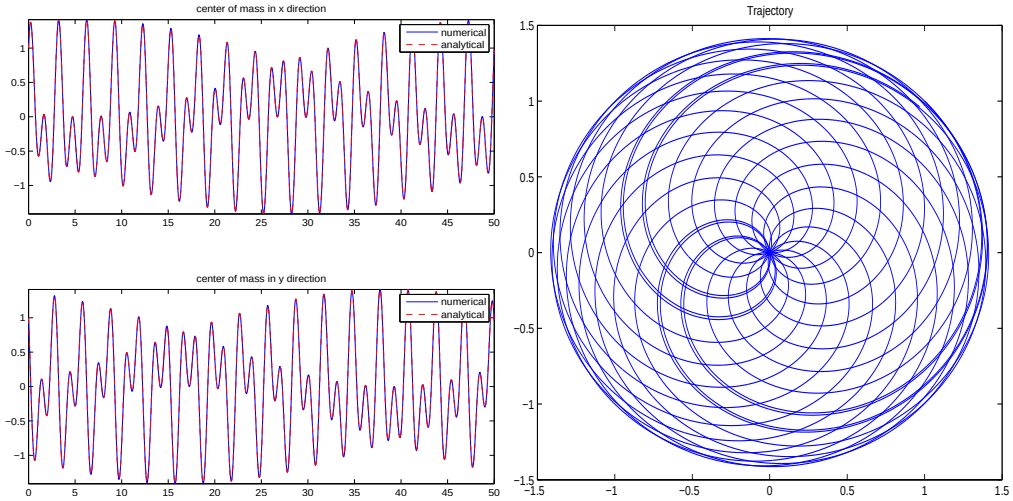

Figure 2.17: Trajectory of center of mass under original frame when $\Omega = \pi, \gamma_x = \gamma_y = 1$.

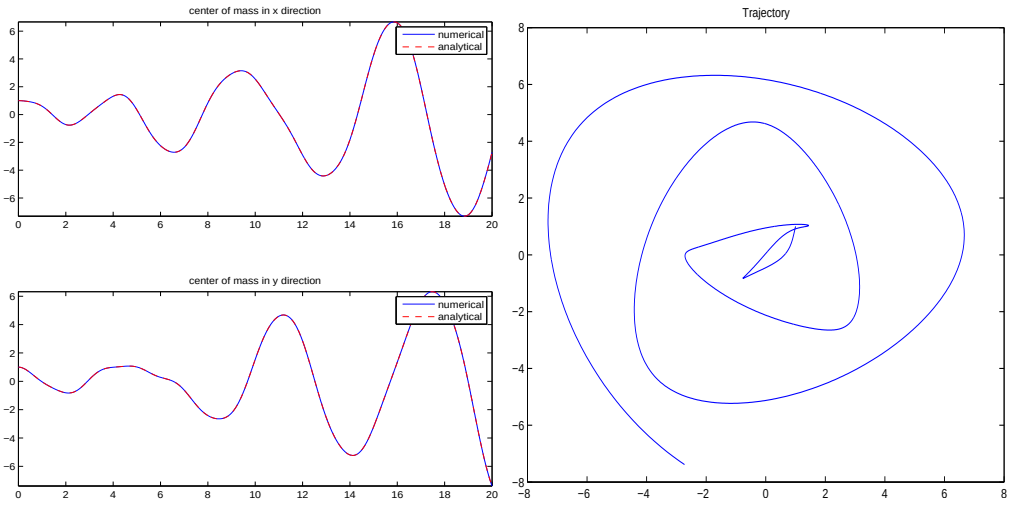

Figure 2.18: Trajectory of center of mass under transformed frame when $\Omega = 1, \gamma_x = 1, \gamma_y = 2, (x_0, y_0) = (1, 1)$.

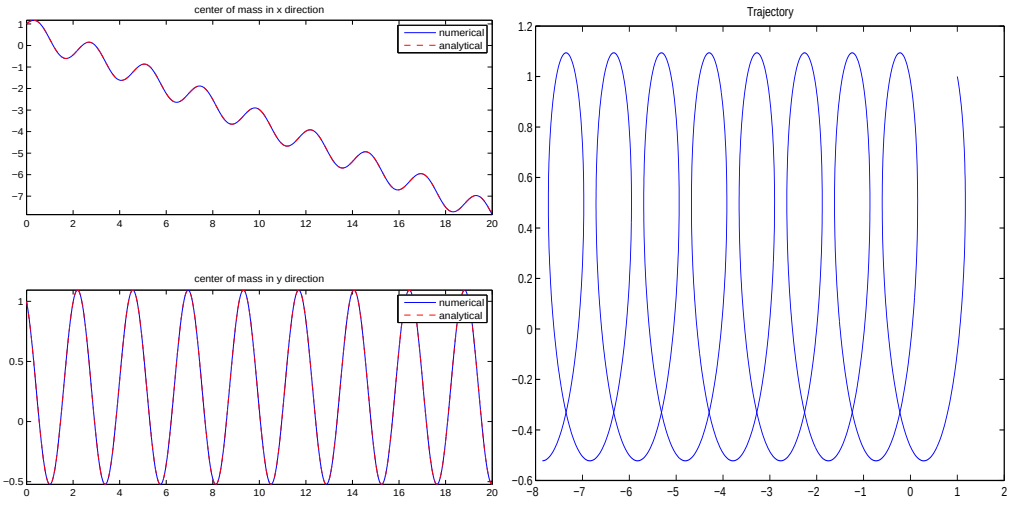

Figure 2.19: Trajectory of center of mass under original frame when $\Omega = 1, \gamma_x = 1, \gamma_y = 2, (x_0, y_0) = (1, 1)$.

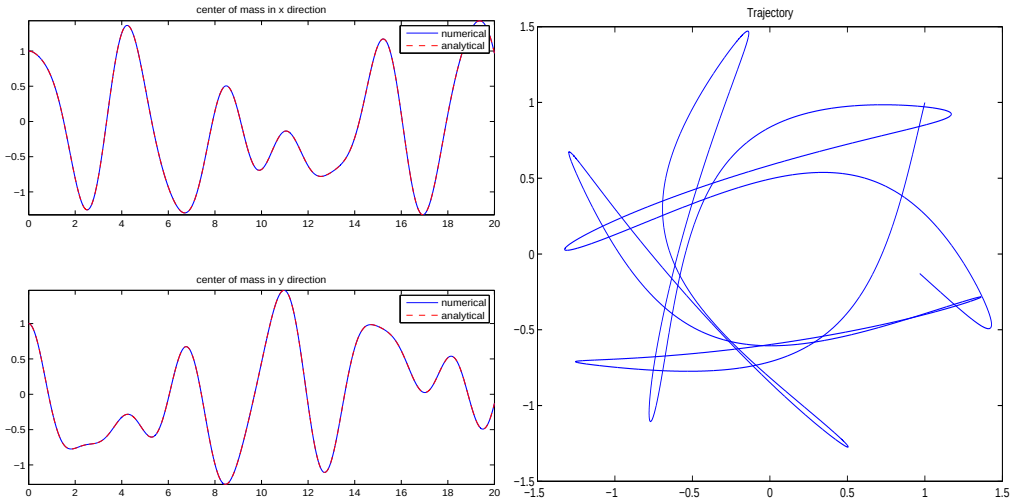

Figure 2.20: Trajectory of center of mass under transformed frame when $\Omega = 1/2, \gamma_x = 1, \gamma_y = 2$.

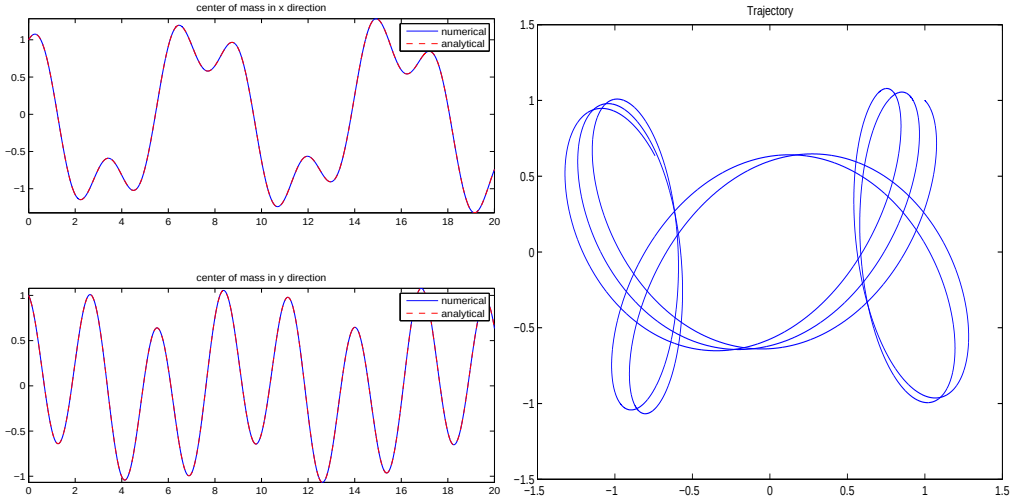

Figure 2.21: Trajectory of center of mass under original frame when $\Omega = 1/2, \gamma_x = 1, \gamma_y = 2$.

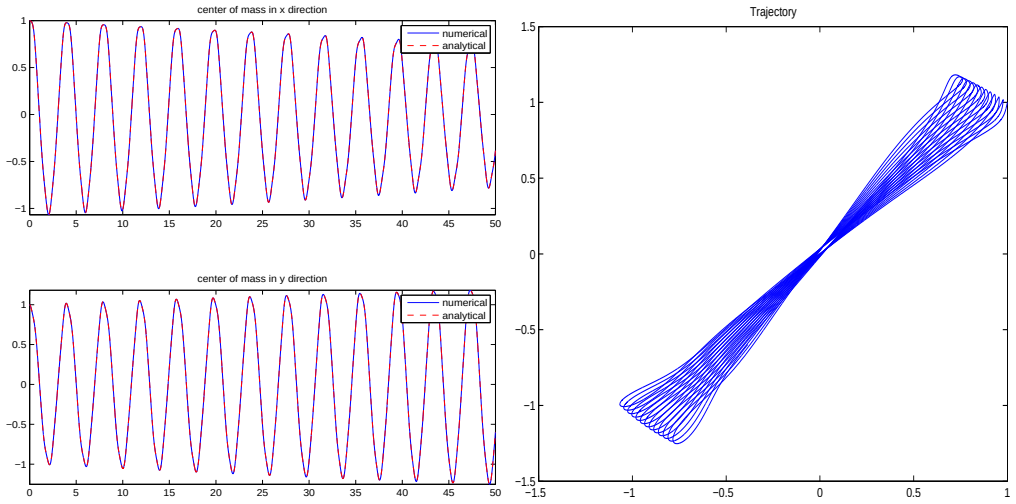

Figure 2.22: Trajectory of center of mass under transformed frame when $\Omega = 4, \gamma_x = 1, \gamma_y = 2$.

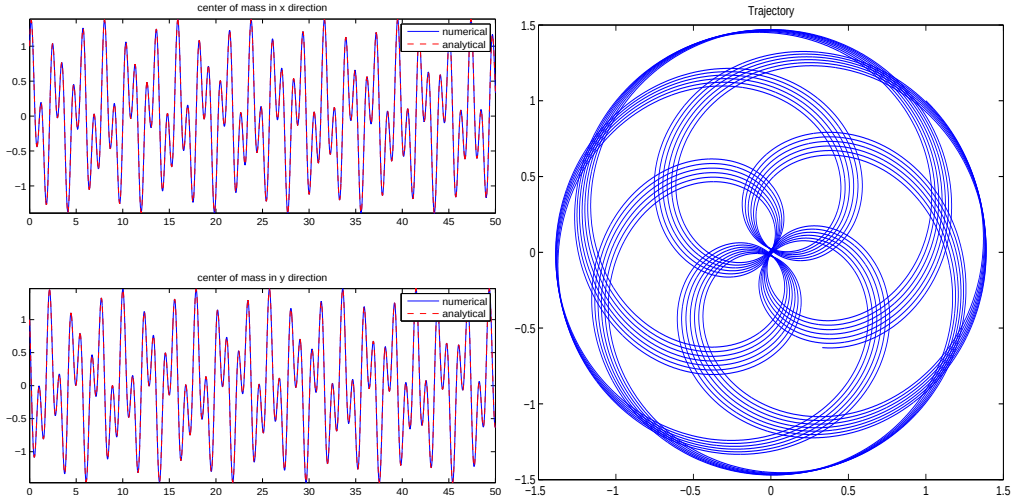

Figure 2.23: Trajectory of center of mass under original frame when $\Omega = 4, \gamma_x = 1, \gamma_y = 2$.

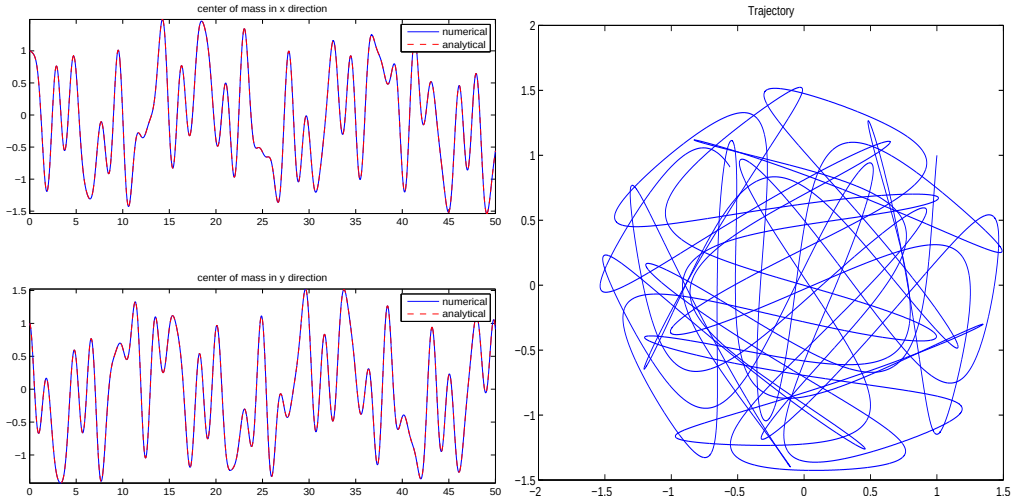

Figure 2.24: Trajectory of center of mass under transformed frame when $\Omega = 1/2, \gamma_x = 1, \gamma_y = \pi$.

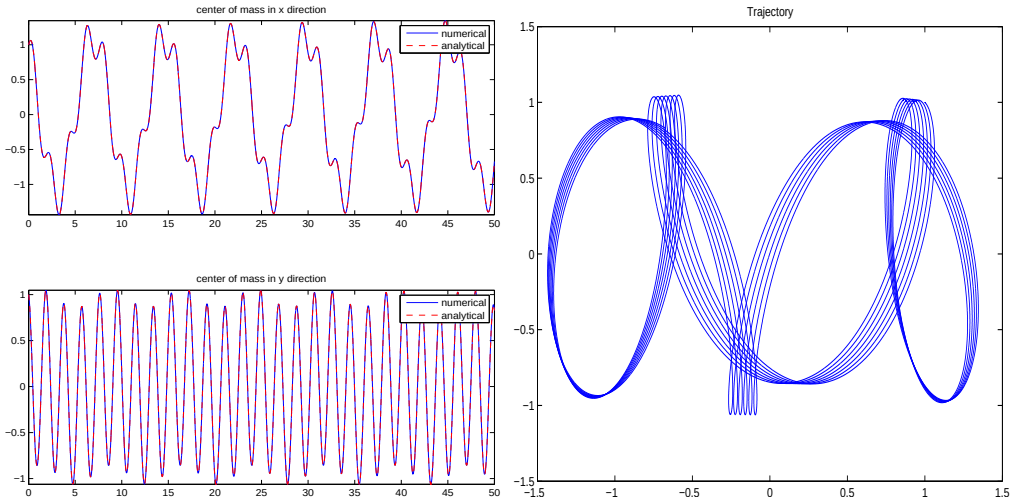

Figure 2.25: Trajectory of center of mass under original frame when $\Omega = 1/2, \gamma_x = 1, \gamma_y = \pi$.

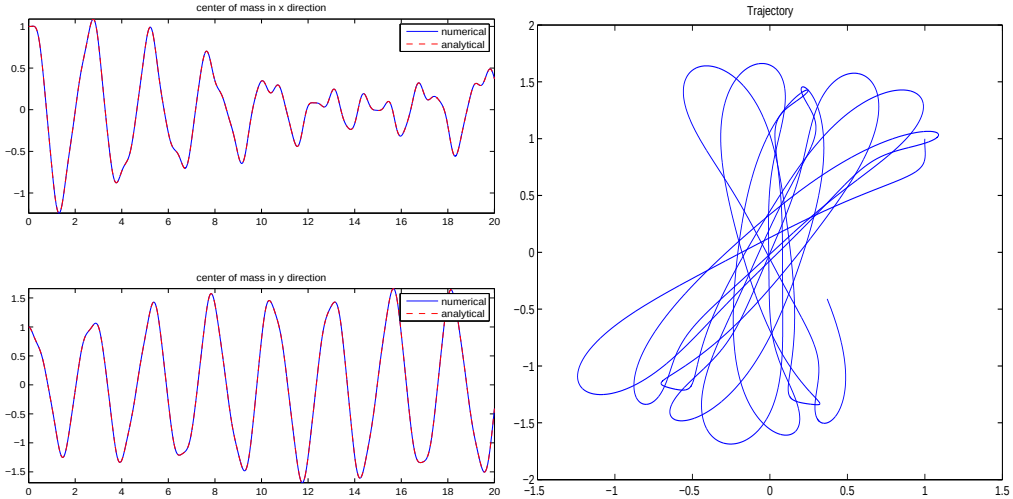

Figure 2.26: Trajectory of center of mass under transformed frame when $\Omega = 4, \gamma_x = 1, \gamma_y = \pi$.

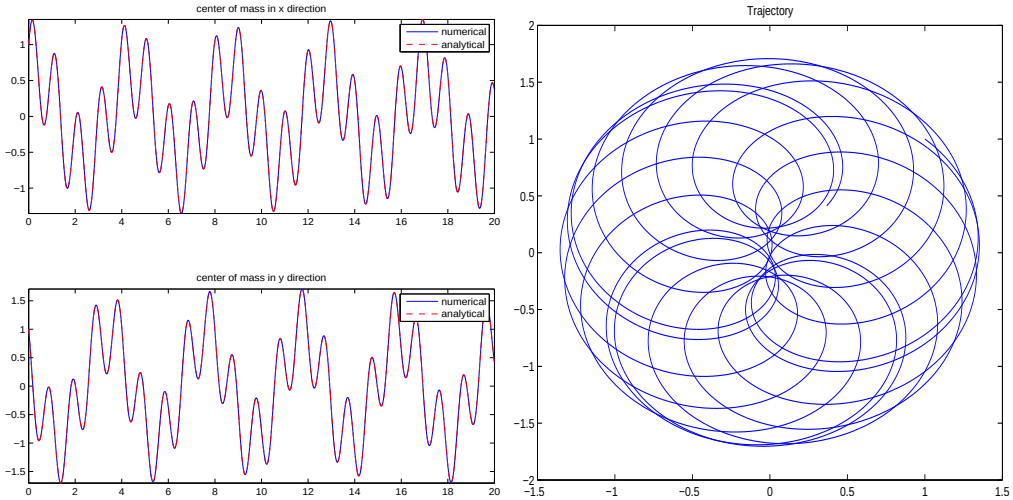

Figure 2.27: Trajectory of center of mass under original frame when $\Omega = 4, \gamma_x = 1, \gamma_y = \pi$.

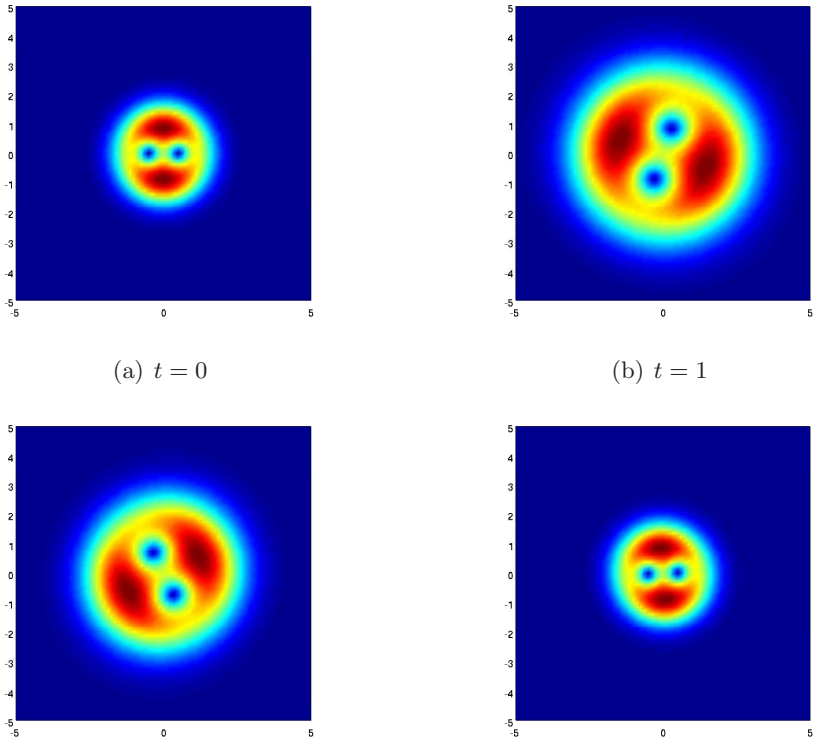

(a) $t = 0$ (b) $t = 1$

(c) $t = 2.4$ (d) $t = 3.2$

Figure 2.28: Case I density contour plot, $\mathbf{x}_1^0 = (0.5, 0), \mathbf{x}_2^0 = (-0.5, 0), (m_1, m_2) = (1, 1)$.

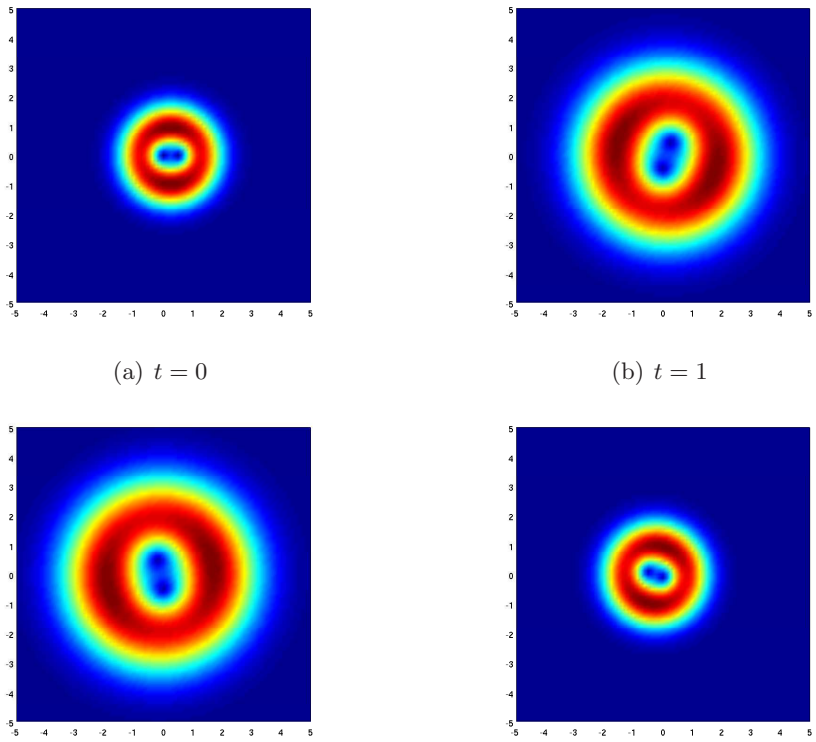

(a) $t = 0$ (b) $t = 1$

(c) $t = 2$ (d) $t = 3$

Figure 2.29: Case II density contour plot, $\mathbf{x}_1^0 = (0.5, 0), \mathbf{x}_2^0 = (0, 0), (m_1, m_2) = (1, 1)$.

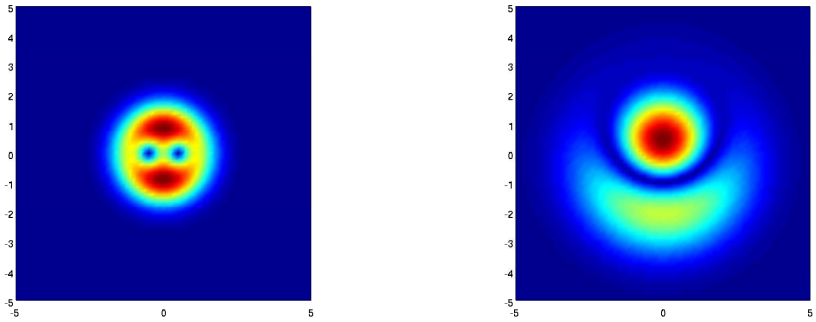

(a) $t = 0$ (b) $t = 2$

(c) $t = 3.2$ (d) $t = 4$

Figure 2.30: Case III density contour plot, $\mathbf{x}_1^0 = (0.5, 0), \mathbf{x}_2^0 = (-0.5, 0), (m_1, m_2) = (1, -1)$.

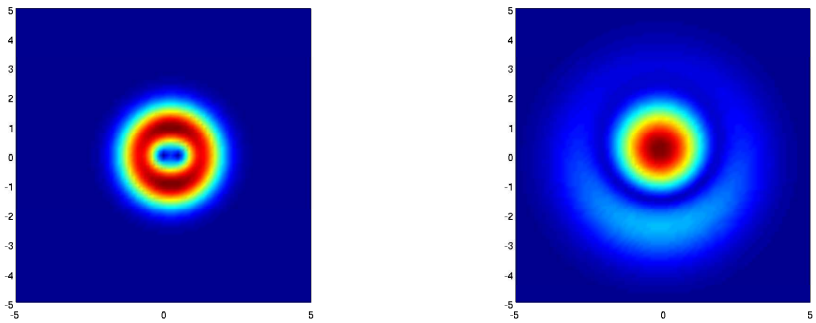

(a) $t = 0$ (b) $t = 2$

(c) $t = 3.2$ (d) $t = 4$

Figure 2.31: Case IV density contour plot, $\mathbf{x}_1^0 = (0.5, 0), \mathbf{x}_2^0 = (0, 0), (m_1, m_2) = (1, -1)$.

Chapter 3

Extention to rotating two-component BEC

In this chapter, we extend the results obtained previously for rotating single-component BEC to rotating two-component BEC. We base the analysis on the coupled Gross-Pitaevskii equations (CGPEs) with an angular momentum rotational term. We follow the previous approach by applying a Lagrangian transformation to investigate the dynamical laws and propose an efficient and accurate method for numerical simulations. Finally, numerical results have been presented and discussed in details.

3.1 Introduction

After the study of single rotational BEC, attentions have been broadened to the system of two or more condensates [43, 46] to better understand superfluidity [1, 54]. The first experiment involving multi-component BEC interaction was realized with atoms evaporatively cooled in the $|F = 2, m_f = 2\rangle$ and $|F = 1, m_f = -1\rangle$ spin states of ^{87}Rb [60]. The possibility of producing long-lived multiple condensate systems has hence been well demonstrated and the existence of inter-component interactions dramatically affect the condensate's dynamics. Great excitement has been spurred in the atomic physics community to study the static and dynamic phenomena occurred in a system of rotating

two-component BEC.

Theoretical treatment first began for super fluid helium mixtures and spin polarized hydrogen. It has been extended to Bose condensates of alkalis atoms[32, 44, 49, 63]. The realization of BEC experimentally has dramatically advanced the theoretical study in this area since the theoretical predictions of multi-component condensates can now be compared to the experimental results.

3.2 Coupled Gross-Pitaevskii equations

Similar to a single component BEC, at temperature T which is much smaller than the critical temperature T_c, a two-component BEC can be described by the macroscopic wave function $\Psi(\tilde{\mathbf{x}},t) = (\psi_1(\tilde{\mathbf{x}},t), \psi_2(\tilde{\mathbf{x}},t))$, with $\tilde{\mathbf{x}} \in R^d$, $d = 2, 3$, whose evolution is governed by two self-consistent, mean field nonlinear Schrödinger equations (NLSEs) in a rotational frame, also known as the coupled Gross-Pitaevkii equation (CGPEs) with the angular momentum rotation term [40, 47, 52, 50]:

$$i\partial_t \psi_j(\tilde{\mathbf{x}},t) = \left[-\frac{1}{2}\nabla^2 + V^j_{hos}(\tilde{\mathbf{x}}) - \Omega L_z + \sum_{l=1}^{2} \beta_{jl}|\psi_l|^2\right]\psi_j - \lambda\psi_{k_j}, \quad j = 1, 2, \tag{3.1}$$

Here, $\psi_j(\tilde{\mathbf{x}},t)$ is the dimensionless wave function of the jth ($j = 1, 2$) component. $V^j_{hos}(\tilde{\mathbf{x}})$ is the dimensionless external trapping potential, which is often harmonic and thus can be written as $\frac{1}{2}(\gamma^2_{x,j}x^2 + \gamma^2_{y,j}y^2)$ in 2D, and resp., $V^j_{hos}(\tilde{\mathbf{x}}) = \frac{1}{2}(\gamma^2_{x,j}\tilde{x}^2 + \gamma^2_{y,j}\tilde{y}^2 + \gamma^2_{z,j}\tilde{z}^2)$ in 3D with $\gamma_{x,j} > 0, \gamma_{y,j} > 0$ and $\gamma_{z,j} > 0$ constants. $L_{\tilde{z}} = -i(\tilde{x}\partial_y - \tilde{y}\partial_x) = iJ_{\tilde{z}}$ is the $\tilde{z}-$component of the angular momentum, and Ω is the dimensionless angular momentum rotating speed. β_{jl} is a constant characterizing the interactions between the jth and lth component, with $\beta_{jl} = \beta_{lj}$. The integers k_j in (3.1) are chosen as

$$k_j = \begin{cases} 2, & j = 1, \\ 1, & j = 2. \end{cases} \tag{3.2}$$

3.3 Dynamical laws in the Cartesian coordinate

Many researches have been done to study the dynamical laws of rotating two-component BEC [77, 7]. We will briefly present the analytical results for rotating two-component BECs in the Cartesian coordinate without given further proofs.

I). Energy and density.

We have two important invariants: density and energy and they are defined as follows:

$$N(t) = N_1(t) + N_2(t) \equiv \| \psi_1 \|^2 + \| \psi_2 \|^2 = 1, \quad t \geq 0, \tag{3.3}$$

with

$$N_j(t) = \| \psi_j(\tilde{\mathbf{x}}, t) \|^2 := \int_{\mathbb{R}^d} |\psi_j(\tilde{\mathbf{x}}, t)|^2 \, \mathrm{d}\tilde{\mathbf{x}}, \quad t \geq 0, j = 1, 2, \tag{3.4}$$

and the energy

$$\begin{aligned} E(\psi_1, \psi_2) \quad = \quad & \int_{\mathbb{R}^d} \Bigg[\sum_{j=1}^{2} \Bigg(\frac{1}{2} |\nabla \psi_j|^2 + V_{hos}^j(\tilde{\mathbf{x}}) |\psi_j|^2 + \sum_{j=1}^{2} \frac{\beta_{jl}}{2} |\psi_j|^2 |\psi_l|^2 \\ & - \Omega \mathbf{Re}(\psi_j^* L_{\tilde{z}} \psi_j) \Bigg) - 2\lambda \mathbf{Re}(\psi_1^* \psi_2) \Bigg] \mathrm{d}\tilde{\mathbf{x}}. \end{aligned}$$

We have the following lemma for density of each component:

Lemma 3.3.1. *Suppose $(\psi_1(\tilde{\boldsymbol{x}}, t), \psi_2(\tilde{\boldsymbol{x}}, t))$ is the solution of the CGPEs (3.1); then we have, for $j = 1, 2$,*

$$N_j''(t) = -2\lambda^2 \left[2N_j(t) - 1 \right] + \tilde{F}_j(t), \quad t \geq 0, \tag{3.5}$$

with initial conditions:

$$N_j(0) = N_j^{(0)} = \int_{\mathbb{R}^d} |\psi_j^0(\tilde{\boldsymbol{x}})|^2 \, \mathrm{d}\tilde{\boldsymbol{x}} = \frac{N_j^0}{N}, \tag{3.6}$$

$$N_j'^{(0)} = N_j^{(1)} = 2\lambda \int_{\mathbb{R}^d} Im \left[\psi_j^0(\tilde{\boldsymbol{x}}) (\psi_{k_j}^0(\tilde{\boldsymbol{x}}))^* \right] \, \mathrm{d}\tilde{\boldsymbol{x}}; \tag{3.7}$$

where for $t \geq 0$,

$$\begin{aligned}\tilde{F}_j(t) &= \lambda \int_{\mathbb{R}^d} (\psi_j^* \psi_{k_j} + \psi_j \psi_{k_j}^*) \Big[V_{hos}^{k_j}(\tilde{\boldsymbol{x}}) - V_{hos}^{j}(\tilde{\boldsymbol{x}}) - (\beta_{jj} - \beta_{k_j j})|\psi_j|^2 \\ &\quad + (\beta_{k_j k_j} - \beta_{j k_j})|\psi_{k_j}|^2 \Big] \mathrm{d}\tilde{\boldsymbol{x}}, \quad t \geq 0. \end{aligned} \tag{3.8}$$

II). Angular momentum expectation.

The angular momentum is defined as:

$$\langle L_{\tilde{z}} \rangle (t) = \langle L_{\tilde{z}} \rangle_1 (t) + \langle L_{\tilde{z}} \rangle_2 (t), \quad t \geq 0, \tag{3.9}$$

where

$$\langle L_{\tilde{z}} \rangle_j (t) = \int_{\mathbb{R}^d} \psi_j^* L_{\tilde{z}} \psi_j \, \mathrm{d}\tilde{\mathbf{x}}, \quad j = 1, 2, \quad t \geq 0, \quad d = 2, 3. \tag{3.10}$$

It satisfies the following theorem:

Theorem 3.3.2. *Suppose* $(\psi_1(\tilde{\boldsymbol{x}}, t), \psi_2(\tilde{\boldsymbol{x}}, t))$ *is the solution of the CGPE (3.1), we have:*

$$\begin{aligned}\frac{d \langle L_{\tilde{z}} \rangle_j (t)}{dt} &= \frac{\gamma_{x,j}^2 - \gamma_{y,j}^2}{2} \int_{\mathbb{R}^d} \tilde{x}\tilde{y} |\psi_j|^2 \, \mathrm{d}\tilde{\boldsymbol{x}} - i \int_{\mathbb{R}^d} \beta_{j k_j} |\psi_j|^2 L_{\tilde{z}} |\psi_{k_j}|^2 \, \mathrm{d}\tilde{\boldsymbol{x}} \\ &\quad - 2\lambda \boldsymbol{Re} \left[\int_{\mathbb{R}^d} \psi_{k_j}^* L_{\tilde{z}} \psi_j \, \mathrm{d}\tilde{\boldsymbol{x}} \right]. \end{aligned} \tag{3.11}$$

We have the conservation of angular momentum expectation, at least in the following cases, when $\gamma_{x,j} = \gamma_{y,j}$ *for* $j = 1, 2$, *i.e. the trapping potential is radially symmetric:*

(i): For any given initial data, we have the conservation of total angular momentum expectation and the energy for non-rotating part. (ii) Moreover if the initial data $(\psi_1^0(\tilde{\boldsymbol{x}}), \psi_2^0(\tilde{\boldsymbol{x}}))$ *is further chosen as*

$$\psi_j^0(\tilde{\boldsymbol{x}}) = f_j(r) e^{i m_j \theta}, \ \textit{with } m_j \in \boldsymbol{Z} \textit{ and } f_j(0) = 0 \textit{ when } m_j \neq 0. \tag{3.12}$$

If $\lambda = 0$, *then* $\langle L_{\tilde{z}} \rangle_1 (t)$ *and* $\langle L_{\tilde{z}} \rangle_2 (t)$ *are conserved.*

On the other hand, if $m_1 = m_2 := m$ in (3.42), then for any given λ, $\left\langle \tilde{Lz} \right\rangle_1 (t)$ and $\left\langle \tilde{Lz} \right\rangle_2 (t)$ are conserved, i.e.

$$\left\langle \tilde{L}_{\tilde{z}} \right\rangle_j (t) \equiv \left\langle \tilde{L}_{\tilde{z}} \right\rangle_j (t) = m, \quad t \geq 0, j = 1, 2. \tag{3.13}$$

III). Condensate width

With the condensate width defined as:

$$\langle \sigma_\alpha \rangle (t) = \sqrt{\delta_\alpha(t)} = \sqrt{\delta_{\alpha,1}(t) + \delta_{\alpha,2}(t)}, \tag{3.14}$$

where

$$\delta_{\alpha,j} = \langle \alpha^2 \rangle (t) = \int_{\mathbb{R}^d} \alpha^2 |\psi_j|^2 \, \mathrm{d}\tilde{\mathbf{x}}, \quad \alpha = \tilde{x}, \tilde{y}, \tilde{z}. \tag{3.15}$$

we have the following dynamical laws:

Theorem 3.3.3. *i). Generally, for d=2,3, and any potential and initial data, the condensate width satisfies:*

$$\begin{cases} \dfrac{d^2\delta_\alpha(t)}{d^2 t} = \displaystyle\int_{\mathbb{R}^d} \sum_{j=1}^{2} \Big[(\partial_y \alpha - \partial_x \alpha)(4i\Omega \psi_j^* (\tilde{x}\partial_y + \tilde{y}\partial_x)\psi_j + 2\Omega^2(\tilde{x}^2 - \tilde{y}^2)|\psi_j|^2 \\ \qquad\qquad +2|\partial_\alpha \psi_j|^2 - 2\alpha |\psi_j|^2 \partial_\alpha V_{hos}^j + |\psi_j|^2 \displaystyle\sum_{l=1}^{2} \beta_{jl} |\psi_l|^2 \Big] \, \mathrm{d}\tilde{\boldsymbol{x}}, \\ \delta_\alpha(0) =: \delta_\alpha^{(0)} = \int_{\mathbb{R}^d} \alpha^2 (|\psi_1^0|^2 + |\psi_1^0|^2) \, \mathrm{d}\tilde{\boldsymbol{x}}, \\ \dot{\delta}_\alpha(0) =: \delta_\alpha^{(1)} = 2 \displaystyle\sum_{j=1}^{2} \int_{\mathbb{R}^d} \alpha Im((\psi_j^0)^* \partial_\alpha \psi_j^0) - \Omega |\psi_j^0|^2 (\tilde{x}\partial_y - \tilde{y}\partial_x)\alpha \, \mathrm{d}\tilde{\boldsymbol{x}}. \end{cases} \tag{3.16}$$

IV). Center of mass.

The center of mass is defined as follows:

$$\langle \tilde{\mathbf{x}} \rangle_j (t) = \int_{\mathbb{R}^d} \tilde{\mathbf{x}} |\psi_j|^2 \, \mathrm{d}\tilde{\mathbf{x}} =: (\tilde{x}_j^c(t), \tilde{y}_j^c(t), \tilde{z}_j^c(t))^T. \tag{3.17}$$

By [77], the center of mass satisfies a 2nd order ODE and can be solved analytically.

3.4 The Lagragian transformation

Similar to single component BEC discussed in Chapter 2, we apply the orthogonal transition matrix $A(t)$ (2.11) for 2D and (2.12) for 3D. Take transformation $\mathbf{x} = A(t)\tilde{\mathbf{x}}$, $\Phi(\mathbf{x},t) = \Psi(A(t)\tilde{\mathbf{x}},t)$, and we substitute them into (3.1). We notice that

$$L_{\tilde{z}}\Psi = L_z\Phi,\ i\partial_t\Psi = i\partial_t\Phi + \Omega L_z\Phi,$$

we can therefore cancel the rotational term in (3.1) and instead solve the following problem:

$$\begin{cases} i\partial_t\phi_j(\mathbf{x},t) = \left[-\frac{1}{2}\nabla^2 + V_j(\mathbf{x},t) + \sum_{l=1}^{2}\beta_{jl}|\phi_l|^2\right]\phi_j - \lambda\phi_{k_j}, \\ \phi_j(\mathbf{x},0) = \phi_j^0(\mathbf{x}), \qquad j = 1,2, \mathbf{x}\in R^d,\ d = 2,3, \end{cases} \tag{3.18}$$

where the external potentials are given as:

$$V_j(\mathbf{x},t) := V_{rot}^j(\mathbf{x}.t) + V_{hos}^j(\mathbf{x}), \tag{3.19}$$

with

$$\begin{aligned} V_{rot}^j(\mathbf{x}.t) &:= \frac{(\gamma_{x,j}^2 - \gamma_{j,y}^2)\left[\sin^2(\Omega t)(y^2-x^2) + \sin(2\Omega t)xy\right]}{2}, \\ V_{hos}^j(\mathbf{x}) &:= \begin{cases} \frac{\gamma_{x,j}^2x^2+\gamma_{j,y}^2y^2}{2}, & d=2, \\ \frac{\gamma_{x,j}^2x^2+\gamma_{j,y}^2y^2+\gamma_{j,z}^2z^2}{2}, & d=3, \end{cases} \end{aligned}$$

and the initial data are normalized as:

$$\| \phi_1^0 \|^2 + \| \phi_2^0 \|^2 := \int_{\mathbb{R}^d}(|\phi_1(\mathbf{x})|^2 + |\phi_2(\mathbf{x})|^2)\,\mathrm{d}\mathbf{x} = 1. \tag{3.20}$$

The two important invariants of (3.18), which are the total density and energy are now respectively of the following forms:

$$N(t) = N_1(t) + N_2(t) \equiv \| \phi_1 \|^2 + \| \phi_2 \|^2 = 1, \quad t \geq 0, \tag{3.21}$$

with

$$N_j(t) = \| \phi_j(\mathbf{x},t) \|^2 := \int_{\mathbb{R}^d} |\phi_j(\mathbf{x},t)|^2 \, \mathrm{d}\mathbf{x}, \quad t \geq 0, j = 1,2, \tag{3.22}$$

and

$$E(\phi_1,\phi_2) := E_n(\phi_1,\phi_2) + E_{rot}(\phi_1,\phi_2), \tag{3.23}$$

where

$$\begin{aligned} E_n(\phi_1,\phi_2) &= \int_{\mathbb{R}^d} \Bigg[\sum_{j=1}^{2} \left(\frac{1}{2}|\nabla\phi_j|^2 + V_j(\mathbf{x})|\phi_j|^2 + \sum_{l=1}^{2} \frac{\beta_{jl}}{2}|\phi_j|^2|\phi_l|^2 \right) \\ &\quad -2\lambda \mathbf{Re}(\phi_1^*\phi_2) \Bigg] \mathrm{d}\mathbf{x}, \end{aligned} \tag{3.24}$$

$$E_{rot}(\phi_1,\phi_2) = -\int_{\mathbb{R}^d} \left[\sum_{j=1}^{2} \left(\int_0^t \partial_s V(\mathbf{x},s)|\phi_j|^2 ds \right) \right] \mathrm{d}\mathbf{x}. \tag{3.25}$$

3.5 Dynamical laws in the Lagrangian coordinate

In this section, we provide some analytical results on the definition and the dynamical laws of the following quantities for the inhomogeneous CGPEs (3.18): energy, density, angular momentum expectation, condensate width and the center of mass.

I). Dynamics of the density

As we know, when $\lambda = 0$ in (3.18), the density of each component is conserved as specified in (3.22). While when $\lambda \neq 0$, we have the following lemmas for the dynamics of each component:

Lemma 3.5.1. *Suppose $(\phi_1(\boldsymbol{x},t), \phi_2(\boldsymbol{x},t))$ is the solution of the CGPEs (3.18); then we have, for $j = 1,2$,*

$$N_j'(t) = 2\lambda \boldsymbol{Re} \left[\int_{\mathbb{R}^d} (i\phi_j^* \phi_{k_j}) \, \mathrm{d}\boldsymbol{x} \right], \quad t \geq 0, \tag{3.26}$$

$$N_j''(t) = -2\lambda^2 \left[2N_j(t) - 1 \right] + F_j(t), \quad t \geq 0, \tag{3.27}$$

with initial conditions:

$$N_j(0) = N_j^{(0)} = \int_{\mathbb{R}^d} |\phi_j^0(\boldsymbol{x})|^2 \, \mathrm{d}\boldsymbol{x}, \tag{3.28}$$

$$N_j^{'(0)} = N_j^{(1)} = 2\lambda \int_{\mathbb{R}^d} Im\left[\phi_j^0(\boldsymbol{x})(\phi_{k_j}^0(\boldsymbol{x}))^*\right] \, \mathrm{d}\boldsymbol{x}, \tag{3.29}$$

where for $t \geq 0$,

$$\begin{aligned} F_j(t) &= \lambda \int_{\mathbb{R}^d} (\phi_j^* \phi_{k_j} + \phi_j \phi_{k_j}^*) \Big[V_{k_j}(\boldsymbol{x}) - V_j(\boldsymbol{x}) - (\beta_{jj} - \beta_{k_j j})|\phi_j|^2 \\ &\quad + (\beta_{k_j k_j} - \beta_{j k_j})|\phi_{k_j}|^2 \Big] \, \mathrm{d}\boldsymbol{x}, \quad t \geq 0. \end{aligned} \tag{3.30}$$

Proof. By differentiating (3.22) with respect to t and apply integration by parts, we obtain for $j = 1, 2$:

$$\begin{aligned} N_j'(t) &= \frac{d}{dt} \parallel \phi_j(\mathbf{x}, t) \parallel^2 = \frac{d}{dt} \int_{\mathbb{R}^d} |\phi_j(\mathbf{x}, t)|^2 \, \mathrm{d}\mathbf{x} \\ &= \int_{\mathbb{R}^d} (\partial_t \phi_j \phi_j^* + \phi_j \partial_t \phi_j^*) \, \mathrm{d}\mathbf{x} \\ &= -i \int_{\mathbb{R}^d} \left[(i\partial_t \phi_j)\phi_j^* - \phi_j (i\partial_t \phi_j)^* \right] \, \mathrm{d}\mathbf{x} \\ &= \int_{\mathbb{R}^d} i\lambda (\phi_j^* \phi_{k_j} - \phi_j \phi_{k_j}^*) \, \mathrm{d}\mathbf{x} \\ &= 2\lambda \mathbf{Re}\left[\int_{\mathbb{R}^d} i\phi_j^* \phi_{k_j} \, \mathrm{d}\mathbf{x} \right], \quad t \geq 0. \end{aligned}$$

Similarly, we apply the same approach to compute $N_j''(t)$. □

Lemma 3.5.2. *(i) If the inter/intra-component s-wave scattering lengths are the same and so are the external trapping potentials, i.e.*

$$V_1(\boldsymbol{x}) = V_2(\boldsymbol{x}), \boldsymbol{x} \in R^d, \beta_{11} = \beta_{12} = \beta_{22}, \tag{3.31}$$

for any initial condition, for $j = 1, 2$, *we have:*

$$N_j(t) = |\phi_j(\boldsymbol{x}, t)|^2 = \left(N_j^{(0)} - \frac{1}{2} \right) cos(2\lambda t) + \frac{N_j^{(1)}}{2\lambda} sin(2\lambda t) + \frac{1}{2}, \quad t \geq 0. \tag{3.32}$$

In this special case, the density of each component is a periodic function with period $T = \frac{\pi}{|\lambda|}$, *which is only dependent on* λ.

When $\lambda = 0$,

$$N_j(t) \equiv N_j^{(0)}.$$

(ii) For more general cases, for $j = 1, 2$, $t \geq 0$, *we have*

$$N_j(t) = |\phi_j(\boldsymbol{x}, t)|^2 = \left(N_j^{(0)} - \frac{1}{2}\right) cos(2\lambda t) + \frac{N_j^{(1)}}{2\lambda} sin(2\lambda t) + \frac{1}{2} + f_j(t), \quad (3.33)$$

where $f_j(t)$ *satisfies the following second-order ODE:*

$$\begin{cases} f_j^{''}(t) + 4\lambda^2 f_j(t) = F_j(t), \\ f_j(0) = f_j^{'}(0) = 0. \quad t \geq 0. \end{cases} \quad (3.34)$$

Proof. (i) By Lemma 3.5.1, when the special equalities (3.31) are satisfied, we have $F_j(t) = 0$, and

$$N_j^{''}(t) = -2\lambda^2 \left[2N_j(t) - 1\right], \quad t \geq 0,$$

which gives us the unique solution (3.32). (ii) Based on the result in (i), we apply superposition principle and get the unique ODE solution stated above for (3.27) in Lemma 3.5.1. □

II). Angular momentum expectation.

Angular momentum is another important quantity to study the dynamics of rotating BEC. It is a measure of the vortex flux and is defined as follows:

$$\langle L_z \rangle (t) = \langle L_z \rangle_1 (t) + \langle L_z \rangle_2 (t), \quad t \geq 0, \quad (3.35)$$

where

$$\langle L_z \rangle_j (t) = \int_{\mathbb{R}^d} \phi_j^* L_z \phi_j \, \mathrm{d}\mathbf{x}, \quad j = 1, 2, \quad t \geq 0, \quad d = 2, 3. \quad (3.36)$$

We denote

$$J_z = y\partial_x - x\partial_y = -iL_z. \quad (3.37)$$

For any $t, \mathbf{x}$, we have the following equalities:

$$\begin{aligned}\partial_t V_j(\mathbf{x},t) &= \Omega J_z V_j(\mathbf{x},t)\\ &= \Omega(y\partial_x - x\partial_y)V_j(\mathbf{x},t)\\ &= \Omega\frac{\gamma_{x,j}^2-\gamma_{j,y}^2}{2}\left[2\cos(2\Omega t)xy + (y^2-x^2)\sin(2\Omega t)\right]. \quad (3.38)\end{aligned}$$

We define $\eta_j(t)$ as

$$\begin{aligned}\eta_j(t) &= \int_{\mathbb{R}^2}\left[2\cos(2\Omega t)xy + (y^2-x^2)\sin(2\Omega t)\right]|\phi_j(\mathbf{x},t)|^2\,\mathrm{d}\mathbf{x}\\ &= \frac{2}{\gamma_{x,j}^2-\gamma_{j,y}^2}\int_{\mathbb{R}^d} J_z V|\phi_j|^2\,\mathrm{d}\mathbf{x}, \quad t\geq 0. \quad (3.39)\end{aligned}$$

The dynamical law of angular momentum expectation in rotating BEC is shown as follows:

Theorem 3.5.3. *Suppose $(\phi_1(\boldsymbol{x},t),\phi_2(\boldsymbol{x},t))$ is the solution of the CGPE (3.18), we have:*

$$\begin{aligned}\frac{d\langle L_z\rangle_j(t)}{dt} &= \frac{\gamma_{x,j}^2-\gamma_{y,j}^2}{2}\eta_{x,y,j}(t) + \int_{\mathbb{R}^d}\beta_{jk_j}|\phi_j|^2 J_z|\phi_{k_j}|^2\,\mathrm{d}\boldsymbol{x}\\ &\quad +2\lambda\boldsymbol{Re}\left[\int_{\mathbb{R}^d}\phi_{k_j}^* J_z\phi_j\,\mathrm{d}\boldsymbol{x}\right], \quad (3.40)\end{aligned}$$

with J_z defined as in (3.37).

Hence, we can define the energy in another equivalent form:

$$\begin{aligned}E(\phi_1,\phi_2) &= \int_{\mathbb{R}^d}\left[\sum_{j=1}^2\left(\frac{1}{2}|\nabla\phi_j|^2 + V_j(\boldsymbol{x})|\phi_j|^2 - \Omega\boldsymbol{Re}(\phi_j^* L_z\phi_j)\right.\right.\\ &\quad \left.\left.+\sum_{l=1}^2\frac{\beta_{jl}}{2}|\phi_j|^2|\phi_l|^2\right) - 2\lambda\boldsymbol{Re}(\phi_1^*\phi_2)\right]\mathrm{d}\boldsymbol{x}. \quad (3.41)\end{aligned}$$

Thus, we have the conservation of angular momentum expectation, at least in the following cases:

(i): For any given initial data, if we have $\gamma_{x,j}=\gamma_{y,j}$ for $j=1,2$, i.e. the trapping potential is radially symmetric;

(ii): For any given $\gamma_{x,j},\gamma_{y,j}$, if we have $\Omega=0$ and the initial data ϕ_j^0 is even in

either x or y for $j = 1, 2$.

We have the following conservation laws

$$\langle L_z \rangle (t) = \langle L_z \rangle (0), \quad E_n(\phi_1, \phi_2) = E_n(\phi_1^0, \phi_2^0),$$

where E_n is defined in (3.25).

Moreover, when the traps are radially symmetric as defined in (i), if the initial data $(\phi_1^0(\boldsymbol{x}), \phi_2^0(\boldsymbol{x}))$ is further chosen as

$$\phi_j^0(\boldsymbol{x}) = f_j(r)e^{im_j\theta}, \text{ with } m_j \in \boldsymbol{Z} \text{ and } f_j(0) = 0 \text{ when } m_j \neq 0. \tag{3.42}$$

If $\lambda = 0$, then $\left\langle \tilde{L}_z \right\rangle_1 (t)$ and $\left\langle \tilde{L}_z \right\rangle_2 (t)$ are conserved.
On the other hand, if $m_1 = m_2 := m$ in (3.42), then for any given λ, $\left\langle \tilde{L}_z \right\rangle_1 (t)$ and $\left\langle \tilde{L}_z \right\rangle_2 (t)$ are conserved, i.e.

$$\left\langle \tilde{L}_z \right\rangle_j (t) \equiv \left\langle \tilde{L}_z \right\rangle_j (0) = m, \quad t \geq 0, j = 1, 2. \tag{3.43}$$

Proof. Differentiating (3.36) with respect to t, noticing (3.18), integrating by parts, and taking into account that ϕ_j decreases to 0 when $|\mathbf{x}| \to \infty$, we have

$$\begin{aligned}
\frac{d \langle L_z \rangle_j (t)}{dt} &= \int_{\mathbb{R}^d} (\partial_t \phi_j^* L_z \phi_j + \phi_j^* L_z \partial_t \phi_j) \, \mathrm{d}\mathbf{x} \\
&= -\int_{\mathbb{R}^d} \left[-(i\partial_t \phi_j)^* J_z \phi_j + \phi_j^* J_z (i\partial_t \phi_j) \right] \mathrm{d}\mathbf{x} \\
&= -\int_{\mathbb{R}^d} \left[\left(-\frac{1}{2}\nabla^2 \phi_j + V_j(\mathbf{x}, t)\phi_j + \phi_j \sum_{l=1}^{2} \beta_{jl} |\phi_l|^2 - \lambda \phi_{kj} \right) J_z \phi_j^* \right. \\
&\quad \left. + \left(-\frac{1}{2}\nabla^2 \phi^* + V(\mathbf{x}, t)\phi^* + \phi_j^* \sum_{l=1}^{2} \beta_{jl} |\phi_l|^2 - \lambda \phi_{kj}^* \right) J_z \phi_j \right] \mathrm{d}\mathbf{x} \\
&= \frac{1}{2} \int_{\mathbb{R}^d} \left[\nabla^2 \phi_j J_z \phi_j^* + \nabla^2 \phi_j^* J_z \phi_j \right] \mathrm{d}\mathbf{x} \\
&\quad - \int_{\mathbb{R}^d} V_j(\mathbf{x}, t)(\phi_j J_z \phi_j^* + \phi_j^* J_z \phi_j) \, \mathrm{d}\mathbf{x} \\
&\quad - \int_{\mathbb{R}^d} (\phi_j^* J_z \phi_j + \phi_j J_z \phi_j^*)(\beta_{jj} |\phi_j|^2 + \beta_{jk_j} |\phi_{k_j}|^2) \, \mathrm{d}\mathbf{x} \\
&\quad + \int_{\mathbb{R}^d} \lambda (\phi_{k_j}^* J_z \phi_j + \phi_{k_j} J_z \phi_j^*) \, \mathrm{d}\mathbf{x}
\end{aligned}$$

$$
\begin{aligned}
&= -\frac{1}{2}\int_{\mathbb{R}^d}[\nabla\phi\nabla(J_z\phi^*)]\,\mathrm{d}\mathbf{x} - \frac{1}{2}\int_{\mathbb{R}^d}[\nabla\phi^*\nabla(J_z\phi)]\,\mathrm{d}\mathbf{x}\\
&- \int_{\mathbb{R}^d} V(\mathbf{x},t)\phi J_z\phi^*\,\mathrm{d}\mathbf{x}\\
&+ \int_{\mathbb{R}^d}\phi\left[V(\mathbf{x},t)J_z\phi^* + \phi^* J_z V(\mathbf{x},t)\right]\mathrm{d}\mathbf{x}\\
&= \frac{\gamma_{x,j}^2-\gamma_{y,j}^2}{2}\eta_j(t) + \int_{\mathbb{R}^d}\beta_{jk_j}|\phi_j|^2 J_z|\phi_{k_j}|^2\,\mathrm{d}\mathbf{x}\\
&+ 2\lambda\mathbf{Re}\left[\int_{\mathbb{R}^d}\phi_{k_j}^* J_z\phi_j\,\mathrm{d}\mathbf{x}\right],
\end{aligned}
$$

where $\eta_j(t)$ is defined above in (3.39).

For case (i), when $\gamma_{x,j}=\gamma_{y,j}$ for $j=1,2$, we can easily arrive at the conclusion that the total angular momentum expectation $\langle L_z\rangle$ is conserved from the ODE:

$$\frac{d\langle L_z\rangle(t)}{dt}=0,\quad t\geq 0.$$

For case (ii), we know that the solution $\phi_j(\mathbf{x},t)$ is even in first variable x or second variable y due to the assumption of the initial data and symmetry of $V_j(\mathbf{x})$, for $j=1,2$. Then when $\Omega=0$, with $|\phi_j(\mathbf{x},t)|$ even in either x or y, we easily have the conservation of angular momentum.

By (3.41), we have:

$$E(\phi_1,\phi_2)=E_n(\phi_1,\phi_2)-\Omega\langle L_z\rangle(t),$$

hence

$$\frac{dE_n(t)}{dt}=\frac{dE(t)}{dt}+\Omega\frac{d}{dt}\langle L_z\rangle(t)=0. \tag{3.44}$$

□

III). Condensate width

We define the condensate width as follows along the α-axis ($\alpha=x,y,z$ for 3D), to quantify the dynamics of the problem (3.18):

$$\langle\sigma_\alpha\rangle(t)=\sqrt{\delta_\alpha(t)}=\sqrt{\delta_{\alpha,1}(t)+\delta_{\alpha,2}(t)}, \tag{3.45}$$

where

$$\delta_{\alpha,j} = \left\langle \alpha^2 \right\rangle (t) = \int_{\mathbb{R}^d} \alpha^2 |\phi_j|^2 \, \mathrm{d}\mathbf{x}, \quad \alpha = x, y, z, \tag{3.46}$$

we have the following dynamical law for the condensate width:

Theorem 3.5.4. *i). Generally, for d=2,3, and any potential and initial data, the condensate width satisfies:*

$$\begin{cases} \dfrac{d^2\delta_\alpha(t)}{d^2t} + 2\gamma_\alpha^2 \delta_\alpha(t) = \displaystyle\int_{\mathbb{R}^d} \sum_{j=1}^{2} \Big[2|\partial_\alpha \phi_j|^2 - 2\alpha |\phi_j|^2 \partial_\alpha V_{j,rot} \\ \qquad\qquad + |\phi_j|^2 \displaystyle\sum_{l=1}^{2} \beta_{jl} |\phi_l|^2 \Big] \, \mathrm{d}\boldsymbol{x}, \\ \delta_\alpha(0) =: \delta_\alpha^{(0)} = \int_{\mathbb{R}^d} \alpha^2 (|\phi_1^0|^2 + |\phi_1^0|^2) \, \mathrm{d}\boldsymbol{x}, \\ \dot{\delta}_\alpha(0) =: \delta_\alpha^{(1)} = 2 \displaystyle\sum_{j=1}^{2} \int_{\mathbb{R}^d} \alpha Im \left[(\phi_j^0)^* \partial_\alpha \phi_j^0 \right] \, \mathrm{d}\boldsymbol{x}. \end{cases} \tag{3.47}$$

ii). In 2D with a radially symmetric trap, i.e. $d = 2$, and $\gamma_{x,j} = \gamma_{y,j} := \gamma_r$, if there is no external driving field, i.e. $\lambda = 0$, for any initial data (ϕ_1^0, ϕ_2^0), we have:

$$\begin{cases} \delta_r(t) = \frac{E(\phi_1^0, \phi_2^0) + \Omega \langle L_z \rangle (0)}{\gamma_r^2} \left[1 - \cos(2\gamma_r t) \right] + \delta_r^{(0)} \cos(2\gamma_r t) + \frac{\delta_r^{(1)}}{2\gamma_r} \sin(2\gamma_r t), \\ \delta_r(0) =: \delta_r^{(0)} = \delta_x(0) + \delta_y(0) = \int_{\mathbb{R}^d} (x^2 + y^2) |\phi^0|^2 \, \mathrm{d}\boldsymbol{x}, \\ \dot{\delta}_r(0) =: \delta_r^{(1)} = \dot{\delta}_x(0) + \dot{\delta}_y(0). \end{cases} \tag{3.48}$$

Moreover, if the initial data $(\phi_1^0(\boldsymbol{x}), \phi_2^0(\boldsymbol{x}))$ is chosen as in (3.42), we have, for any $t \geq 0$,

$$\begin{aligned} \delta_x(t) &= \delta_y(t) = \frac{1}{2} \delta_r(t) \\ &= \frac{E(\phi_1^0, \phi_2^0) + \Omega \langle L_z \rangle (0)}{2\gamma_r^2} \left[1 - \cos(2\gamma_r t) \right] \\ &\quad + \delta_x^{(0)} \cos(2\gamma_r t) + \frac{\delta_x^{(1)}}{2\gamma_r} \sin(2\gamma_r t). \end{aligned} \tag{3.49}$$

Thus the condensate widths are periodic functions with frequency equals to two times of the trapping frequency.

iii). For the other cases with a radially symmetric trap, we have , for $t \geq 0$,

$$\begin{aligned}\delta_r(t) &= \frac{E(\phi_1^0,\phi_2^0)+\Omega\langle L_z\rangle(0)}{\gamma_r^2}\left[1-\cos(2\gamma_r t)\right]\\ &\quad +\delta_r^{(0)}\cos(2\gamma_r t)+\frac{\delta_r^{(1)}}{2\gamma_r}\sin(2\gamma_r t)+g_r(t),\end{aligned} \tag{3.50}$$

where $g_r(t)$ *is the solution of the following equations:*

$$\frac{d^2 g_r(t)}{d^2 t}+4\gamma_r^2 g_r(t)=G_r(t),\quad g_r(0)=\frac{dg_r(0)}{dt}=0,$$

with $G_r(t)=8\lambda\int_{\mathbb{R}^d}\boldsymbol{Re}(\phi_1^*\phi_2)\,\mathrm{d}\boldsymbol{x}$.

Proof. i). Differentiate (3.46) directly with respect to t, noticing (3.18), integrate by parts, we have:

$$\begin{aligned}\frac{d\delta_{\alpha,j}(t)}{dt} &= \frac{d}{dt}\int_{\mathbb{R}^d}\alpha^2|\phi_j|^2\,\mathrm{d}\mathbf{x}=\int_{\mathbb{R}^d}\alpha^2(\phi_j\partial_t\phi_j^*+\phi_j^*\partial_t\phi_j)\,\mathrm{d}\mathbf{x}\\ &= i\int_{\mathbb{R}^d}\alpha^2\left[\phi_j(i\partial_t\phi_j)^*-\phi_j^*(i\partial_t\phi_j)\right]\,\mathrm{d}\mathbf{x}\\ &= \frac{i}{2}\int_{\mathbb{R}^d}\Big[\nabla\phi^*(\alpha^2\nabla\phi+\phi\nabla\alpha^2)-\nabla\phi(\alpha^2\nabla\phi^*+\phi^*\nabla\alpha^2)\\ &\quad +2\lambda\alpha^2(\phi_j^*\phi_{k_j}-\phi_j\phi_{k_j}^*)\Big]\,\mathrm{d}\mathbf{x}\\ &= \int_{\mathbb{R}^d}\left[i\alpha(\phi_j\partial_\alpha\phi_j^*-\phi_j^*\partial_\alpha\phi_j)+i\lambda\alpha^2(\phi_j^*\phi_{k_j}-\phi_j\phi_{k_j}^*)\right]\,\mathrm{d}\mathbf{x}.\end{aligned}$$

And we differentiate again with respect to t:

$$\begin{aligned}\frac{d^2\delta_{\alpha,j}(t)}{dt^2} &= i\int_{\mathbb{R}^d}\alpha(\phi_t\phi_\alpha^*+\phi\phi_{t\alpha}^*-\phi_t^*\phi_\alpha-\phi^*\phi_{t\alpha})\,\mathrm{d}\mathbf{x}\\ &= i\int_{\mathbb{R}^d}\Big[2i\alpha(\partial_t\phi_j\partial_\alpha\phi_j^*-\partial_t\phi_j^*\partial_\alpha\phi_j)+i(\phi_j^*\partial_t\phi_j-\phi_j\partial_t\phi_j^*)\\ &\quad +i\lambda\alpha^2(\partial_t\phi_j^*\phi_{k_j}-\partial_t\phi_j\phi_{k_j}^*+\phi_j^*\partial_t\phi_{k_j}+\phi_j\partial_t\phi_{k_j}^*)\Big]\,\mathrm{d}\mathbf{x}\\ &:= I+II+III.\end{aligned}$$

Applying integration by parts, we have:

$$\begin{aligned}
I &:= \int_{\mathbb{R}^d} 2\alpha \left[(i\partial_t\phi_j)\partial_\alpha\phi_j + (-i\partial_t\phi_j^*)\partial_\alpha\phi_j)\right] \,\mathrm{d}\mathbf{x} \\
&= \int_{\mathbb{R}^d}\Bigg[-\alpha(\partial_\alpha\phi_j^*\nabla^2\phi_j + \partial_\alpha\phi_j\nabla^2\phi_j^*) \\
&\quad +2\alpha(V_j(\mathbf{x}) + \sum_{l=1}^{2}\beta_{jl}|\phi_l|^2)(\phi_j\partial_\alpha\phi_j^* + \phi_j^*\partial_\alpha\phi_j) \\
&\quad -4\lambda\alpha\mathbf{Re}(\phi_{k_j}\partial_\alpha\phi_j^*)\Bigg] \,\mathrm{d}\mathbf{x} \\
&= \int_{\mathbb{R}^d}\Bigg[-|\nabla\phi_j|^2 + 2|\partial_\alpha\phi_j|^2 - 2V_j(\mathbf{x})|\phi_j|^2 - 2\alpha|\phi_j|^2\partial_\alpha(V_j(\mathbf{x})) - \beta_{jj}|\phi_j|^4 \\
&\quad +2\beta_{jk_j}\alpha|\phi_{k_j}|^2\partial_\alpha|\phi_j|^2 - 2\lambda\alpha(\phi_{k_j}\partial_\alpha\phi_j^* + \phi_{k_j}^*\partial_\alpha\phi_j)\Bigg] \,\mathrm{d}\mathbf{x}.
\end{aligned}$$

$$\begin{aligned}
II &:= \int_{\mathbb{R}^d}\left[(\phi_j^*(i\partial_t\phi_j) + (-i\partial_t\phi_j^*)\phi_j\right] \,\mathrm{d}\mathbf{x} \\
&= 2\int_{\mathbb{R}^d}\left[\frac{1}{2}|\nabla\phi_j|^2 + V_j(\mathbf{x})|\phi_j|^2 + \sum_{l=1}^{2}\beta_{jl}|\phi_l|^2|\phi_j|^2 - \lambda\mathbf{Re}(\phi_j^*\phi_{k_j})\right] \,\mathrm{d}\mathbf{x}
\end{aligned}$$

$$III := i\lambda\int_{\mathbb{R}^d}\alpha^2(\partial_t\phi_j^*\phi_{k_j} - \partial_t\phi_j\phi_{k_j}^* + \phi_j^*\partial_t\phi_{k_j} - \phi_j\partial_t\phi_{k_j}^*)\,\mathrm{d}\mathbf{x}$$

Hence we have, for $j = 1, 2$:

$$\begin{aligned}
\frac{d^2\delta_{\alpha,j}(t)}{d^2t} &= \int_{\mathbb{R}^d}\left[2|\partial_\alpha\phi_j|^2 - 2\alpha|\phi_j|^2\partial_\alpha(V_j(\mathbf{x})) + \beta_{jj}|\phi_j|^4 - 2\beta_{jk_j}\alpha|\phi_j|^2\partial_\alpha|\phi_{k_j}|^2\right] \,\mathrm{d}\mathbf{x} \\
&\quad -2\lambda\int_{\mathbb{R}^d}\Big[\mathbf{Re}(\phi_j^*\phi_{k_j}) + 2\alpha\mathbf{Re}(\phi_{k_j}^*\partial_\alpha\phi_j)\Big] \,\mathrm{d}\mathbf{x} \\
&\quad +i\lambda\int_{\mathbb{R}^d}\alpha^2(\partial_t\phi_j^*\phi_{k_j} - \partial_t\phi_j\phi_{k_j}^* + \phi_j^*\partial_t\phi_{k_j} - \phi_j\partial_t\phi_{k_j}^*)\,\mathrm{d}\mathbf{x}. \qquad (3.51)
\end{aligned}$$

Hence we have:

$$\frac{d^2\delta_\alpha(t)}{d^2t} + 2\gamma_\alpha^2\delta_\alpha(t) = \int_{\mathbb{R}^d}\sum_{j=1}^{2}\left[2|\partial_\alpha\phi_j|^2 - 2\alpha|\phi_j|^2\partial_\alpha V_{j,rot} + |\phi_j|^2\sum_{l=1}^{2}\beta_{jl}|\phi_l|^2\right] \,\mathrm{d}\mathbf{x}.$$

(ii). If $d = 2$, and $\gamma_{x,j} = \gamma_{y,j} := \gamma_r$ for $j = 1, 2$, we have:

$$\begin{cases} \frac{d^2\delta_x(t)}{d^2t} + 2\gamma_r^2\delta_x(t) = \int_{\mathbb{R}^d} \sum_{j=1}^{2} \left[2|\partial_x\phi_j|^2 - 2x|\phi_j|^2\partial_x V_{j,rot} + |\phi_j|^2 \sum_{l=1}^{2} \beta_{jl}|\phi_l|^2 \right] \mathrm{d}\mathbf{x}, \\ \frac{d^2\delta_y(t)}{d^2t} + 2\gamma_r^2\delta_y(t) = \int_{\mathbb{R}^d} \sum_{j=1}^{2} \left[2|\partial_y\phi_j|^2 - 2y|\phi_j|^2\partial_y V_{j,rot} + |\phi_j|^2 \sum_{l=1}^{2} \beta_{jl}|\phi_l|^2 \right] \mathrm{d}\mathbf{x}. \end{cases} \tag{3.52}$$

Add (3.52) and we have the ODE for $\delta_r(t)$:

$$\begin{aligned} \frac{d^2\delta_r(t)}{d^2t} &= -4\gamma_r^2\delta_r(t) + 4E(\phi_1(\mathbf{x},t), \phi_2(\mathbf{x},t)) + 4\Omega \langle L_z \rangle (t) \\ &\quad +8\lambda \int_{\mathbb{R}^d} \mathbf{Re}(\phi_1^*\phi_2)\, \mathrm{d}\mathbf{x} \\ &= -4\gamma_r^2\delta_r(t) + 4E(\phi_1^0, \phi_2^0) + 4\Omega \langle L_z \rangle (0) + 8\lambda \int_{\mathbb{R}^d} \mathbf{Re}(\phi_1^*\phi_2)\, \mathrm{d}\mathbf{x}. \end{aligned}$$

When $\lambda = 0$, the above ODE collapses to

$$\frac{d^2\delta_r(t)}{d^2t} = -4\gamma_r^2\delta_r(t) + 4E(\phi_1^0, \phi_2^0) + 4\Omega \langle L_z \rangle (0), \quad t \geq 0, \tag{3.53}$$

with the initial condition as:

$$\begin{cases} \delta_r(0) =: \delta_r^{(0)} = \delta_x(0) + \delta_y(0), \\ \dot{\delta}_r(0) =: \delta_r^{(1)} = \dot{\delta}_x(0) + \dot{\delta}_y(0). \end{cases} \tag{3.54}$$

We solve the ODE (3.46) with the initial data given in (3.54), we could find the following unique solution:

$$\delta_r(t) = \frac{E(\phi_1^0, \phi_2^0) + \Omega \langle L_z \rangle (0)}{\gamma_r^2} [1 - \cos(2\gamma_r t)] + \delta_r^{(0)} \cos(2\gamma_r t) + \frac{\delta_r^{(1)}}{2\gamma_r} \sin(2\gamma_r t). \tag{3.55}$$

In addition, if the initial data has radially symmetric structure as shown in (3.42), then $V_j(\mathbf{x}) = V_{j,hos}(\mathbf{x})$. we have, for any $t \geq 0$,

$$\begin{aligned} \delta_x(t) &= \int_{\mathbb{R}^d} x^2|\phi|^2\, \mathrm{d}\mathbf{x} = \int_0^\infty \int_0^{2\pi} r^2 \cos^2\theta |f(r,t)|^2 r d\theta dr \\ &= \pi \int_0^\infty r^2|f(r,t)|^2 r dr = \int_0^\infty \int_0^{2\pi} r^2 \sin^2\theta |f(r,t)|^2 r d\theta dr \\ &= \int_{\mathbb{R}^d} y^2|\phi|^2\, \mathrm{d}\mathbf{x} = \delta_y(t) = \frac{1}{2}\delta_r(t). \end{aligned}$$

Thus we could show the result above in (3.49).

(iii). In general, when $\lambda \neq 0$, the second-order ODE has the following form:

$$\frac{d^2\delta_r(t)}{d^2t} = -4\gamma_r^2\delta_r(t) + 4E(\phi_1^0, \phi_2^0) + 4\Omega \langle L_z \rangle (0) + G_r(t). \tag{3.56}$$

We solve the second-order ODE and could get a unique solution as defined in (3.50). □

IV). Center of mass.

In this section, we would like to study the analytical solutions for the center of mass. Let $(\phi_1(\mathbf{x}), \phi_2(\mathbf{x}))$ be a solution of the transformed CGPEs (3.18). For any initial data given, we then define the center of mass as follows:

$$\langle \mathbf{x} \rangle_j (t) = \int_{\mathbb{R}^d} \mathbf{x} |\phi_j|^2 \, \mathrm{d}\mathbf{x} =: (x_j^c(t), y_j^c(t), z_j^c(t))^T. \tag{3.57}$$

By this definition, we have:

Lemma 3.5.5. *When $\lambda = 0$, we have the following equations:*

$$\begin{cases} \frac{d^2 \langle \boldsymbol{x} \rangle_j (t)}{dt^2} + B(t) \langle \boldsymbol{x} \rangle_j (t) = 0, \\ \langle \boldsymbol{x} \rangle_j (0) = \boldsymbol{x}_j^0, \\ \langle \dot{\boldsymbol{x}} \rangle_j (0) = 0, \end{cases} \tag{3.58}$$

with $B(t) = A^T(t)\Lambda A(t)$, where $\Lambda = diag(\gamma_{x,j}, \gamma_{j,y})$ in 2-d and $diag(\gamma_{x,j}, \gamma_{j,y}, \gamma_{j,z})$ in 3-d, i.e.

$$B(t) = \frac{1}{2} \begin{bmatrix} \gamma_{x,j}^2 + \gamma_{j,y}^2 & 0 \\ 0 & \gamma_{x,j}^2 + \gamma_{j,y}^2 \end{bmatrix} + \frac{\gamma_{x,j}^2 - \gamma_{j,y}^2}{2} \begin{bmatrix} \cos(2\Omega t) & \sin(2\Omega t) \\ \sin(2\Omega t) & -\cos(2\Omega t) \end{bmatrix}, \tag{3.59}$$

if $d = 2$, and

$$B(t) = \frac{1}{2} \begin{bmatrix} \gamma_{x,j}^2 + \gamma_{j,y}^2 & 0 & 0 \\ 0 & \gamma_{x,j}^2 + \gamma_{j,y}^2 & 0 \\ 0 & 0 & 2\gamma_{j,z}^2 \end{bmatrix} + \frac{\gamma_{x,j}^2 - \gamma_{j,y}^2}{2} \begin{bmatrix} \cos(2\Omega t) & \sin(2\Omega t) & 0 \\ \sin(2\Omega t) & -\cos(2\Omega t) & 0 \\ 0 & 0 & 0 \end{bmatrix}, \tag{3.60}$$

for $d = 3$.

Proof. We can follow exactly the same proof as in rotational BEC in Lemma 2.3.4. □

The ODE system (3.58) governing the motion of center of mass for rotating two-component BEC is the same as the one for single-component BEC, which as been discussed in Lemma 2.3.4. And the ODE system was solved analytically and classified in details based on parameters $\Omega, \gamma_{x,j}, \gamma_{y,j}, \gamma_{z,j}$.
Different cases and their respected results will be presented in section 3.7.

3.6 Numerical methods

Similar to the section 2.4 for single-component BEC, we present an accurate and efficient numerical method which solves the transformed rotating CGPEs under a rotating Lagrangian coordinate as shown in (3.18). Without loss of generality, we take $d = 2$.
We begin by applying the second order time splitting method, and then proceed with Fourier spectral method in x_j and y_j direction.
We take $\Delta t > 0$ as a time step. For $n = 0, 1, 2, \ldots, N$ from time $t = t_n = n\Delta t$ to $t = t_{n+1} = t_n + \Delta t$, we could solve the transformed CGPEs (3.18) in the following three steps:

Step I:

$$\begin{cases} i\partial_t \phi_j = -\frac{1}{2}\nabla^2 \phi_j, \\ \phi_j(\mathbf{x}, 0) = \phi_j^0(\mathbf{x}), \quad \mathbf{x} \in R^d, \ d = 2, 3. \end{cases} \tag{3.61}$$

Step II:

$$\begin{cases} i\partial_t \phi_j = V_j(\mathbf{x}, t)\phi_j + \sum_{l=1}^{2} \beta_{jl}|\phi_l|^2 \phi_j, \\ \phi_j(\mathbf{x}, 0) = \phi_j^0(\mathbf{x}), \quad \mathbf{x} \in R^d, \ d = 2, 3. \end{cases} \tag{3.62}$$

Step III:

$$\begin{cases} i\partial_t \phi_j = -\lambda \phi_{k_j}, \\ \phi_j(\mathbf{x}, 0) = \phi_j^0(\mathbf{x}), \quad \mathbf{x} \in R^d, \ d = 2, 3. \end{cases} \tag{3.63}$$

These three steps are solved for the same time of length Δt. For step I (3.61), we will apply Fourier spectral methods which are the same as single-component BEC, as discussed in subsection 2.4.2 and 2.4.3. Step II (3.62) and Step III (3.62) can be solved analytically. For Step II, similar to single-component BEC, we have

$$|\phi_j(\mathbf{x},t)|^2 = |\phi_j(\mathbf{x},t_n)|^2, \quad t \in [t_n, t_{n+1}]\,. \tag{3.64}$$

Then solve the ODE in (3.62) directly which gives us:

$$\phi_j(\mathbf{x},t) = \phi_j(\mathbf{x},t_n) exp\left[-i\left(\int_{t_n}^{t} V_j(\mathbf{x},s)ds + \sum_{l=1}^{2}\beta_{jl}|\phi_l(\mathbf{x},t_n)|^2\right)(t-t_n)\right]. \tag{3.65}$$

Take $d = 2$ and substitute (3.19) in (2.52) and integrate, we have the exact analytical solution given by:

For $\gamma_{x,j} = \gamma_{j,y} = \gamma_{j,r}$,

$$\int_{t_n}^{t} V_j(\mathbf{x},s)ds = \frac{1}{2}\gamma_{j,r}^2(x^2+y^2)(t-t_n). \tag{3.66}$$

For $\gamma_{x,j} \neq \gamma_{j,y}$,

$$\begin{aligned}\int_{t_n}^{t} V_j(\mathbf{x},s)ds \;=\; & \frac{1}{2}(\gamma_{x,j}^2x^2+\gamma_{j,y}^2y^2)(t-t_n) \\ & +\frac{1}{4}(\gamma_{x,j}^2-\gamma_{j,y}^2)\Bigg[(y^2-x^2)\Bigg(t-t_n \\ & -\frac{1}{2\Omega}(\sin 2\Omega t - \sin 2\Omega t_n)\Bigg) \\ & +\frac{xy}{\Omega}(\cos 2\Omega t - \cos 2\Omega t_n)\Bigg].\end{aligned} \tag{3.67}$$

As discussed in the single-component BEC, we can also apply numerical quadrature method to approximate $V_j(\mathbf{x},t)$.

For Step III (3.63), we can rewrite it as

$$i\partial_t\phi = -\lambda A\phi, \quad A := \begin{bmatrix}0 & 1\\ 1 & 0\end{bmatrix}, \quad \phi := \begin{bmatrix}\phi_1\\ \phi_2\end{bmatrix}. \tag{3.68}$$

Since A is real and diagonalizable, we can solve (3.68) analytically and obtain:

$$\phi(\mathbf{x},t) = e^{i\lambda A(t-t_n)}\phi(\mathbf{x},t_n) = \begin{bmatrix} \cos(\lambda(t-t_n)) & i\sin(\lambda(t-t_n)) \\ i\sin(\lambda(t-t_n)) & \cos(\lambda(t-t_n)) \end{bmatrix} \phi(\mathbf{x},t_n). \tag{3.69}$$

In practice, we often apply the second order Strang splitting method [70, 76].

3.7 Numerical results

3.7.1 Dynamics of energy and density

To verify the dynamics of the densities $N_j(t) = \| \phi_j(\mathbf{x},t) \|^2$, for $j = 1, 2$, we take $\lambda = 1$, $\Omega = 0.6$, $\gamma_{x,j} = \gamma_{y,j} = 1$. The initial data in (3.18) is chosen as

$$\phi_1^0(\mathbf{x}) = \frac{x+iy}{\sqrt{\pi}} \exp(-\frac{x^2+y^2}{2}), \quad \phi_2^0(\mathbf{x}) \equiv 0, \quad \mathbf{x} \in \mathbb{R}^2. \tag{3.70}$$

We take the following two cases to compare the dynamics of total density and density of each component:

i $\beta_{11} = \beta_{12} = \beta_{22} = 500$,

ii $\beta_{11} = 500$, $\beta_{12} = 300$ and $\beta_{22} = 400$.

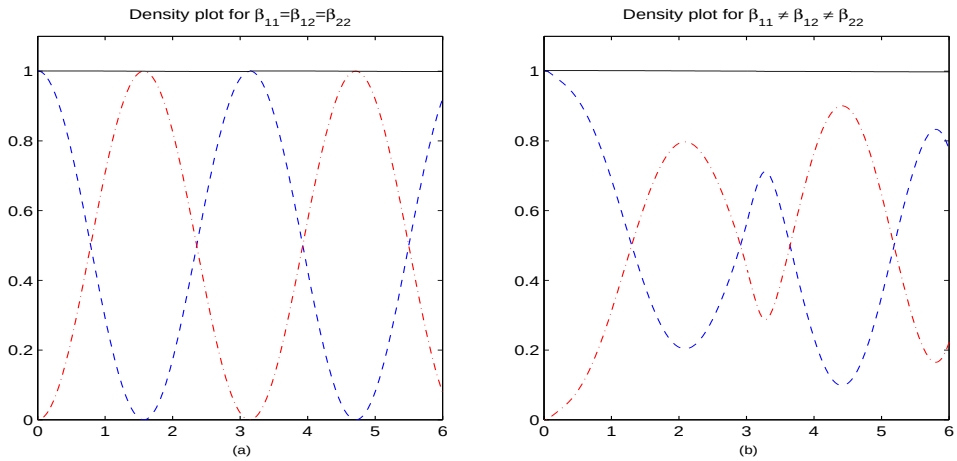

Figure 3.1: Dynamics of total density and density of each component for case i. (left) and case ii. (right).

Fig . 3.1 shows the time evolution of the total density as well as densities of each component for case i. and case ii. We can conclude that: (i) the total density is always conserved; (ii) When $\beta_{11} = \beta_{12} = \beta_{22}$, the densities of both components are periodic functions with period $T = \pi/|\lambda|$; (iii) otherwise when $\beta_{11} \neq \beta_{12} \neq \beta_{22}$, the densities of both components are quasiperiodic[1] and oscillate at period $T = \pi$ with a perturbation.

3.7.2 Conservation of angular momentum expectation

According to Lemma 3.5.3, we take the initial data as shown in (3.42), with $\Omega = 0.6$, $\beta_{11} = 400, \beta_{12} = 388$ and $\beta_{22} = 376$. We are interested in the following cases, for $j = 1, 2$,

i. $\lambda \neq 0$, $m_1 = m_2$ and $\gamma_{x,j} = \gamma_{y,j}$,

ii. $\lambda \neq 0$, $m_1 = m_2$ and $\gamma_{x,j} \neq \gamma_{y,j}$,

iii. $\lambda = 0$, $m_1 = m_2$ and $\gamma_{x,j} \neq \gamma_{y,j}$.

We take Following the Fig. 3.2-3.4, we can see that $\gamma_{x,j} = \gamma_{y,j}$, i.e. both of the external trapping energy being symmetric is a sufficient condition for the total expectation of angular momentum to be conserved and is necessary for angular momentum expectation conservation of each component.

3.7.3 Center of mass

In this subsection, we study the time evolution of center of mass as well as how the density evolves.

$$\phi_j^0(\mathbf{x}) = \phi_j^v(\mathbf{x} - \mathbf{x}_j^0), \quad \mathbf{x} \in \mathbb{R}^d. \tag{3.71}$$

where ϕ_j^v is the central vortex state with winding number $+1$ in the two component BEC with parameters of $\Omega = 1$, $\beta_{11} = 200, \beta_{12} = 194$ and $\beta_{22} = 188$, and $\mathbf{x}_j^0$ is a given point in $\mathbb{R}^d$. We study the time evolution of the density and center of mass for three different cases:

[1] A function f is said to be quasiperiodic with quasiperiod ω if there exists a function g such that $f(x + \omega) = g(x)f(x)$. When g is identically equal to 1, we call f a periodic function.

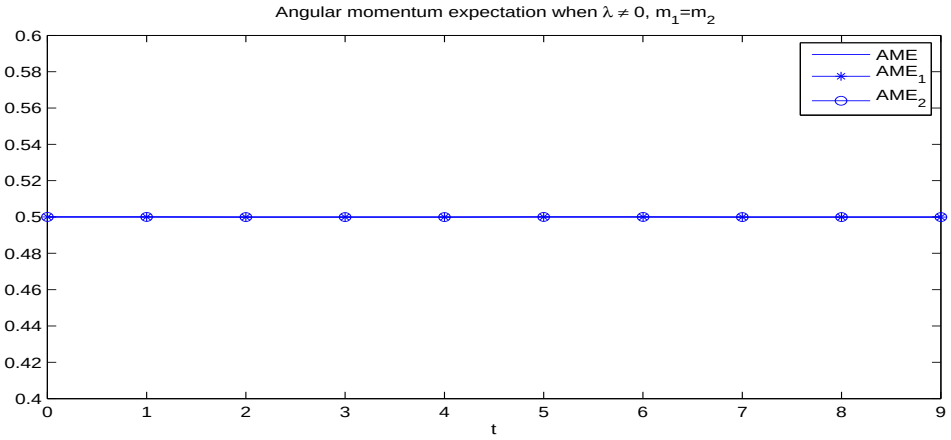

Figure 3.2: Dynamics of angular momentum expectation $\langle L_z \rangle (t)$ (solid line), $\left\langle \tilde{L}_z \right\rangle_1 (t)$ ('-*') and $\left\langle \tilde{L}_z \right\rangle_2 (t)$ ('-o') when $\lambda \neq 0$ and $\gamma_{x,j} = \gamma_{y,j}$ for $j = 1, 2$.

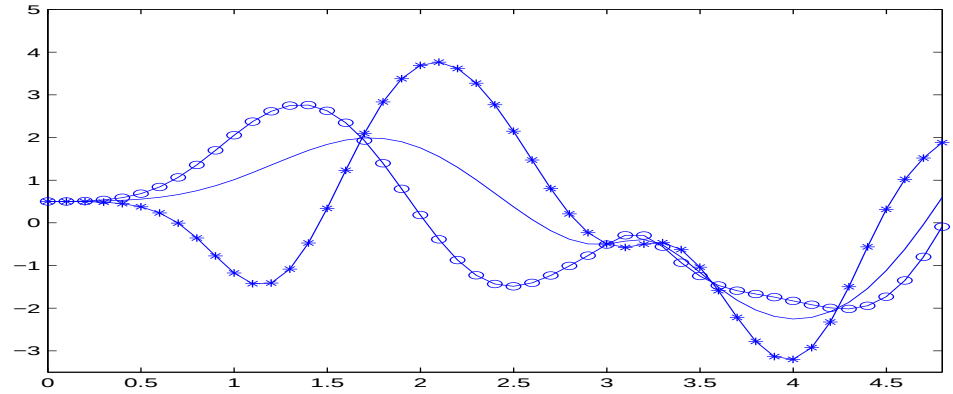

Figure 3.3: Dynamics of angular momentum expectation $\langle L_z \rangle (t)$ (solid line), $\left\langle \tilde{L}_z \right\rangle_1 (t)$ ('-*') and $\left\langle \tilde{L}_z \right\rangle_2 (t)$ ('-o') when $\lambda \neq 0$ and $\gamma_{x,j} \neq \gamma_{y,j}$ for $j = 1, 2$.

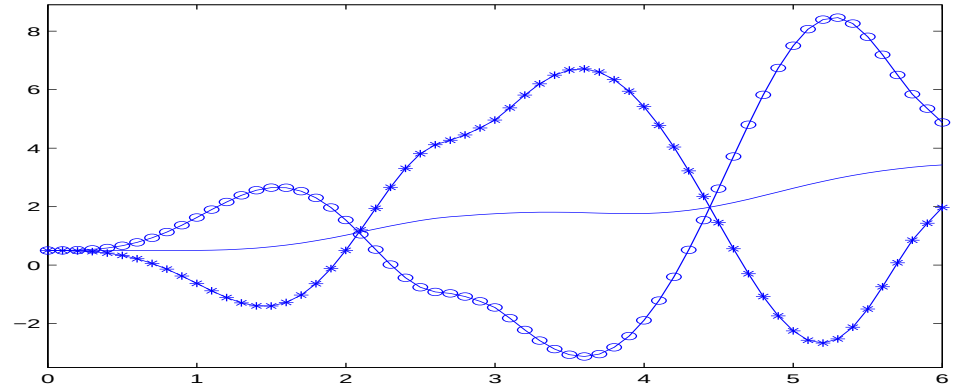

Figure 3.4: Dynamics of angular momentum expectation $\langle L_z \rangle (t)$ (solid line), $\left\langle \tilde{L}_z \right\rangle_1 (t)$ ('-*') and $\left\langle \tilde{L}_z \right\rangle_2 (t)$ ('-o') when $\lambda = 0$ and $\gamma_{x,j} \neq \gamma_{y,j}$ for $j = 1, 2$.

i. Traps and centers shifted are the same: i.e. $\mathbf{x}_1^0 = \mathbf{x}_2^0 = \mathbf{x}^0 = (2,2)^T$, and $\gamma_{x,j} = \gamma_{y,j} = 1$, for $j = 1, 2$.

ii. Traps are the same but centers shifted are different: i.e. $\mathbf{x}_1^0 = -\mathbf{x}_2^0 = \mathbf{x}^0 = (2,2)^T$, and $\gamma_{x,j} = \gamma_{y,j} = 1$, for $j = 1, 2$.

iii. Centers shifted are the same but traps are different: i.e. $\mathbf{x}_1^0 = \mathbf{x}_2^0 = \mathbf{x}^0 = (2,2)^T$, and $\gamma_{x,1} = \gamma_{y,1} = 1$, $\gamma_{x,2} = \gamma_{y,2} = 2$.

Fig. 3.5-3.7 depicts the density surface of $|\phi_1|^2$ and $|\phi_2|^2$ at different times for case (i)-(iii). And Fig. 3.8 shows the dynamics of total center of mass as well as center of mass for each component under the new coordinate system for case (i). Fig. 3.9 transforms the movement of center of mass back to the original coordinate system. We can conclude that in case (i), when $\mathbf{x}_1^0 = \mathbf{x}_2^0$, and $\gamma_{x,j} = \gamma_{y,j}$, the density functions of the two components move like solitary waves in 2D and their shapes do not change throughout time (c.f. Fig. 3.5). While in other cases, their shapes change dramatically (c.f. Figs. 3.6 and3.7).

3.7.4 Condensate width

To verify the dynamical laws of condensate width presented in Theorem 3.5.4, we take initial data as (3.71), with $\gamma_{x,j} = \gamma_{y,j}$ for $j = 1, 2$,

i $\lambda = 0$ and $V_1(\mathbf{x}) = V_2(\mathbf{x})$,

ii $\lambda \neq 0$ and $V_1(\mathbf{x}) = V_2(\mathbf{x})$,

iii $\lambda = 0$ and $V_1(\mathbf{x}) \neq V_2(\mathbf{x})$.

We take $\Omega = 0.6$, $\lambda = 0$, $\beta_{11} = 400, \beta_{12} = 388$ and $\beta_{22} = 376$. Fig. 3.10-3.12 show the time evolution of condensate width corresponding the above three cases: (i). $\lambda = 0$ and $\gamma_{x,j} = \gamma_{y,j} = 1$, for $j = 1, 2$; (ii). $\lambda = 1$ and $\gamma_{x,j} = \gamma_{y,j} = 1$, for $j = 1, 2$; (iii). $\lambda = 0$ and $\gamma_{x,1} = \gamma_{y,2} = 1$, $\gamma_{x,2} = \gamma_{y,1} = 1.2$.

We can see that in case (i) (c.f. Fig 3.10), $\sigma_r(t), \sigma_x(t), \sigma_y(t)$ are periodic functions with $\sigma_x(t) = \sigma_y(t) = \frac{1}{2}\sigma_r(t)$, and period $T = \pi/\gamma_{x,1} = \pi$. In case (ii), with $\gamma_{x,j} = \gamma_{y,j} = 1$, for $j = 1, 2$, we still have $\sigma_x(t) = \sigma_y(t) = \frac{1}{2}\sigma_r(t)$, but they

oscillate with a perturbation and are quasi-periodic functions. In case (iii), we can observe that $\sigma_x(t) \neq \sigma_y(t)$ and as case (ii), they oscillate with a perturbation.

3.7.5 Dynamics of vortex lattices

We are interested in the time evolution of vortex lattices. We take the initial data as:

$$\phi_1^0(\mathbf{x}) = \prod_{l=1}^{M} \frac{x + im_l y}{\sqrt{\pi}} \exp(-\frac{x^2+y^2}{2}), \quad \phi_2^0(\mathbf{x}) \equiv 0, \quad \mathbf{x} \in R^2, \tag{3.72}$$

where M is the total number of interacting vortices. We take $M = 4$ and 9 to analyse separately. For $M = 4$, we take $\Omega = 0.6$, $\gamma_{x,j} = \gamma_{y,j} = 1$, for $j = 1, 2$, $\mathbf{x}_1^0 = \mathbf{x}_2^0 = (0, 0)$, $\lambda = 1$, $\beta_{11} = \beta_{12} = \beta_{22} = 100$ (c.f. Fig. 3.13). For $M = 9$, we take $\Omega = 01$, $\gamma_{x,j} = \gamma_{y,j} = 5$, for $j = 1, 2$, $\mathbf{x}_1^0 = \mathbf{x}_2^0 = (0, 0)$, $\lambda = 1$, $\beta_{11} = \beta_{12} = \beta_{22} = 500$ (c.f. Fig. 3.14).

According to dynamics of mass, for both cases, $N_1(t)$ and $N_2(t)$ are periodic functions with $T = \pi$. We notice that for both cases, initially the density is only observed in component one, as given in initial condition (3.72), gradually, at $t = T/4$, the densities are equally distributed into two components; at $t = T/2$, the densities are totally transformed to component two; at $t = 3T/4$, the densities redistribute to both two components; and at $t = T = \pi$, the densities are almost transformed back to component one (c.f. Fig 3.13 and Fig. 3.14).

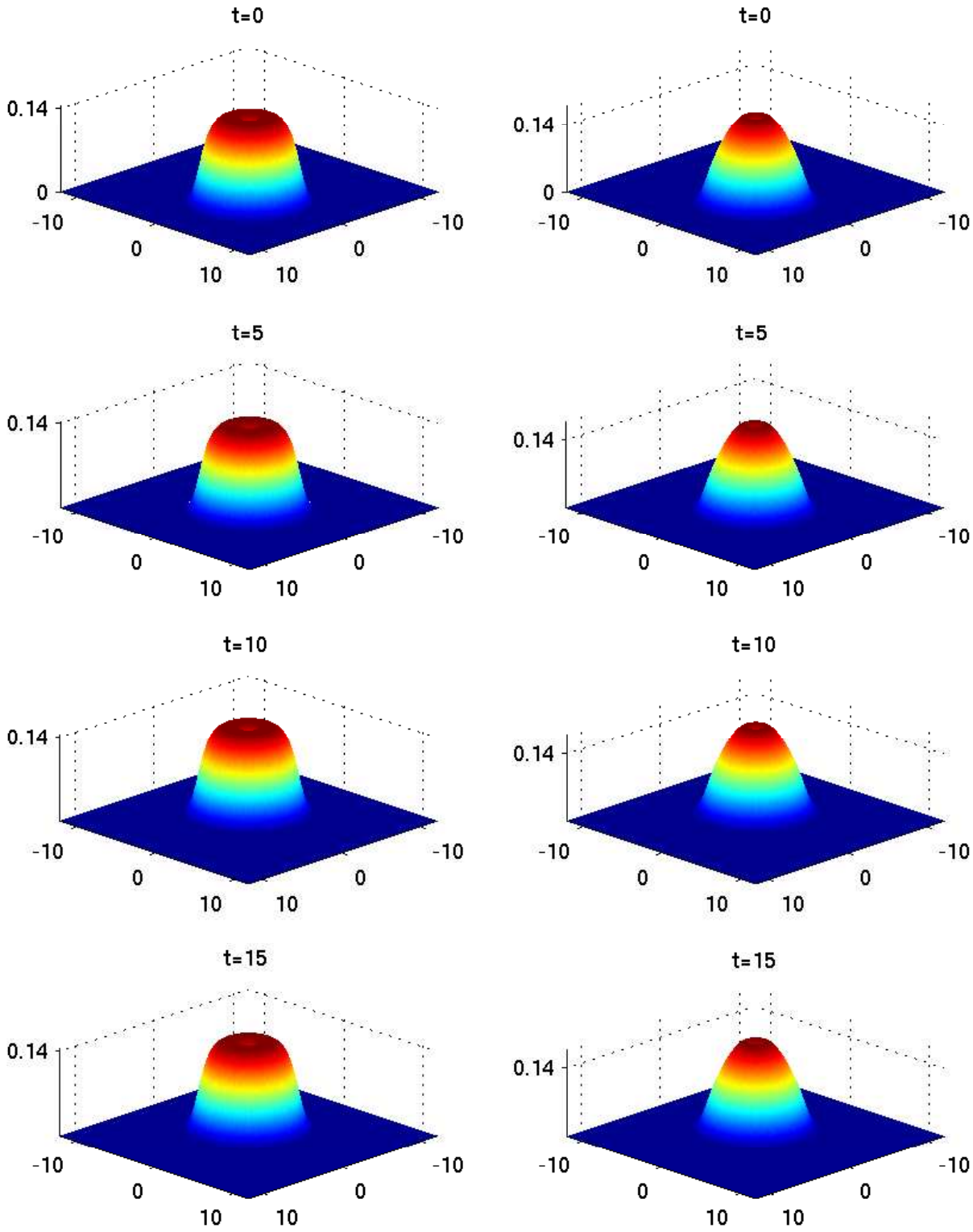

Figure 3.5: Time evolution of density surfaces for component one (left) and component two (right) at different times for case I. From top to bottom: $t = 0, 5, 10, 15$.

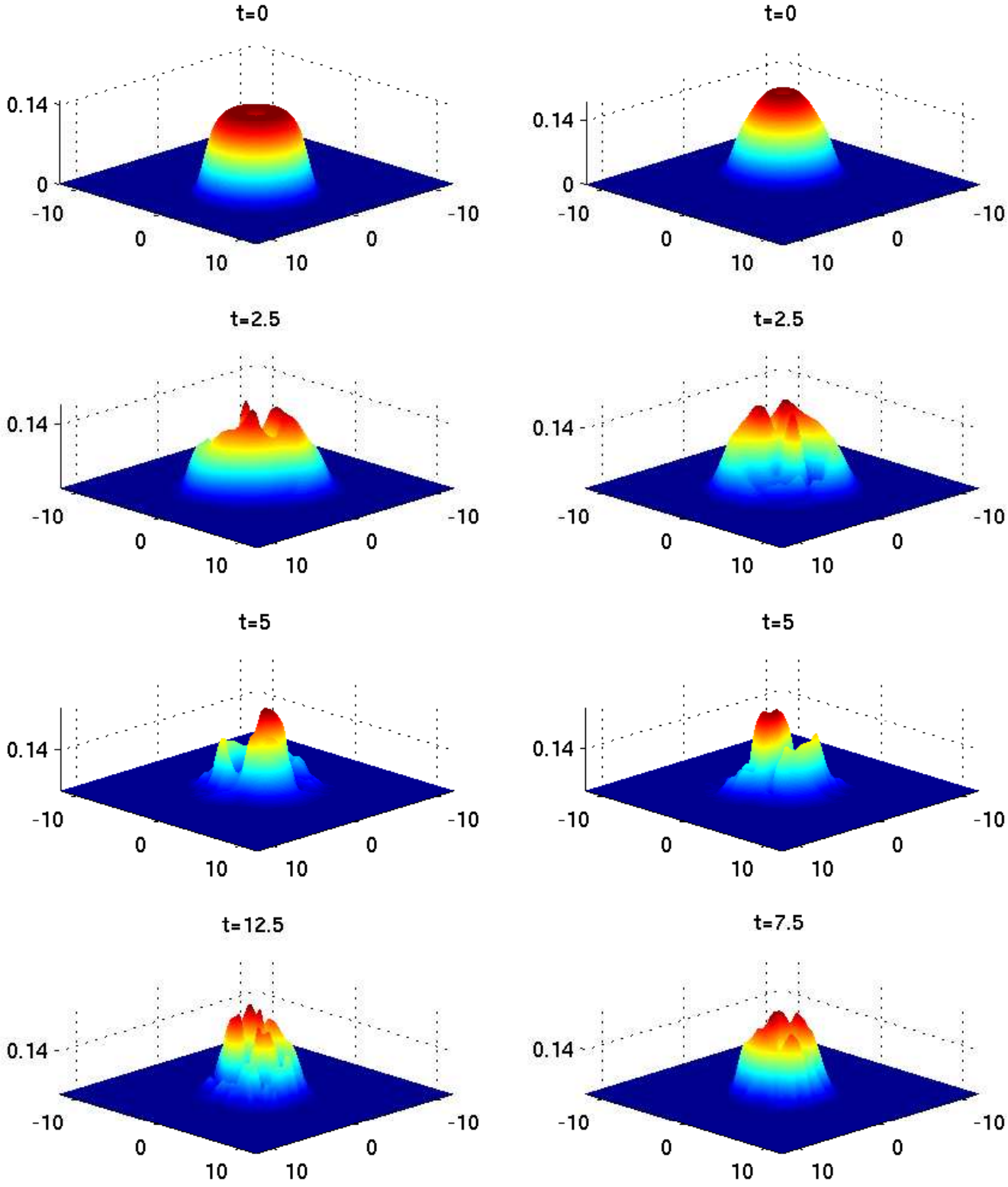

Figure 3.6: Time evolution of density surfaces for component one (left) and component two (right) at different times for case II. From top to bottom: $t = 0, 2.5, 5, 7.5$.

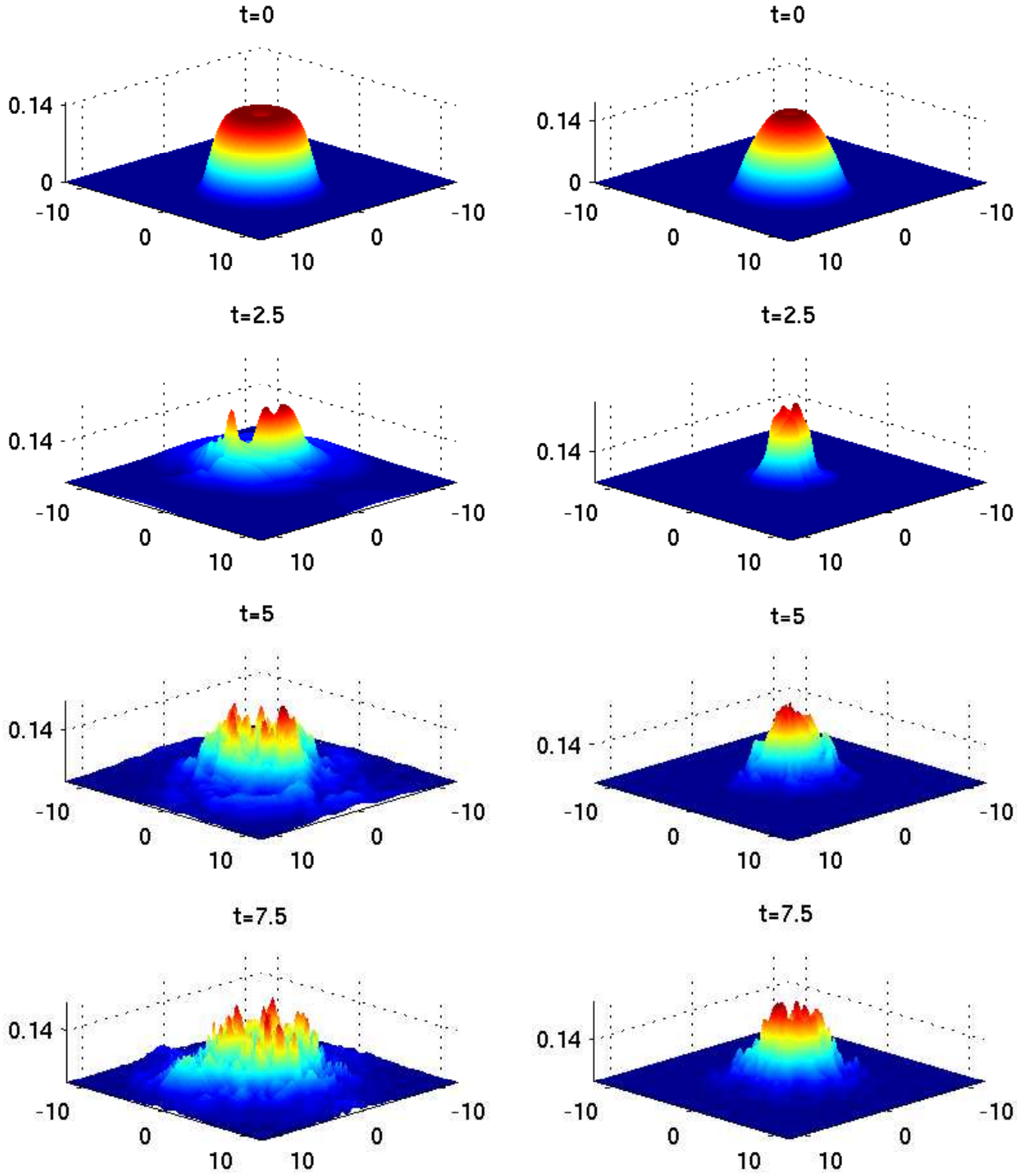

Figure 3.7: Time evolution of density surfaces for component one (left) and component two (right) at different times for case III. From top to bottom: $t = 0, 2.5, 5, 7.5$.

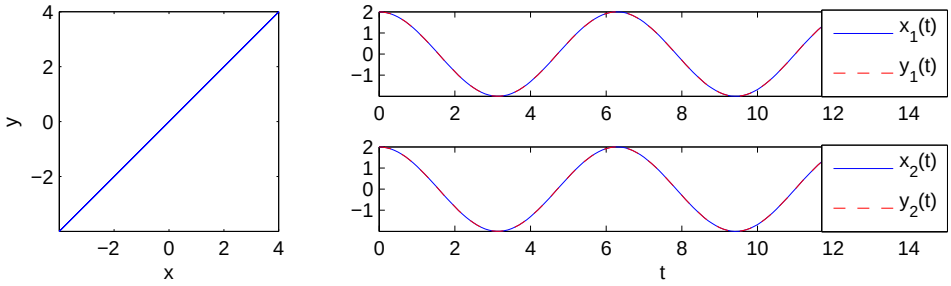

Figure 3.8: Dynamics of center of mass. Left: trajectory of total center of mass. Right: the time evolution of center of mass of component one (top), time evolution of center of mass of component two (bottom).

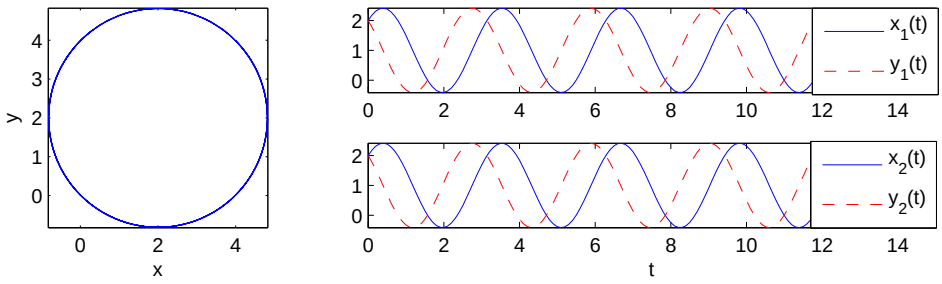

Figure 3.9: Dynamics of center of mass. Left: trajectory of total center of mass. Right: the time evolution of center of mass of component one (top), time evolution of center of mass of component two (bottom).

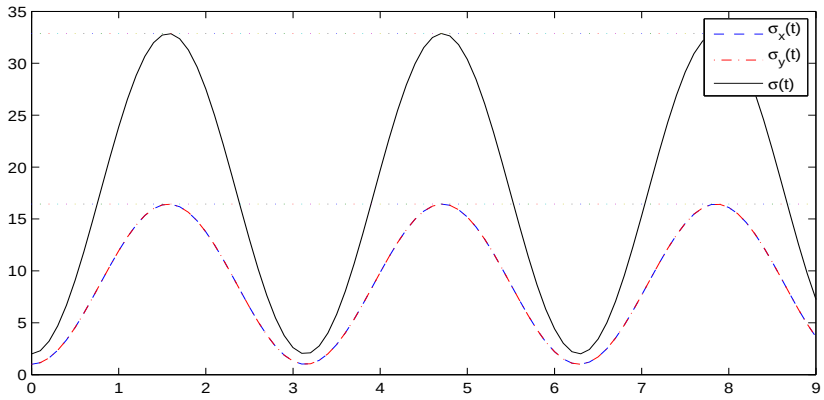

Figure 3.10: Dynamics of condensate widths $\sigma_x(t), \sigma_y(t)$ and $\sigma_r(t)$ when $\lambda = 0$ and $V_1(\mathbf{x}) = V_2(\mathbf{x})$.

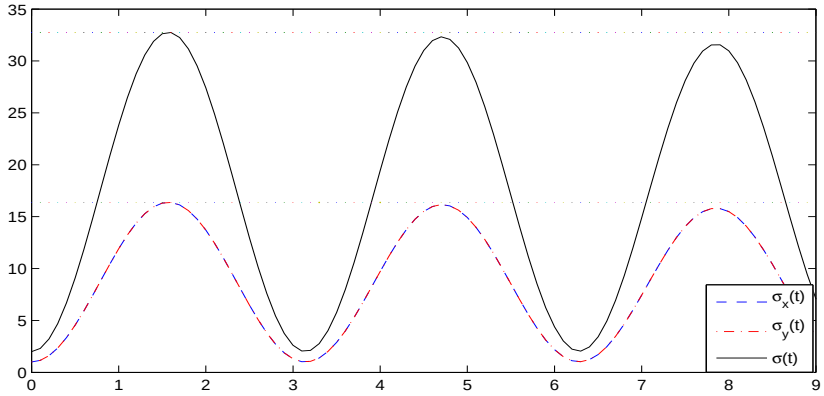

Figure 3.11: Dynamics of condensate widths $\sigma_x(t), \sigma_y(t)$ and $\sigma_r(t)$ when $\lambda \neq 0$ and $V_1(\mathbf{x}) = V_2(\mathbf{x})$.

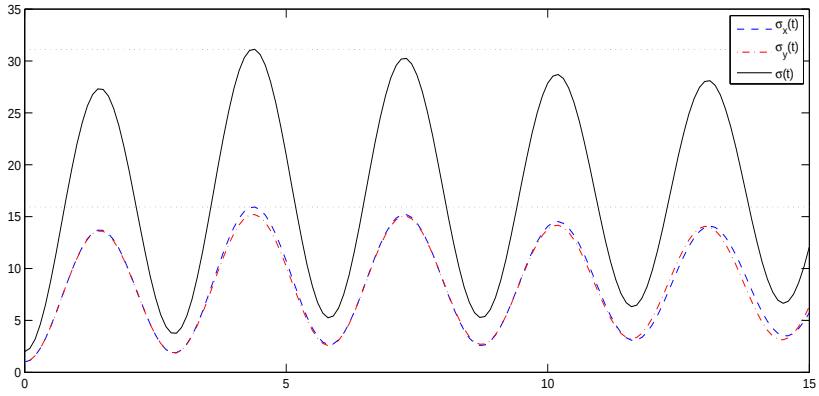

Figure 3.12: Dynamics of condensate widths $\sigma_x(t), \sigma_y(t)$ and $\sigma_r(t)$ when $\lambda = 0$ and $V_1(\mathbf{x}) \neq V_2(\mathbf{x})$.

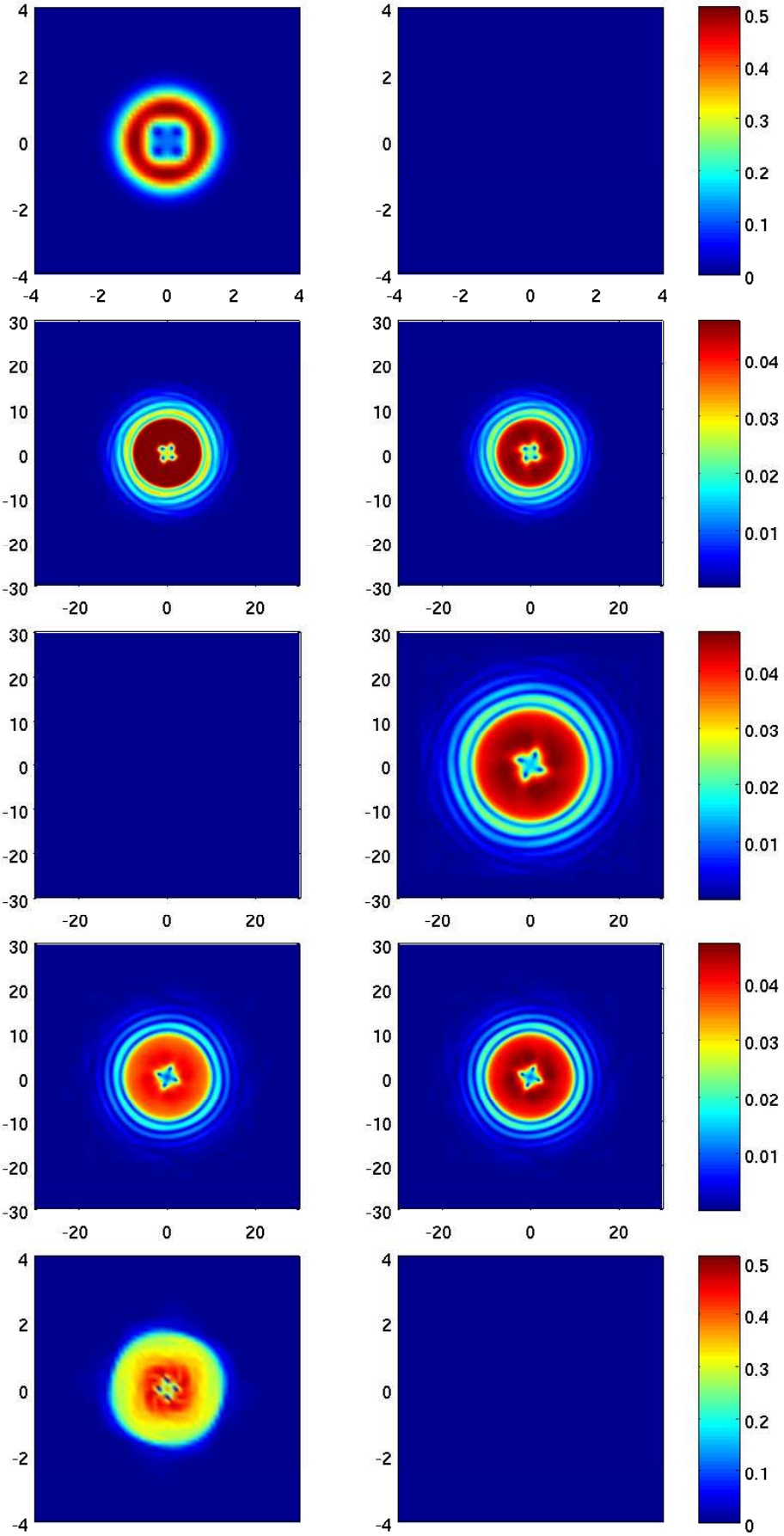

Figure 3.13: Dynamics of vortex lattices when $N = 4$ for component one (left) and component two (right); From top to bottom, $t = 0, 0.7, \pi/2, 2.3, \pi$.

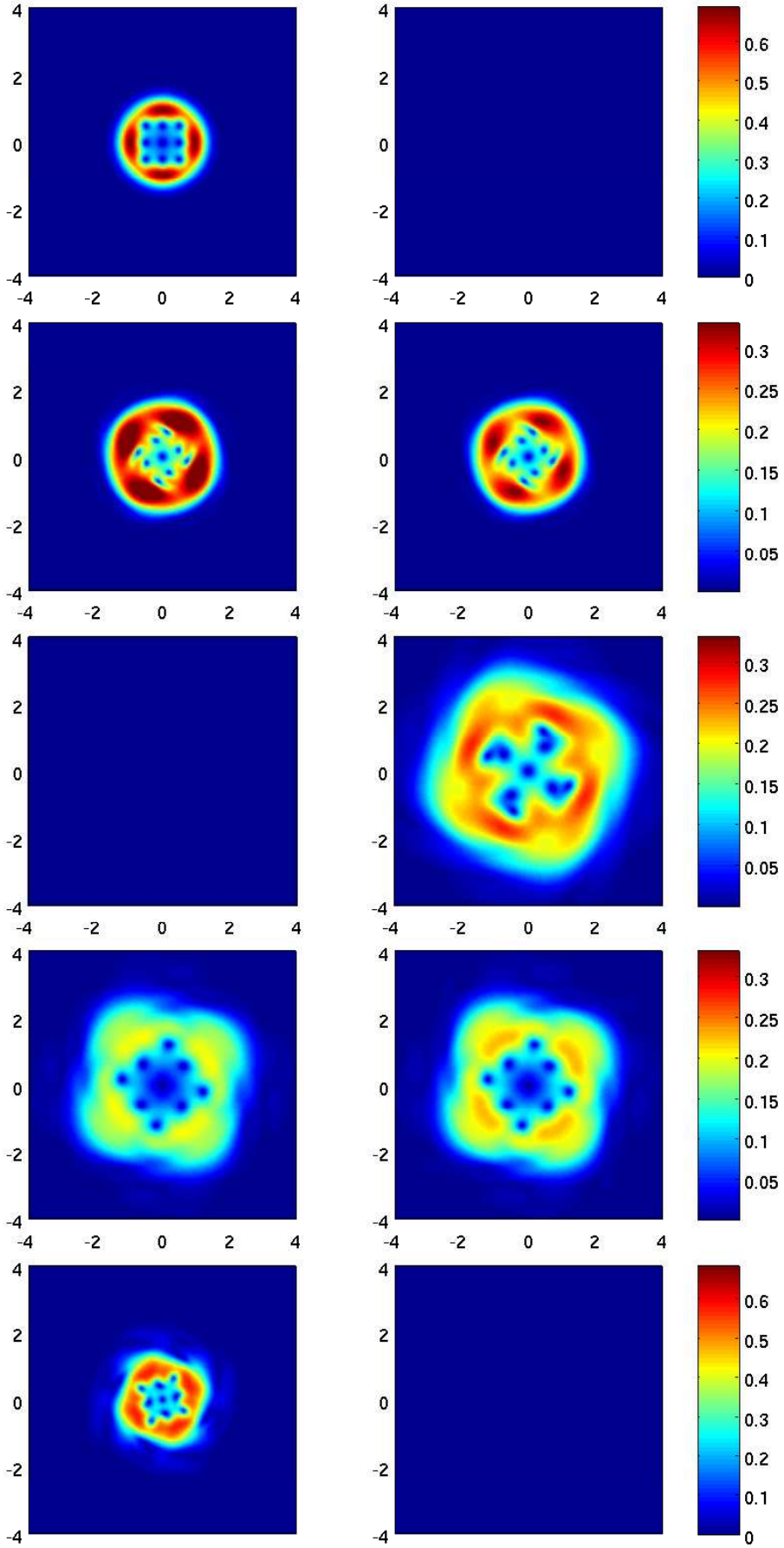

Figure 3.14: Dynamics of vortex lattices when $N = 9$ for component one (left) and component two (right); From top to bottom, $t = 0, 0.7, \pi/2, 2.3, \pi$.

Chapter 4

Conclusion and future studies

In this thesis, we have proposed a new method to study the dynamics of rotating single component Bose-Einstein condensates (BEC) both analytically and numerically and extend our results to rotating two-component BEC. Under the new Lagrangian coordinate system, on the analytical side, we have redefined the analytical form of density, energy, angular momentum expectation, condensate width as well as center of mass. We proved the conservation of density and energy, as well as the angular momentum expectation when the trapping potential is radially symmetric in 2D, and cylindrically symmetric in 3D. We presented an ODE system for the motion of center of mass, and solved it analytically. Along the numerical front, we have applied a second order time splitting method and Fourier pseudo spectral method in space to study numerically the dynamics of condensate, including the energy, angular momentum, condensate width, the motion of center of mass as well as the interaction of central vortices.

We then proceed to extend the numerical methods and results to the rotating coupled-Gross-Pitaevskii equation. We follow the same approach by first presenting the existing dynamical laws. Then applying the Lagrangian coordinate transformation and redefine dynamical laws and analyse their properties. In the end, we present the numerical results.

The dynamics of rotating BEC and rotating two-component BEC have been investigated in the thesis. A further extension can be the case for rotating spin-1

and dipolar BEC. We can apply the orthogonal time dependent matrix transformation method to study the dynamics. We could also include the collision terms in the kinetic equation for mean field to treat finite temperature effects [61, 74].

Bibliography

[1] J. R. Abo-Shaeer, C. Raman, J. M. Vogels, and W. Ketterle, *Observation of vortex lattices in Bose-Einstein condensation in a dilute atomic vapor*, Science **292** (2001), 476–479.

[2] S. K. Adhikari, *Numerical solution of the two-dimensional Gross-Pitaevskii equation for trapped interacting atoms*, Phys. Lett. A. **265** (2000), 91–96.

[3] S. K. Adhikari and P. Muruganandam, *Effect of an impulsive force on vortices in a rotating Bose-Einstein condensate*, Phys. Lett. A. **301** (2002), 333–339.

[4] A. Aftalion and Q. Du, *Vortices in a rotating Bose-Einstein condensate: Critical angular velocities and energy diagrams in the Thomas-Fermi regime*, Phys. Rev. A. **64** (2001), 063603.

[5] M. H. Anderson, J. R. Ensher, M. R. Matthews, C. E. Wieman, and E. A. Cornell, *Observation of Bose-Einstein condensation in a dilute atomic vapor*, Science **269** (1995), 198.

[6] W. Bao, *Ground states and dynamics of multicomponent Bose-Einstein condensates*, Multiscale Model. Simul **2** (2004), 210–236.

[7] ———, *Analysis and efficient computation for the dynamics of two-component Bose-Einstein condensates*, Contemporary Mathematics **473** (2008), 1–26.

[8] W. Bao, Q. Du, and Y. Zhang, *Dynamics of rotating Bose-Einstein condensates and their efficient and accurate numerical computation*, SIAM J. Appl. Math. **66** (2006), 758–786.

[9] W. Bao, S. Jin, and P. A. Markowish, *On time-splitting spectral approximations for the Schrödinger equation in the semiclassical regime*, J. Comput. Phys. **175** (2002), 487–524.

[10] ———, *Numerical study of time-splitting spectral discretizations of nonlinear the Schrödinger equations in the semiclassical regime*, SIAM J. Sci. Comput. **25** (2003), 27–64.

[11] W. Bao and J. Shen, *A fourth-order time splitting Laguerre-Hermite pseudospectral method for Bose-Einstein condensates*, SIAM J. Sci. Comput. **26** (2005), 2010–2028.

[12] W. Bao, H. Wang, and P. A. Markowich, *Ground, symmetric and central vortex state in rotating Bose-Einstein condensate*, Comm. Math. Sci. **3** (2005), 57–88.

[13] W. Bao and Y. Zhang, *Dynamics of the ground state and central vortex states in Bose-Einstein condensates*, Math. Models Meth. Appl. Sci. **15** (2005), 1863–1896.

[14] S. N. Bose, *Plancks gesetz und lichtquantenhypothese*, Zeitschift Für Physik A **26** (1924), 178–181.

[15] S. N. Bose, *The λ-phenomenon of liquid helium and the Bose-Einstein degeneracy*, Nature **141** (1938), 643–644.

[16] C. C. Bradley, C. A. Sackett, and R. G. Hulet, *Evidence of Bose-Einstein condensation in an atomic gas with attractive interactions*, Phys. Rev. Lett. **75** (1995), 1687.

[17] V. Bretin, S. Stock, Y. Seurin, and J. Dalibard, *Fast rotation of a Bose-Einstein condensate*, Phys. Rev. Lett. **92** (2004), 050403.

[18] Y. Cai, *Mathematical theory and numerical methods for Gross-Pitaevskii equations and applications*, Ph.D. thesis, National University of Singapore, 2011.

[19] B. M. Caradoc-Davis, R. J. Ballagh, and P. B. Blakie, *Coherent dynamics of vortex formation in trapped Bose-Einstein condensates*, Phys. Rev. Lett. **83** (1999), 895.

[20] ———, *Three-dimensional vortex dynamics in Bose-Einstein condensates*, Phys. Rev. A **62** (2000), 011602.

[21] Y. Castin and R. Dum, *Bose-Einstein condensates with vortices in rotating traps*, Eur. Phys. J. DAt. Mol. Opt. Phys. **7** (1999), 399–412.

[22] M. M. Cerimele, M. L. Chiofalo, F. Pistella, S. Succi, and M. P. Tosi, *Numerical solution of the Gross-Pitaevskii equation using an explicit finite different scheme: an application to trapped Bose-Einstein condensates*, Phys. Rev. E. **62** (2000), 1382–1389.

[23] P. M. Chaikin and T. C. Lubensky, *Principles of condensed matter physics*, Cambridge, Cambridge, 2007.

[24] M. L. Chiofalo, S. Succi, and M. P. Tosi, *Ground state of trapped interacting Bose-Einstein condensates by an explicit imaginary-time algorithm*, Phys. Rev. E. **62** (2000), 7438.

[25] S. T. Chui, V. N. Ryzhov, and E. E. Tareyeva, *Phase separation and vortex states in the binary mixture of Bose-Einstein condensates*, J. Exp. Theor. Phys. **91** (2000), 1183–1189.

[26] I. Coddington, P. C. Haljan, P. Engels, V. Schweikhard, S. Tung, and E. A. Cornell, *Experimental studies of equilibrium vortex properties in a Bose-condensed gas*, Phys. Rev. A. **70** (2004), 063607.

[27] S. L. Cornish, N. R. Claussen, J. L. Roberts, E. A. Cornell, and C. E. Wieman, *Stable ^{85}Rb Bose-Einstein condensations with widely tunable interactions*, Phys. Rev. Lett. **85** (2000), 1795–1798.

[28] F. Dalfovo and S. Giorgini, *Theory of Bose-Einstein condensation in trapped gases*, Rev. Mod.Phys. **71** (1999), 463.

[29] K. B. Davis, M. O. Mewes, M. R. Andrews, N. J. van Druten, D. S. Durfee, D. M. Kurn, and W. Ketterle, *Bose-Einstein condensation in a gas of sodium atoms*, Phys. Rev. Lett. **75** (1995), 3969.

[30] R. J. Donnelly, *Quantized vortices in Helium II*, Cambridge University Press, Oxford.

[31] A. Einstein, *Quantentheorie des einatomigen idealen gases*, Sitzber. Kgl. Preuss. Akad. Wiss. **261** (1924).

[32] B. D. Esry, C. H. Greene, J. P. Burke Jr, and J. L. Bohn, *Hartree-Fock theory for double condensates*, Phys. Rev. Lett. **78** (1997), 3594–3597.

[33] D. L. Feder, C. W. Clark, and B. I. Schneider, *Nucleation of vortex arrays in rotating anisotropic of an impulsive force on vortices in a rotating Bose-Einstein condensates*, Phys. Rev. A. **61** (1999), 011601.

[34] D. L. Feder, A. A. Svidzinsky, A. L. Fetter, and C. W. Clark, *Anomalous modes drive vortex dynamics in confined Bose-Einstein condensates*, Phys. Rev. Lett. **86** (2001), 564–567.

[35] A. L. Fetter and A. A. Svidzinsky, *Vortices in a trapped dilute Bose-Einstein condensate*, Phys. Condens. Matter **13** (2001), R135–194.

[36] D. G. Fried, T. C. Killian, L. Willmann, D. Landhuis, S. C. Moss, D. Kleppner, and T. J. Greytak, *Bose-Einstein condensation of atomic hydrogen*, Phys. Rev. Lett. **81** (1998), 3811–3814.

[37] J. J. Garcia-Ripoll and V. M. Perez-Garcia, *Stability of vortices in inhomogeneous Bose-Einstein condensates subject to rotation: A three dimensional analysis*, Phys. Rev. A. **60** (1999), 4864–4874.

[38] ———, *Stable and unstable vortices in multicomponent Bose-Einstein condensates*, Phys. Rev. Lett. **81** (2000), 4264.

[39] ———, *Nucleation of bended vortices in Bose-Einstein condensates in elongated traps*, Condensed Matter. (2002), 0006368.

[40] ———, *Split vortices in optically coupled Bose-Einstein condensates*, Phys. Rev. A. **66** (2002), 021602.

[41] A. Griffin, D. Snoke, and S. Stringaro, *Bose-Einstein condensation*, Cambridge University Press, 1995.

[42] E. P. Gross, *Structure of a quantized vortex in boson systems*, Il Nuovo Cimento **20** (1961), 454–457.

[43] D. S. Hall, M. R. Matthews, J. R. Ensher, C. E. Wieman, and E. A. Cornell, *Dynamics of component separation in a binary mixture of Bose-Einstein condensates*, Phys. Rev. Lett. **81** (1998), 15391542.

[44] T. L. Ho and V. B. Shenoy, *Binary mixtures of Bose condensates of alkali atoms*, Phys. Rev. Lett. **77** (1996), 3276–3279.

[45] B. Jackson, J. F. McCann, and C. S. Adams, *Dissipate Bose-Einstein condensates with vortices in rotating traps*, Eur. Phys. J. D: At. Mol. Opt. Phys. **7** (1999), 399–412.

[46] D. Jaksch, S. A. Gardiner, K. Schulze, J. I. Cirac, and P. Zoller, *Uniting Bose-Einstein condensates in optical resonators*, Phys. Rev. Lett. **86** (2001), 4733–4736.

[47] K. Kasamatsu, M. Tsubuta, and M. Ueda, *Vortex phase diagram in rotating two-component Bose-Einstein condensates*, Phys. Rev. Lett. **91** (2003), 150406.

[48] ———, *Vortices in a multicomponent Bose-Einstein condensates*, Int.J.Mod.Phys. B. **19** (2005), 1835.

[49] C. K. Law, H. Pu, N. P. Bigelow, and J. H. Eberly, *"stability signature" in two species dilute Bose-Einstein condensates*, Phys. Rev. Lett. **79** (1997), 3105–3108.

[50] E. H. Lieb and R. Seiringer, *Derivation of the Gross-Pitaevskii equation for rotating Bose gases*, Comm. Math. Phys. **264** (2006), 505–537.

[51] E. H. Lieb, R. Seiringer, and J. Yngvason, *Bosons in a trap: A rigorous derivation of the Gross-Pitaevskii energy functional*, Phys. Rev. A **61** (2000), 3602.

[52] E. H. Lieb and J. P. Solovej, *Ground state energy of the two component charged Bose gas*, Comm. Math. Phys. **252** (2004), 485–534.

[53] F. London, *Superfluids*, vol. I and II, Dover, 1964.

[54] K. W. Madison, F. Chevy, W. Wohlleben, and J. Dalibard, *Vortex formation in a stirred Bose-Einstein condensates*, Phys. Rev. Lett. **84** (2000), 806.

[55] ———, *Vortex formation in a stirred Bose-Einstein condensates*, J. Mod. Opt. **47** (2000), 2725.

[56] M. R. Matthews, B. P. Anderson, P. C. Haljan, D. S. Hall, C. E. Wieman, and E. A. Cornell, *Vortices in a Bose-Einstein condensate*, Phys. Rev. Lett. **83** (1999), 2498.

[57] G. Modugno, G. Ferrari, G. Roati, R. J. Brecha, A. Simoni, and M. Inguscio, *Bose-Einstein condensation of potassium atoms by sympathetic cooling*, Science **294** (2001), 1320–1322.

[58] E. J. Mueller and T. L. Ho, *Two-component Bose-Einstein condensates with a large number of vortices*, Phys. Rev. Lett. **88** (2002), 180403.

[59] P. Muruganandam and S. K. Adhikari, *Bose-Einstein dynamics in three dimensions by the pseudospectral and finite-difference methods*, J. Phys. B: At. Mol. Opt. Phys. **36** (2003), 2501–2513.

[60] C. J. Myatt, E. A. Burt, R. W. Ghrist, E. A. Cornell, and C. E. Wietman, *Production of two overlapping Bose-Einstein condensates by sympathetic cooling*, Phys. Rev. Lett. **78** (1997), 586–589.

[61] C. J. Pethick and H. Smith, *Bose-Einstein condensation in dilute gases*, Cambridge University Press, 2002.

[62] L. P. Pitaevskii, *Vortex lines in an imperfect Bose gas*, Solviet Physics JETP **13** (1961), 451–454.

[63] H. Pu and N. P. Bigelow, *Properties of two-species Bose condensates*, Phys. Rev. Lett. **80** (1998), 1130–1133.

[64] C. Raman, J. R. Abo-Shaeer, J. M. Vogels, K. Xu, and W. Ketterle, *Vortex nucleation in a stirred Bose-Einstein condensate*, Phys. Rev. Lett. **87** (2001), 210402.

[65] A. Robert, O. Sirjean, A. Browaeys, J. Poupard, S. Nowak, D. Boiron, C. I. Westbrook, and A. Aspect, *A Bose-Einstein condensate of metastable atoms*, Science **292** (2001), 461–464.

[66] P. A. Ruprecht, M. J. Holland, K. Burnett, and M. Edwards, *Time-dependent solution of the nonlinear Schrödinger equation for Bose-condensed trapped neutral atoms*, Phys. Rev. A. **51** (1995), 4704–4711.

[67] F. P. Dos Santos, J. Leonard, J. Wang, C. J. Barrelet, F. Perales, E. Rasel, C. S. Unnikrishnan, M. Leduc, and C. Cohen-Tannoudji, *Bose-Einstein condensation of metastable helium*, Phys. Rev. Lett. **86** (2001), 3459–3462.

[68] V. Schweikhard, I. Coddington, P. Engels, V. P. Mogendorff, and E. A. Cornell, *Rapidly rotating Bose-Einstein condensates in and near the lowest Landau level*, Phys. Rev. Lett. **92** (2004), 040404.

[69] ———, *Vortex lattice dynamics in rotating Bose-Einstein condensates*, Phys. Rev. Lett. **93** (2004), 210403.

[70] G. Strang, *On the construction and comparison of different schemes*, SIAM J. Numer. Anal. **5** (1968), 506–517.

[71] M. Tsubota, K. Kasamatsu, and T. Araki, *Dynamics of quantized vortices in superfluid helium and rotating Bose-Einstein condensates*, cond-mat, 0309364.

[72] H. Wang, *Quantized vortex states and dynamics in Bose-Einstein condensates*, Ph.D. thesis, National University of Singapore, 2006.

[73] T. Weber, J. Herbig, M. Mark, H. C. Nägerl, and R. Grimm, *Bose-Einstein condensation of cesium*, Science **299** (2003), 232.

[74] E. Zaremba, T. Nikuni, and A. Griffin, *Dynamics of trapped Bose gases at finite temperatures*, Journal of Low Temperature Physics **116** (1999), 277–345.

[75] Y. Zhang, *Mathematical analysis and numerical simulation of Bose-Einstein condensation*, Ph.D. thesis, National University of Singapore, 2006.

[76] Y. Zhang and W. Bao, *Dynamics of the center of mass in rotating Bose-Einstein condensates*, Appl. Numer. Math. **57** (2007), 697–709.

[77] Y. Zhang, W. Bao, and H. Li, *Dynamics of rotating two-component Bose-Einstein condensates and its efficient computation*, Physica D **234** (2007), 49–69.

NUMERICAL STUDIES OF ROTATING BOSE-EINSTEIN CONDENSATES VIA ROTATING LAGRANGIAN COORDINATES

CAO XIAOMENG

NATIONAL UNIVERSITY OF SINGAPORE

2012

NUMERICAL STUDIES OF ROTATING BOSE-EINSTEIN CONDENSATES VIA ROTATING LAGRANGIAN COORDINATES